



# HHS Public Access

Author manuscript

*Chem Rev.* Author manuscript; available in PMC 2021 December 20.

Published in final edited form as:

*Chem Rev.* 2021 May 12; 121(9): 5193–5239. doi:10.1021/acs.chemrev.0c01005.

## Iron Acquisition Systems of Gram-negative Bacterial Pathogens Define TonB-Dependent Pathways to Novel Antibiotics

**Phillip E. Klebba,**

Department of Biochemistry and Molecular Biophysics, Kansas State University, Manhattan, Kansas 66506, United States

**Salete M. C. Newton,**

Department of Biochemistry and Molecular Biophysics, Kansas State University, Manhattan, Kansas 66506, United States

**David A. Six,**

Venatorx Pharmaceuticals, Inc., Malvern, Pennsylvania 19355, United States

**Ashish Kumar,**

Department of Biochemistry and Molecular Biophysics, Kansas State University, Manhattan, Kansas 66506, United States

**Taihao Yang,**

Department of Biochemistry and Molecular Biophysics, Kansas State University, Manhattan, Kansas 66506, United States

**Brittany L. Nairn,**

Department of Biological Sciences, Bethel University, St. Paul, Minnesota 55112, United States

**Colton Munger,**

Department of Biochemistry and Molecular Biophysics, Kansas State University, Manhattan, Kansas 66506, United States

**Somnath Chakravorty**

Jacobs School of Medicine and Biomedical Sciences, SUNY Buffalo, Buffalo, New York 14203, United States

### Abstract

Iron is an indispensable metabolic cofactor in both pro- and eukaryotes, which engenders a natural competition for the metal between bacterial pathogens and their human or animal hosts. Bacteria secrete siderophores that extract  $\text{Fe}^{3+}$  from tissues, fluids, cells, and proteins; the ligand gated porins of the Gram-negative bacterial outer membrane actively acquire the resulting ferric

---

**Corresponding Author Phillip E. Klebba** – *Department of Biochemistry and Molecular Biophysics, Kansas State University, Manhattan, Kansas 66506, United States; Phone: (785)532-6268; peklebba@ksu.edu.*

Supporting Information

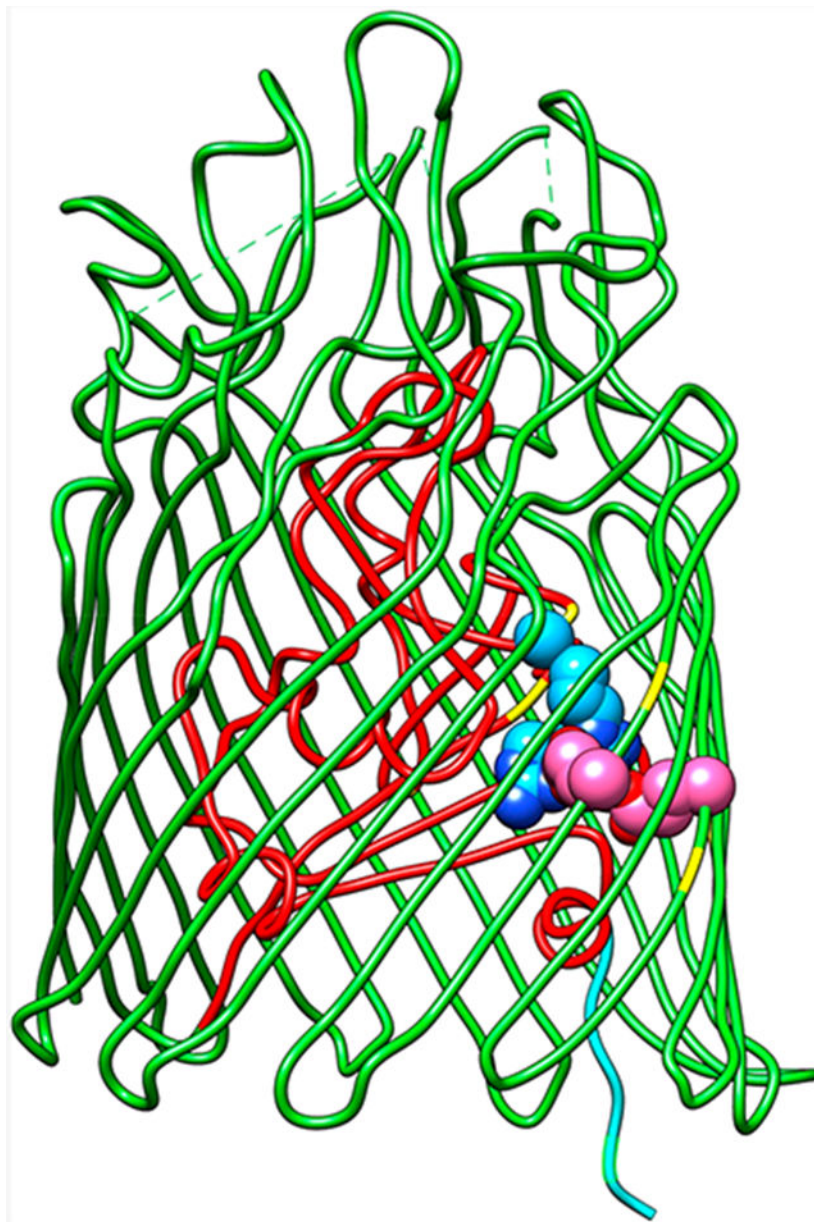
The Supporting Information is available free of charge at <https://pubs.acs.org/doi/10.1021/acs.chemrev.0c01005>.

Phylogenetic relationships of Gram (–) bacterial LGP, derived from pairwise comparisons of the mature protein sequences listed below the cladogram/phylogram (PDF)

The authors declare the following competing financial interest(s): D.A.S. is employed and compensated by Venatorx, and may own stock or stock options in Venatorx as part of his remuneration for employment.

siderophores, as well as other iron-containing molecules like heme. Conversely, eukaryotic hosts combat bacterial iron scavenging by sequestering  $\text{Fe}^{3+}$  in binding proteins and ferritin. The variety of iron uptake systems in Gram-negative bacterial pathogens illustrates a range of chemical and biochemical mechanisms that facilitate microbial pathogenesis. This document attempts to summarize and understand these processes, to guide discovery of immunological or chemical interventions that may thwart infectious disease.

## Graphical Abstract



## INTRODUCTION

Since 1947, when Pappenheimer saw the regulation of diphtheria toxin production by iron availability,<sup>1</sup> the link between iron acquisition and bacterial pathogenesis seemed logical. Twenty years later, Bullen and Rogers<sup>2</sup> noted the impact of excess iron on innate immune defense to infection, which began a series of their articles describing the antagonism between prokaryotic iron requirements and iron sequestration by human hosts.<sup>2-10</sup> The research that validated those ideas exponentially expanded over the ensuing 50 years to create an immense body of data. This paper will review those findings to the present day, especially as they relate to iron uptake by Gram (–) bacterial pathogens that acquire different forms of Fe<sup>3+</sup> through TonB-dependent transport systems in their cell envelopes. One goal is to explain the transport strategies that carbapenem-resistant Enterobacteriales<sup>11,12</sup> (formerly Enterobacteriaceae<sup>13-15</sup>) (CRE; see Abbreviations for a list of all abbreviations and acronyms) and the notorious group of *Enterococcus*, *Staphylococcus*, *Klebsiella*, *Acinetobacter*, *Pseudomonas*, and *Enterobacter* (ESKAPE) pathogens<sup>16,17</sup> and other dangerous or multiply drug resistant organisms, utilize to circumvent the innate immune defenses of eukaryotic hosts. In the process, we will consider the nature and relationships of dozens of Gram (–) bacterial outer membrane (OM) receptor proteins that bind and transport organic iron complexes. These summaries consider genetic, microbiological, biochemical, and structural biological data with both clinical and mechanistic relevance. Our discourse focuses on the iron uptake systems of pathogenic organisms of current worldwide concern as a result of their unrelenting development of antibiotic resistance. Our overview is not all-inclusive of Gram (–) bacterial iron uptake systems, nor comprehensive with regard to clinical remedies that may arise against such phenomena. Instead, we address the possibility of antibiotic discovery against TonB-dependent iron uptake in the target bacteria. TonB is a ubiquitous, essential protein component of Gram (–) bacterial iron uptake pathways, so inhibition of TonB action is potentially effective to limit bacterial growth, and thereby stem the severity of CRE/ESKAPE pathogenesis. To simplify designation of the many small molecules and proteins under consideration, we adopted the convention of abbreviating prokaryotic molecules with a capitalized first-letter (*e.g.*, enterobactin, Ent) and eukaryotic proteins with all capitals (*e.g.*, siderocalin, SCN).

### 1. NOVEL THERAPEUTICS AGAINST GRAM (–) BACTERIAL PATHOGENS

Today's world faces a long-standing threat that intensified over the past several decades: the uncertain outcomes of bacterial infection. In 2009, for example, Gram (–) bacteria caused two-thirds of the mortality among ~100 000 bacteria-associated deaths in U.S. hospitals; 20% were resistant to all known antibiotics.<sup>18</sup> At that time, the WHO identified Gram (–) CRE/ESKAPE pathogens as critical priorities for antibiotic discovery.<sup>19</sup> Ten years later, in 2019, the CDC reported more than 35,000 US deaths,<sup>20</sup> as a result of more than 2.8 million infections with ESKAPE and other antibiotic-resistant bacteria. During the same time, pharmaceutical companies lessened efforts to combat microbial pathogens.<sup>21-25</sup> Antimicrobial treatments are typically either inhibitors of essential biochemical pathways in the pathogen (antibiotics) or molecular constructs (vaccines) that stimulate adaptive immunity in the host. Both approaches have a history of clinical applications that saved millions of lives. Unfortunately, natural selection of variations in the pathogens that lead

to resistance undermines both approaches. Antibiotic resistance often arises from mutations that alter cell envelope permeability or decrease the susceptibility of target enzymes to inhibition or other mechanisms.<sup>26-28</sup> Vaccine inefficacy stems from changes in the antigenic determinants of the pathogen that supersede the epitopes of the vaccine construct. Hence, one challenge is to identify new pathways, proteins, or other molecules that are vulnerable targets for drug or vaccine development.

Gram (–) bacterial antibiotic resistance largely derives from the selective permeability of the OM and inner membrane (IM) of the cell envelope. The former excludes large or hydrophobic antibiotics but internalizes solutes and nutrients,<sup>27,28</sup> whereas the latter contains pumps that expel antibiotics.<sup>29,30</sup> Without new antibiotics,<sup>31,32</sup> soon no therapeutic options will exist for an expanding number of bacterial pathogens. Many multidrug resistant bacteria became problematic in the past decade, including members of the CRE/ESKAPE pathogen group.<sup>33,34</sup> Plus, in 2019, the CDC added other Gram (–) species as urgent or serious threats: *Campylobacter*, *Neisseria*, *Salmonella*, and *Shigella*.<sup>20</sup> The high rate of antibiotic resistance in such strains, that produce the majority of nosocomial infections in the U.S., makes them potentially lethal. These bacteria also often contain uniquely adapted systems for “iron piracy”<sup>35</sup> from humans and animals. The clinical options against CRE are so limited that physicians must resort to abandoned toxic drugs like colistin,<sup>36</sup> an old antibiotic that was kept in reserve as a last resort against bacterial infections. If CRE acquire colistin resistance, then they become predicted “superbugs”<sup>31,32</sup> that are untreatable by all known antibiotics. Colistin resistant *Escherichia coli* already appeared in the U.S.,<sup>37</sup> underscoring the urgent need for new antibacterial agents.

## 2. IRON ACQUISITION AND BACTERIAL PATHOGENESIS

From a biochemical or metabolic perspective, iron is the most valuable metal in biological systems. Over 80 enzymes require iron-containing heme (Hn) or non-Hn cofactors that help catalyze the metabolic biochemistry of bacteria, fungi, and animals. Examples include aconitase and succinate dehydrogenase in the Krebs cycle, proton-pumping oxidoreductases in the electron transport chain, class Ia ribonucleotide reductases in *de novo* DNA synthesis, monooxygenases like cytochrome P<sub>450</sub>, and catalases and superoxide dismutases that detoxify reactive oxygen species. This central role of iron in aerobic biochemistry makes it a determinant of bacterial pathogenesis, invasiveness, and molecular competition at the host–pathogen interface: the eukaryotic innate immune system sequesters iron, but successful pathogens overcome this defense mechanism and capture the metal.<sup>38-51</sup> The eukaryotic components of cellular iron trafficking include the Fe<sup>3+</sup>-binding proteins transferrin (TF), lactoferrin (LF) and ferritin (FTN), an intricate intracellular network of regulatory and delivery proteins hepcidin, hephaestin, hemoglobin-haptoglobin, Hn-hemopexin, ferroportin, ceruloplasmin, serum albumin, and lipocalins (LCN),<sup>52-54</sup> including LCN2, that is now called siderocalin<sup>55</sup> (SCN). Their prokaryotic counterparts are components of diverse, omnipresent iron uptake systems that bacteria employ to obtain iron in the host. In Gram (–) cells, iron acquisition usually begins with the elaboration of siderophores (*Gr. iron carrier*), low molecular weight organic chelators<sup>56,57</sup> that complex adventitious, or sequestered iron with unparalleled high affinity: Ent has a binding affinity constant of 10<sup>52</sup> M<sup>-1</sup>.<sup>58,59</sup> Over 500 different siderophores are known and characterized.<sup>60</sup> The second

part of Gram (–) bacterial iron uptake is an equally large group of discriminating, high affinity cell surface receptors that bind ferric siderophores and other iron complexes ( $K_D \sim 10^{-10} \text{ M}^{61,62}$ ). Since their discovery,<sup>63,64</sup> these ~80 kDa proteins were recognized as the OM components of multiprotein, energy- and TonB-dependent cell envelope transport systems.<sup>65</sup> Their nomenclature has evolved with the understanding of their properties, as iron-regulated membrane proteins (IRMP<sup>66</sup>), iron-regulated OM proteins (IROMP<sup>67</sup>), ligand-gated porins (LGP<sup>68</sup>), or TonB-dependent transporters (TBDT<sup>69</sup>). None of these acronyms is perfect (see following), but LGP perhaps best describes their mechanistic attributes. Like ligand-gated ion channels,<sup>70-72</sup> the binding of a ferric siderophore, other metal complex, or eukaryotic iron-containing protein activates LGP to conformational motion<sup>35,73,74</sup> that signals their occupancy and stimulates interactions with TonB. The ensuing actions of TonB, as energized by electrochemical proton motive force (PMF), enable uptake of the iron complex or free iron through the OM into the periplasm.

Since about 1970,<sup>6</sup> the biochemical connections between pro- and eukaryotic iron homeostasis were apparent, and many researchers, but especially J. J. Bullen,<sup>4,8,75,76</sup> noted the relationship between bacterial iron acquisition and infection. Fifty years of research on these systems confirmed that bacteria need iron for metabolism, they produce biosynthetic and transport systems to obtain it, and their success toward this end influences the outcome of their infections. Conversely, iron deprivation, or disruption of iron uptake processes, retards bacterial growth,<sup>66,77-81</sup> reducing or eliminating virulence.<sup>35,82-89</sup> Although none of the prokaryotic uptake systems are yet fully understood,<sup>69,90,91</sup> Gram (–) bacterial  $\text{Fe}^{3+}$  transport begins when LGP adsorb iron complexes, and facilitated by TonB, internalize them through the OM bilayer. TonB-dependent iron acquisition systems contribute to colonization of eukaryotic hosts.<sup>48,92-99</sup> Overall, an assortment of experimental approaches accumulated comprehensive evidence that iron acquisition is a determinant of pathogenesis:

- Iron deprivation slows bacterial growth;<sup>100,66,77,79-82,101</sup> bacteria secrete siderophores to combat low-iron stress.<sup>60,66,81</sup>
- Gram (–) bacterial pathogens, including species of *Escherichia*, *Salmonella*, *Neisseria*, *Vibrio*, *Acinetobacter*, *Klebsiella*, *Yersinia*, *Pseudomonas*, *Hemophilus*, and more, acquire iron with TonB-dependent transporters.<sup>73,88,102-120</sup>
- Microbial iron scavenging and host iron sequestration are antagonistic processes that influence infection.<sup>4,7,75,121</sup>
- Iron sequestration reduces or eliminates bacterial virulence.<sup>35,82-89,122-131</sup>
- Successful pathogens capture iron from their hosts.<sup>35,38,39,41-51,83,96,132-147</sup>
- Vaccination with bacterial iron transporters creates protective humoral and/or cellular immunity.<sup>148-157</sup>
- “Trojan Horse” siderophore antibiotics, that enter bacteria through iron transporters, show broad-spectrum activity against Gram (–) bacteria.<sup>158-163</sup>

Despite the many connections between iron and infectious disease, and the variety of studies that repeatedly verified the relationship between iron acquisition and bacterial

colonization<sup>164</sup> or virulence,<sup>92,94,99,165-167</sup> some findings challenged the idea that iron uptake promoted bacterial pathogenesis.<sup>168</sup> The explanation of this discrepancy is that bacterial pathogens often elaborate multiple siderophores and acquire even more ferric siderophores. So, single mutations that abrogate a particular iron uptake pathway may not impair host colonization or virulence<sup>168</sup> because other iron uptake pathways compensate for the deficiency. Laboratory *E. coli* K-12 strains, for example, produce at least seven TonB-dependent transport systems for ferric iron,<sup>51,104,169-171</sup> and wild *E. coli* clinical isolates encode even more<sup>172-174</sup> that either internalize ferric siderophores<sup>57,175</sup> or extract iron from eukaryotic proteins.<sup>35,74</sup> Other bacterial pathogens, like *Acinetobacter baumannii*, produce as many as 10 different siderophores in iron deficient environments.<sup>176</sup>

Once this knowledge of iron uptake multiplicity and redundancy was known, it raised doubts that siderophore pathways are appropriate targets for antibiotic development. However, all Gram (–) bacteria acquire ferric iron with TonB-dependent LGP, so TonB itself is a conserved common component of all these OM uptake reactions. The actions of TonB are ostensibly susceptible chemical inhibition, which will reduce iron acquisition and therefore also reduce bacterial proliferation in humans and animals. Furthermore, mutant bacteria lacking TonB, or producing mutant TonB proteins, will not obtain iron in the host environment and therefore fail to thrive or colonize.<sup>88,164</sup> So, antibiotics that target TonB may suffer less from resistance. These points suggest that TonB-dependent iron uptake pathways are viable candidates for antibiotic discovery.

A large percentage of existing antibiotics target bacterial cell envelope biochemistry.<sup>177-180</sup> Compounds that block OM iron transport will similarly focus on a process that is uniquely prokaryotic: eukaryotes acquire iron by different mechanisms.<sup>181-184</sup> Iron potentiates the activity of the quinone antibiotic streptonigrin against *E. coli*,<sup>185</sup> *Neisseria gonorrhoeae*,<sup>186,187</sup> and *Haemophilus influenzae*,<sup>188</sup> but not a single natural antibiotic is known to antagonize bacterial iron transport systems, a fact that questions the likelihood of finding new antibiotics against them. Nevertheless, the recent licensing of cefiderocol,<sup>189-191</sup> that utilizes a TonB-dependent LGP to introduce a bacteriocidal antibiotic into the bacterial periplasm, illustrates the clinical potential of such pathways. Finally, it is perhaps most pertinent that the innate immune system encodes numerous proteins that reduce iron availability to invading microbes, underscoring the potential of seeking chemical or immunological interventions that similarly interfere with prokaryotic iron uptake.

### 3. OVERVIEW OF TONB-DEPENDENT IRON TRANSPORT SYSTEMS

Gram (–) bacterial LGP are surface receptors that recognize and bind metal complexes. Then, activated by TonB, they internalize the ferric siderophore or porphyrin through the OM bilayer. Virtually all Gram (–) bacterial pathogens obtain iron with TonB-dependent systems, which explains the interest in blocking TonB action, but the incomplete information about LGP transport mechanisms<sup>74,90,192,193</sup> complicates the use of iron deprivation against pathogenesis. Furthermore, complex multiprotein arrays (in *E. coli*, 13 cell envelope proteins) collaborate in the uptake of each iron atom. Their functions include high affinity ligand recognition, transmembrane signal transduction, internal conformational motion, catalytic protein–protein interactions driven by energy transmission between membranes,

and active transport in two distinct membranes energized by both the electrochemical gradient and ATP hydrolysis. Most notably, active iron OM transport occurs through a closed membrane channel, across a bilayer that is unable to sustain an ion gradient, necessitating a novel means of energization. Hence, besides its clinical potential, the topic has theoretical importance.

LGP are omnipresent in Gram (–) bacterial cell envelopes to varying degrees of representation. Members of Enterobacterales encode many (7–20) that act in iron or other metal uptake, but Proteobacteria in other Families may contain many more (Pseudomonadaceae, 35–38; Caulobacteriaceae, 63; Xanthomonadaceae, 42–70<sup>69</sup>) that are predicted to span other substrate specificities. Most of these functions were assigned by bioinformatic analyses and are not yet experimentally verified. In the case of *Caulobacter crescentus*, five iron-regulated Omps were identified, but only one transport function was identified as the receptor for hemin.<sup>194</sup> The most mechanistically well characterized LGP catalyze iron<sup>195–199</sup> or cobalt<sup>195–199</sup> uptake, but many other transport specificities are proposed in the LGP superfamily.<sup>200</sup> LGP often also act as receptors for bacteriocins and phage. *E. coli* FepA (EcoFepA) (we abbreviate bacterial proteins to also designate the genus and species of their origin: e.g., *Klebsiella pneumoniae* FepA, KpnFepA; *A. baumannii* BauA, AbaBauA; *Pseudomonas aeruginosa* FpvA, PaeFpvA, etc.), for example, is the cognate receptor for the TonB-dependent colicins B and D<sup>64,201,202</sup> and bacteriophage H8.<sup>203</sup> The architecture of EcoFepA<sup>196</sup> typifies the tertiary structure of all LGP: a 150-residue N-terminal globular domain situated within a 22-stranded C-terminal porin  $\beta$ -barrel (Figure 1). The eight LGP of *E. coli* K-12 acquire different types of metal complexes: ferric catecholates (FepA,<sup>196</sup> Fiu,<sup>204</sup> Cir<sup>195</sup>), ferric hydroxamates (FhuA,<sup>198,199</sup> FhuE,<sup>205</sup> IutA<sup>206</sup>), ferric citrate (FecA<sup>197</sup>), and cyanocobalamin (vitamin B<sub>12</sub>; BtuB<sup>207</sup>). FptA<sup>208</sup> and FpvA<sup>209</sup> of *P. aeruginosa*, which show the same overall fold, transport iron complexes of pyochelin<sup>210,211</sup> (Pch) and pyoverdine<sup>212,213</sup> (Pvd), respectively. The discriminating specificity of these receptors for their ligands,<sup>61,202,214</sup> whose binding potentiates the active transport mechanism, is what led to the designation LGP.<sup>61,202,214</sup> They are unlike diffusive porins,<sup>27</sup> in that they bind ligands with high affinity and require energy and TonB action to accomplish ligand internalization. The common designation TBDT<sup>69</sup> is intuitively accurate but potentially confuses these OM uptake systems with completely different active transporters in the IM. Both classes of membrane proteins perform active transport, but they are structurally different, function by different mechanisms, utilize different energy sources, and inhabit different membranes. Hence, we reserve the term “transporter” for ATP-binding cassette (ABC) transporters and electrochemical gradient-coupled (e.g., PMF-dependent) major facilitator transporters in the bacterial IM.

### 3.1. OM Iron Transport: LGP Crystal Structures

In 1990, Weiss *et al.*<sup>215</sup> determined the first detailed crystal structure of a porin from *Rhodobacter capsulatus*. It was followed by the crystal structure of *E. coli* OmpF (EcoOmpF).<sup>216</sup> Buchanan *et al.*<sup>196</sup> submitted a description of the crystal structure of EcoFepA in September of 1998, a few weeks before that of EcoFhuA.<sup>198,199</sup> Since then, 18 more LGP structures were resolved (Table 1). The transmembrane  $\beta$ -barrels of these OM proteins are central to the understanding LGP functionality, because they classify them

in the porin superfamily.<sup>27,200</sup> The 22-stranded  $\beta$ -sheets surround a structurally distinct, N-terminal, ~150 amino acid globule that regulates the movement of molecules through the pore.

**3.1.1. N-Terminal Globular Domain (N-Domain).**—The N-terminal portion of LGP contain structural features that enable its biochemical functions. A four-stranded  $\beta$ -sheet obstructs LGP channels. The N-terminal region contains the “TonB-box”,<sup>217,218</sup> a short sequence (7–11 residues) that mediates signal transduction to TonB. When ferrichrome (Fc) binds to FhuA, or B<sub>12</sub> binds to BtuB, their loops undergo changes that propagate through the N-domain, altering the disposition of the TonB-box at the periplasmic interface.<sup>197,207</sup> The exact sequence and molecular mechanics of these conformational changes are unknown, but they occur in response to high affinity binding of a metal complex to the surface loops of the LGP that coalesce around its ligand by induced fit.<sup>197,219,220</sup> Two large loops sit atop the N-domain globule, and as many as 11 more surface loops ranging from 2 to 40 residues bridge adjacent  $\beta$ -strands in the C-domain  $\beta$ -barrel. Loop motion during ligand binding is the basis for concomitant or ensuing movement of the TonB-box at the internal surface of the receptor, creating a trans-OM signaling pathway that activates the actions of TonB in the periplasm.

**3.1.2. C-Terminal Transmembrane  $\beta$ -Barrel (C-Domain).**—Like other OM proteins (Omp),<sup>215,216,221-223</sup> LGP contain an antiparallel, amphiphilic  $\beta$ -sheet that circumscribes an aqueous channel. The  $\beta$ -strands in the sheet are linked on the periplasmic side by short reverse turns, and on the outer surface by usually expansive loops that are populated with residues involved in ligand recognition and high-affinity binding. The diameter of the 22-stranded C-terminal  $\beta$ -barrel approximates 50 Å, a size that potentially compromises the permeability barrier of the OM bilayer.<sup>28</sup> However, the N-domain restricts passage of molecules through this large hydrophilic pore to ligands that specifically bind and activate the energy- and TonB-dependent uptake mechanism.<sup>68</sup>

### 3.2. TonB/ExbBD Physiology

Genetic studies on iron uptake by *E. coli*, as well as its susceptibility to bacteriophage or colicins,<sup>64,202,224-227</sup> identified the *tonB* locus as a crucial component of the transport system. *tonB* mutants were unable to thrive in iron-deficient media and showed pleiotropic transport deficiencies. *exbBD* strains were similarly implicated,<sup>217,228</sup> but the impact of *exbBD*-deficiency was less dramatic, likely because they may be substituted by TolQR.<sup>229,230</sup> Subsequent research revealed that TonB, ExbB, and ExbD form a multimeric protein complex in the IM,<sup>231</sup> with TonB presumably at the center of this assembly.<sup>232,233</sup> Genetic, biochemical, bioinformatic, and biophysical data<sup>65,233-238</sup> show that TonB is an IM-anchored protein that spans the periplasm (Figure 1). When an LGP binds a metal complex, the TonB-box of its N-domain repositions at the periplasmic interface,<sup>198,199</sup> allowing protein–protein interactions with the TonB C-terminal domain (TonB CTD).<sup>239,240</sup> Binding of the TonB-box of LGP to the TonB C-terminal domain (CTD)<sup>239,240</sup> facilitates the movement of iron through the LGP channel. Models postulate<sup>238,241,242</sup> and evidence exists<sup>237</sup> that TonB transmits energy from the IM to the OM by rotary motion, driven by the electrochemical gradient across the IM [for review see ref 91]. ExbB and ExbD<sup>231</sup>



participate in this reaction. TonB-dependent, PMF-driven activity of LGP<sup>62,227,243,244</sup> allows their accumulation of iron against its concentration gradient. Thus, Gram (–) bacterial pathogens obtain iron from human and animal hosts by TonB-dependent uptake systems that are virulence determinants.<sup>4,7,62,121,227,243,244</sup> The ubiquity of TonB in Gram (–) bacterial metal transport makes it a potential target for drug discovery.

### 3.3. Periplasmic and IM Iron Transport

After traversing the OM through LGP, iron complexes adsorb to periplasmic binding proteins<sup>245,246</sup> (like EcoFepB,<sup>247,248</sup> Figure 2) and then to IM ABC-transporters<sup>249-251</sup> that intake iron into the cytoplasm. For the prototypic FeEnt acquisition system, FepB<sup>247,252,253</sup> (Figures 1 and 2) transfers FeEnt to the IM ABC-transporter complex FepCDG<sup>254</sup> (Figure 1). During or after entry into the cytoplasm, Fes hydrolyzes the lactone scaffold of FeEnt, concomitantly reducing and releasing ferric iron into intracellular pools as Fe<sup>2+</sup>.<sup>255-261</sup>

## 4. SIDEROPHORES

After the isolation of ferrichrome from the smut fungus *Ustilago sphaerogena*,<sup>56</sup> and mycobactin from the acid-fast bacterium *Mycobacterium johnei*,<sup>262</sup> more than 500 other siderophores were discovered. We will not review the basic chemistry of siderophores because numerous other descriptions<sup>57,59,60,263</sup> already exist. Suffice it to say that based on their complexation of Fe<sup>3+</sup>, siderophores fall into three main groups: catecholate, hydroxamate, and mixed chemistry chelators (Figure 2). Compounds in the latter category contain a variety of chemical groups that may share electrons with the iron nucleus: carboxylates, imidazoles, oxazolines, quinones, thiazolidines, and more. Although siderophores in different categories have characteristic properties that affect their affinities for iron(III), the ferric ion favors complexation by oxygen, rather than nitrogen or sulfur, and siderophores reflect this preference.

### 4.1. Complexation of Fe<sup>3+</sup> by Siderophores

Many siderophores are virulence factors of the bacteria that produce them.<sup>264</sup> They capture Fe<sup>3+</sup> in the host environment because they generally possess higher affinity for iron than host proteins.<sup>264,265</sup> Besides the prototypic tricatecholate compound Ent that many Gram (–) bacteria in the Family Enterobacterales produce, and the prototypic trihydroxamate ferrichromes (Fc) that many fungi produce, other siderophores of interest are the monocatecholates dihydroxybenzoic acid (DHBA) and dihydroxybenzoyl serine (DHBS), citrate (Cit), the citrate-based hydroxamate aerobactin (Abn), and the mixed chemistry chelates acinetobactins (Acn), baumannoferrins (Bfn), fimsbactins (Fbn), yersiniabactin (Ybt), pyochelin (Pch), and pyoverdine (Pvd). In nature, the monocatecholates are relevant degradation products of Ent, vibriobactin<sup>266</sup> (Vbn), and corynebactin<sup>267</sup> (Crn; also called bacillibactin<sup>657</sup>) that are all cyclic trimers of 2,3-DHBS. The individual units are joined by ester linkages between the alpha carboxyls and side chain hydroxyl groups of Ser (Figure 3). Additionally, Ent may be derivatized by the addition of glucose to two of its three catechol groups to create glucosylated Ent (GEnt). Both Ent and GEnt are potentially labile compounds because their cyclic lactone backbone is susceptible to acid or base hydrolysis, and their catecholate groups may oxidize to quinones. These chemical processes

produce a series of natural hexadentate, tetradentate, and bidentate catecholate compounds in the prokaryotic microenvironment, each with different metal complexation activities and affinities. Several attributes of trimeric, hexadentate Ent/GEnt contribute to their immense affinity for  $\text{Fe}^{3+}$ , that is, 30 logs higher than that of a bidentate ligand like DHBA or DHBS. First, the architecture of Ent/GEnt locates their catecholate hydroxyls in perfectly symmetrical geometry around the metal center, without strain.<sup>263,268</sup> Second,  $\text{Fe}^{3+}$  prefers a hard acidic ligand, like oxygen, rather than soft basic ligands like nitrogen or sulfur. Lastly, and most importantly, trimeric Ent/GEnt exemplify the chelate effect: metal complexes of polydentate ligands (in this case, hexadentate) are much more stable than complexes of chemically similar mono- or bidentate ligands. Complexation by three isolated bidentate ligands (*i.e.*, DHBA/DHBS) requires three individual productive collisions between the metal and the ligands, whereas chelation by a single hexadentate ligand (*i.e.*, Ent/GEnt) occurs by an initial collision that attaches the first oxygen, followed by binding of the second oxygen by rotation, and the remaining oxygens by motion of the aposiderophore that enables them to surround the iron center. A hexadentate chelate also better resists dissociation. When a mono- or bidentate group is displaced, it is lost into the bulk solution. But, if any of the oxygens of the hexadentate Ent/GEnt are displaced, other oxygens still remain attached, and it is only a matter of time until the displaced oxygen(s) find(s) the metal again and reattach. All of these conditions stabilize the complex with hexadentate Ent/GEnt, relative to an iron chelate formed by bidentate monocatecholate groups.

#### 4.2. Siderophore Biosynthesis in Bacterial Pathogenesis

An average man contains about 5 g of iron, creating an overall concentration of ~3 mM. Most of that iron was acquired in the oxidized ferric [ $\text{Fe}^{3+}$  or Fe(III)] form and then reduced to the ferrous [ $\text{Fe}^{2+}$  or Fe(II)] state within cells. Human proteins complex both ferrous and ferric iron, for use as a biochemical or redox cofactor, as part of intracellular iron homeostasis, and as a means of blocking microbial iron acquisition. As an initial response to bacterial infection mammalian hosts increase the production of LF and TF, two iron binding proteins of the innate immune system. This upregulation minimizes the concentration of adventitious extracellular iron,<sup>269</sup> confronting invading bacteria with an iron-depleted environment.<sup>270</sup> Iron sequestration renders bacteria iron-deficient, which retards their metabolism and propagation.<sup>271,272</sup> Within cells, proteins or small molecules complex iron for metabolic purposes, but also because free iron promotes the formation of reactive oxygen species by the Fenton reaction.<sup>264,273</sup> Faced by iron unavailability, bacteria upregulate their iron acquisition systems, many of which are implicated in bacterial pathogenesis.<sup>5,35,49,274</sup> They usually comprise two components: (i) siderophores, that chelate iron(III) with high affinity, and (ii) OM LGP, that avidly bind ferric siderophore complexes and actively transport them into bacterial cells. Microbial siderophores surmount the low solubility of free  $\text{Fe}^{3+}$  in aqueous solutions ( $10^{-18} \text{ M}$ )<sup>4</sup> and antagonize innate immune proteins that adsorb free iron in blood, serum, and cellular secretions. They capture the extra- and intracellular iron of humans and animals for utilization by invading bacteria that may also directly extract and transport<sup>35,275,276</sup> iron from eukaryotic iron-binding proteins. Ent, the native catecholate siderophore of the family Enterobacterales, has the highest affinity for  $\text{Fe}^{3+}$  ( $K_a = 10^{52} \text{ M}^{-1}$ ),<sup>58</sup> which allows it to remove iron from proteins<sup>277,278</sup> that have lower affinity (*e.g.*, transferrin;  $K_a = 10^{20} \text{ M}^{-1}$ ).<sup>279</sup> Other microbial siderophores also remove iron

from TF, LF, or FTN.<sup>211,212</sup> It is often stated that the host environment is iron deficient, but the siderophores of pathogens invade and scavenge iron from eukaryotic metabolic and storage pools, effectively raising the concentration of available iron from submicromolar to much higher, potentially millimolar levels. In this way, siderophores confer an advantage to bacteria during infection of host tissues,<sup>124,134,264,280-282</sup> so it is not surprising that heightened production of one or more siderophores is a virulence factor<sup>283,284</sup> in Gram (-) bacterial pathogenesis. Siderophore production by invading pathogens overcomes host-imposed iron restriction,

### 4.3. Utilization of Xenosiderophores

Ent and FepA, the receptor for FeEnt, are prototypic components of Gram (-) bacterial TonB-dependent iron uptake systems. FeEnt is recognized and transported by both commensal and pathogenic Gram (-) species in the same and other Families.<sup>120</sup> This natural ferric catecholate uptake system illustrates a common attribute of microbial habitats: utilization of xenosiderophores. The term refers to siderophores that are recognized and acquired by a different organism than the one that produced them. So, although *A. baumannii*, *Yersinia enterocolitica*, *Neisseria gonorrhoeae*, and *P. aeruginosa* lack the ability to synthesize Ent, all four species encode transport systems to assimilate FeEnt.<sup>120,272,285</sup> This ability to utilize gratuitous ferric siderophores is an asset during colonization and pathogenesis.<sup>286</sup> The gut, for example, is populated by thousands of different bacterial species<sup>287-289</sup> that may simultaneously produce dozens or hundreds of different siderophores,<sup>60</sup> so access to this conglomeration of iron chelates is potentially valuable to microbes that do not elaborate their own siderophores (*e.g.*, *Listeria monocytogenes*<sup>290</sup>). In response, host epithelial cells and neutrophils produce SCN<sup>55</sup> that preferentially binds apo- and ferric catecholates (Figure 2). SCN binds FeEnt with about 10-fold less affinity than EcoFepA and about the same affinity as other orthologues of EcoFepA (Table 1), so depending on its concentration, SCN has the ability to compete for ferric catecholates and thereby inhibit bacterial growth.<sup>264,291</sup> Nevertheless, members of Enterobacterales adapted to evade SCN by glucosylating two of the three the catecholate rings of Ent. SCN binds the glucosylated form of the siderophore (GEnt/FeGEnt; also called ferric salmochelin) with much lower affinity.<sup>291</sup> Species of *Klebsiella*, *Salmonella*,<sup>292</sup> *Escherichia*,<sup>293,294</sup> and *Enterobacter*<sup>295</sup> encode the *iroA* gene cluster to glucosylate Ent.<sup>44</sup> The *iroA* system contains the biosynthetic *iroBCDE* genes: IroB glucosylates Ent to form GEnt; IroC mediates GEnt export out of the cell; IroE cleaves the trilactone backbone of GEnt to a linear form that may traverse the IM, while IroD cleaves the linearized aposiderophore to generate a monomer and dimer.<sup>296-299</sup> The *iroA* region also encodes IroN, the cognate receptor for FeGEnt. The ability of numerous pathogenic bacterial genera to glucosylate Ent and transport FeGEnt, even in the presence of SCN, allows proliferation in places that are inhospitable to other Gram (-) bacteria. Surprisingly, because it produces a number of SCN-resistant siderophores,<sup>300</sup> including GEnt, the *E. coli* Nissle 1917 strain<sup>301</sup> is employed as a probiotic treatment.<sup>302-304</sup> It is thought to protect from diarrheal infections (for example, by *S. enterica*) by outcompeting the other pathogens for iron.<sup>305,306,264</sup> These observations, combined with widespread Ent biosynthesis and FeEnt transport by Gram-negative bacteria, highlight the importance of catecholate siderophores in bacterial colonization and/or pathogenesis.<sup>164</sup>

#### 4.4. Exchange of Iron among Siderophore Ligands

The myriad of chemically distinct siderophores<sup>264</sup> warrants the question: why are so many different molecules needed to scavenge iron in the microenvironment? Especially given their prodigious affinity for  $\text{Fe}^{3+}$ , why do not the catecholate siderophores monopolize bacterial iron uptake processes to the exclusion of other less avid microbial chelators? A clue to the answer may reside in the fact that the multitude of siderophores translates into another multitude of unique ferric siderophore receptors in the OM. The variety of ferric siderophore structures requires a variety of LGP recognition specificities that allows individual organisms to preferentially bind and transport particular iron complexes. As explained below, this selectivity for certain ferric siderophores has advantages to proliferation in certain environments. Second, in considering how siderophores of lower affinity compete against Ent and its derivatives for complexation of iron, it is important to note that iron chelation reactions are equilibria: in a solution of multiple aposiderophores, the distribution of iron among them reflects the affinities of the different organic ligands, their concentrations, and the pH because exchange of ferric iron between organic ligands occurs more rapidly at acidic pH. For example, Ent ( $K_A = 10^{52} \text{ M}^{-1}$ ), acquires iron from FcA ( $K_A = 10^{34} \text{ M}^{-1}$ ),<sup>59</sup> but even at millimolar concentrations of both compounds this exchange reaction takes hours to occur ( $t_{1/2} = 4.5 \text{ h}$  at neutrality<sup>307</sup>). In native, even iron-deficient habitats, the concentrations of microbial aposiderophores usually do not exceed micromolar levels, so the rates of ligand exchange around  $\text{Fe}^{3+}$  will be slower. The upshot is that ferric siderophore complexes are relatively kinetically stable regardless of their chelation chemistry. Once formed, a lower affinity iron complex like FeAbn has a sufficient lifespan to provide iron to cells expressing its surface receptor, IutA,<sup>308</sup> even in the presence of Ent or other potent catecholate siderophores. Furthermore, living bacterial cells act as a thermodynamic sink, driving iron–siderophore chelation equilibria toward the ferric complexes that they bind and transport.

#### 4.5. Redundant Iron Acquisition Systems

The advantage of redundancy during iron acquisition becomes apparent when considering *K. pneumoniae*.<sup>309</sup> Hypervirulent *K. pneumoniae*, that causes pyogenic liver abscesses<sup>310,311</sup> (predominantly in Asia<sup>312-315</sup>), elaborates copious amounts of multiple siderophores ( $30 \mu\text{g/mL}$ )<sup>283,316</sup> that are virulence determinants. In this sense, hypervirulent *K. pneumoniae* differs from classical *K. pneumoniae*. Hypervirulent *K. pneumoniae* strains harbor plasmids that encode synthesis of Ent and GEnt, as well as uptake systems for their ferric complexes.<sup>317</sup> Humans and animals respond with serum SCN, that tightly binds Ent and FeEnt, reducing their ability to supply iron to invading bacteria. Serum albumin also adsorbs Ent, albeit with lower affinity.<sup>318</sup> However, glycosylation of Ent by hypervirulent *K. pneumoniae* and other pathogens impedes its recognition by SCN.<sup>55,291,319</sup> Besides catecholates, hypervirulent *K. pneumoniae* secrete the hydroxamate Abn and the mixed chelator Ybt.<sup>320</sup> Deletion of the Abn biosynthetic locus *iucA* reduced the virulence of hypervirulent *K. pneumoniae*; loss of other siderophores did not affect its pathogenesis in a murine infection model.<sup>283</sup> The citrate-based siderophore Abn is well-known to confer bacterial invasiveness,<sup>155,321,322</sup> and its production is a virulence determinant of hypervirulent *K. pneumoniae*.<sup>323</sup> Like GEnt and FeGEnt, neither Abn nor FeAbn bind to SCN or albumin. Thus, despite its much lower affinity for  $\text{Fe}^{3+}$  ( $K_A = 10^{24} \text{ M}^{-1}$ ),<sup>59</sup>

unlike Ent, Abn remains active and available in host fluids and tissues, where it may remove iron from TF and LF ( $K_a = 10^{20} \text{ M}^{-1}$ ).<sup>277</sup> Biosynthesis of all four siderophores, Ent, GEnt, Abn, and Ybt, is common in hypervirulent *K. pneumoniae*. However, studies on the relationships of these four siderophores to the pathogenesis of *K. pneumoniae*<sup>284</sup> reiterated the influence of Abn, that consistently associated with virulence.<sup>284,309,324,325</sup> For instance, the majority of *K. pneumoniae* isolated from pyogenic liver abscesses produced Abn, while only 2% isolated from other sites (respiratory tract, urine, blood, or stool) secreted it.<sup>326</sup> The other siderophores are less involved in the virulence of hypervirulent *K. pneumoniae*. As noted, *K. pneumoniae* glucosylates Ent and produces Ybt, but neither GEnt nor Ybt correlate with its systemic infections. One potential explanation for the persistent presence of GEnt in hypervirulent *K. pneumoniae* is that it may act in concert with the toxin microcin E492 during colonization.<sup>323</sup> In classical *K. pneumoniae*, on the other hand, GEnt production does correlate with invasive colonization of specific lung tissues.<sup>280</sup> Additionally, in extraintestinal pathogenic *E. coli* (ExPEC), the expression of IronN, the cognate receptor for FeGEnt, promotes biofilm formation.<sup>327</sup> Thus overall, the apparent redundancy in the siderophores of bacterial iron acquisition systems is a misconception. They all complex  $\text{Fe}^{3+}$ , but each one has chemical nuances that define their chelation properties, their ability to extract iron from eukaryotic proteins, and their interaction with or persistence in animal fluids or tissues. Together, these properties may produce unique, unexpected contributions to bacterial pathogenesis.

#### 4.6. Siderophores and Tissue Tropism

The production of Ybt by *K. pneumoniae* illustrates other aspects of microbial iron acquisition during pathogenesis. Although named for its discovery in *Yersinia pestis*,<sup>328,329</sup> several other infectious bacteria produce Ybt,<sup>330,331</sup> that is, an atypical siderophore with mixed chelation groups. The genes encoding Ybt reside in the pigmentation (*pgm*) locus of the high pathogenicity island (HPI) of *Y. pestis*, *Yersinia pseudotuberculosis*, and *Yersinia enterocolitica*. The HPI also occurs throughout Enterobacterales in *Citrobacter*, *Enterobacter*, *Klebsiella*, *Salmonella*, *Serratia*, and all known pathotypes of *Escherichia*.<sup>332</sup> Murine infection studies with *Y. pestis* revealed that the siderophore facilitates establishment of the pathogen at peripheral sites.<sup>330</sup> While Ybt is essential for bubonic plague, it is dispensable and has varying degrees of involvement for septicemic and pneumonic plague.<sup>332-334</sup> With regard to *K. pneumoniae*, classical strains that produce Ybt cause pneumonia in the murine infection model, whereas Ybt nonproducers that only produce Ent are at best opportunistic and only establish an infection in SCN-deficient mice. Despite the fact that classical *K. pneumoniae* causes septicemia, wound, and urinary tract infections (UTI), Ybt<sup>+</sup> *K. pneumoniae* strains are predominantly found in the respiratory tract over blood, urine, or stool samples.<sup>326</sup> Hypervirulent *K. pneumoniae* abundantly produces Ybt, but it was not found to enhance its pathogenesis, perhaps because copious Abn production masked the impact of Ybt.<sup>323</sup> For uropathogenic *E. coli*, the noncatecholate siderophores Abn and Ybt were advantageous to colonization, and their receptors IutA and FyuA, respectively, correlated with bacterial invasion of the bladder and kidney.<sup>335</sup> Vaccination of mice with FyuA, furthermore, protected the animals against ascending UTI to the bladder and kidney.<sup>336,337</sup> Next, the mixed chelation chemistry of Ybt, that includes three electron pairs from nitrogen and three pairs from oxygen, imparts multifunctionality: besides  $\text{Fe}^{3+}$ , Ybt

may bind  $\text{Cu}^{2+}$ , which protects *Y. pestis* against reactive oxygen by mimicking a superoxide dismutase that converts oxygen to less harmful forms.<sup>338</sup> In uropathogenic *E. coli*, this property confers a higher intracellular survival rate than that observed for nonpathogenic strains. Lastly, Ybt production illustrates that a particular siderophore may influence the site of an infection and allow the siderophore-producer to capture a replicative niche within the host.<sup>264</sup> Whereas Ybt<sup>+</sup> classical *K. pneumoniae* strains caused bronchopneumonia in normal mice, resulting in moderate bacterial load in the lungs and spleen, otherwise isogenic Ent<sup>+</sup> *K. pneumoniae* caused inflammation and bacterial density in the airways.<sup>280,283,284,326</sup> In SCN-deficient mice, on the contrary, introduction of Ent<sup>+</sup> or Ent<sup>+</sup>, GEnt<sup>+</sup> classical *K. pneumoniae* strains caused perivascular invasion, higher bacterial load, greater involvement of the spleen, and lower survival. These differences likely arise because of the better ability of Ent, relative to Ybt, to strip iron from transferrin, which is rich in the perivascular space. Consequently, in the absence of SCN, that neutralizes Ent but not Ybt, Ent-producers outcompete Ybt-producers for the available iron.<sup>280,326</sup> These data also show the antagonism of bacterial dissemination by SCN. In summary, ferric siderophore uptake systems have multiple attributes that contribute to the infection of humans and animals. When viewed from the perspective of the diversity of their chemistry and iron chelation properties, their individual characteristics allow bacteria to adapt to the different conditions and iron sources in specific tissues.

#### 4.7. Utilization of Hn

Erythrocyte hemoglobin constitutes the biggest source of iron in the mammalian body. Bacteria acquire iron from hemoglobin by hemolysis or cell death that releases Hn into the plasma. Alternatively, Hn may adsorb to cell surfaces, such as the intestinal lumen. Hn utilization is a factor in the virulence and pathogenesis of *A. baumannii*, *E. coli*, *Haemophilus influenzae*, *Neisseriameningitidis*, *P. aeruginosa*, *Shigella dysenteriae*, *Vibrio cholerae* and *Y. pestis*, that all utilize iron from hemoglobin.<sup>339-345</sup> The iron in Hn is usually in the ferrous state, but once removed from the porphyrin by Hn oxidases, and especially in the presence of siderophores, the equilibrium shifts toward ferric iron, that is readily complexed by both siderophores and TF.<sup>346</sup> *A. baumannii* LAC-4, *P. aeruginosa*, and *N. meningitidis* oxidize Hn to biliverdin,<sup>347</sup> concomitantly converting  $\text{Fe}^{2+}$  to  $\text{Fe}^{3+}$ , which is accessible to siderophores for iron supply to the pathogens.

## 5. FERRIC SIDEROPHORE TRANSPORT BY LGP OF BACTERIAL PATHOGENS

Infectious Gram (–) bacteria evolved a variety of molecular strategies to initiate the iron uptake process, that involve many different ferric siderophore or Hn receptors on the cell surface. However, all these specific systems of diverse Gram (–) bacteria share an underlying mechanistic component: the TonB/ExbBD complex that converts PMF-driven bioenergetics in the IM into biochemical processes that drive active transport through the OM (see also sections 3.2 and 8.1). The Gram (–) CRE/ESKAPE bacteria encompass various examples and paradigms with regard to iron acquisition during pathogenesis. These include *K. pneumoniae*, *A. baumannii*, *P. aeruginosa*, and *E. coli*, as well as other Gram (–) pathogens (*S. enterica*, *Y. pestis*, *Serratia marscescens*) that collectively provide

unambiguous evidence of the close relationship between iron acquisition and bacterial virulence.

Just a glance through the activities of the iron-transporting LGP (Table 1) emphasizes the significance of generic and specialized iron uptake mechanisms to bacterial pathogenesis. Starting with pathogenic variants of *E. coli* (UPEC and EHEC), and in pathogens of other genera, uptake of FeAbn, FeGEnt, and Hn consistently associates with invasiveness, tissue tropism, or infectivity. Hn scavengers (*P. aeruginosa*, *Y. pestis*), furthermore, produce both hemophore-dependent and -independent transport systems to obtain it. Utilization of other ferric siderophores is often highly specialized: besides *Y. pestis*, the CRE pathogens *E. coli* and *K. pneumoniae* both acquire FeYbt via FyuA, whereas *P. aeruginosa* does not encode such a receptor in its genome. *A. baumannii* is a general exception to these commonalities, in that most strains transport neither FeAbn nor Hn. However, analyses of genomic sequences suggest that *A. baumannii* encodes several unique iron uptake systems. *A. baumannii* produces three unique siderophores (Acn, Bfn, Fbn), it utilizes FeEnt,<sup>272</sup> and its chromosome encodes at least six other LGP of currently unknown functions. Exclusively genomic inferences are sometimes incorrect,<sup>194,348</sup> so the full understanding of the iron transport capabilities of *A. baumannii* await experimental characterization. After TonB-dependent OM uptake, iron translocation into the cytoplasm involves multiple binding and transport reactions in the periplasm and the IM. Consequently, the identification of a homologous LGP orthologue in the OM does not necessarily guarantee the ability of *A. baumannii* to use a particular ferric siderophore as an iron source.

### 5.1. *E. coli*

Most *E. coli* strains are harmless to animals and humans and live in the gut as commensal microbes. Strains like the probiotic Nissle 1917 are beneficial to human physiology, alleviating symptoms of colitis and inflammatory bowel disease.<sup>349</sup> However, *E. coli* also acquires pathogenesis determinants, including siderophore biosynthetic genes, toxins, or other molecules that promote tissue invasion or tropism. Pathogenic *E. coli* fall into numerous categories: ETEC (entero-toxicogenic), EIEC (entero-invasive), EHEC (enterohemorrhagic (including the widespread O157:H7), EPEC (entero-pathogenic), EAEC (entero-aggregative), and AIEC [adherent-invasive, which includes uropathogenic *E. coli* (UPEC), that causes ~90% of urinary tract infections (UTI)]. These pathogenic isolates often rely on iron acquisition mechanisms that are not found in laboratory strains. For instance, the EHEC pathogen O157:H7 acquires iron from Hn or hemoglobin through the outer membrane receptor ChuA.<sup>118</sup>

Tang and Saier<sup>167</sup> compared the laboratory *E. coli* strain MG1655<sup>350</sup> to serovars in five of the pathogenic categories. Not only are certain LGP exclusively found in the pathogens, but some strains have multiple receptors for a single ferric siderophore or Hn. MG1655 expresses six receptors for iron uptake, whereas UPEC strains produce 10–15, again illustrating the direct connection between iron uptake versatility and virulence. It is noteworthy that 4 of 7 pathogenic strains had two chromosomal *tonB* homologues,<sup>167</sup> although their functional differences are not known.

Prototypic laboratory *E. coli* K-12 strains, like the sequenced paradigm MG1655, do not chromosomally encode the FeAbn receptor IutA, but it is present in the genome of pathogenic *E. coli*, like the AIEC strain O83:H7.<sup>351</sup> As first discovered for EcoIutA,<sup>155</sup> LGP are often encoded and mobilized on plasmids that transfer among bacteria in natural habitats. IutA (NRG857\_30235) and IroN (NRG857\_30015) are encoded on the *E. coli* plasmids pAPECO103-ColBM, pAPEC-O1-ColBM, and pVM01 (from the APEC strain E3), on the *S. enterica* serovar Kentucky plasmid pCVM29188\_146, and on the *K. pneumoniae* CG43 plasmid pVLK. The chromosome of *K. pneumoniae* CG43 also contains another FepA paralogue (NRG857\_02640). Furthermore, in ExPEC the FeGent receptor, IroN, contributes to biofilm formation, independently of Gent production.<sup>327</sup> *E. coli* O157:H7 encodes several novel LGP (Table 1), including ChuA, that recognizes and transports Hn.

## 5.2. *K. pneumoniae*

Classical *K. pneumoniae* is a nonmotile Gram (–) bacillus in the Family Enterobacterales. Most *K. pneumoniae* isolates are encapsulated, nontransformable, nontransducible, and probably virulent. However, mutations in LPS and capsule biosynthesis,<sup>352-356</sup> DNA methylation,<sup>357</sup> and iron acquisition<sup>358</sup> may attenuate *K. pneumoniae*. Besides its ubiquity in surface water and soil, it is a commensal bacterium in the gastrointestinal tract and a common opportunistic nosocomial pathogen. It may infiltrate the urinary tract, bloodstream, or lungs, and it may contaminate surgeries, resulting in wound and urinary tract infections, pneumonia, bacteremia, and sepsis. Infections with classical *K. pneumoniae* may progress to pyogenic liver abscesses, meningitis, endophthalmitis, and sepsis. Such “community-acquired infections” are public health threats, and the increasing propensity of this organism to acquire antibiotic resistance augments its threat to human and animal health. Especially, carbapenem-resistant strains of classical *K. pneumoniae*, that are resistant to nearly all known antibiotics,<sup>359</sup> cause 40–50% mortality from bloodstream infections.<sup>360</sup> Classical *K. pneumoniae* strains that express extended spectrum  $\beta$ -lactamases (ESBLs) are resistant to cephalosporins and monobactams.<sup>253,265</sup> Besides the classical *K. pneumoniae* pathotype, a hypervirulent variant emerged that causes hepatic abscesses, endophthalmitis, meningitis, osteomyelitis, and necrotizing fasciitis, even in otherwise healthy individuals.<sup>361-366</sup> Acquired drug resistance makes classical *K. pneumoniae* difficult to eliminate but does not enhance its virulence. Hypervirulent *K. pneumoniae*, on the other hand, may acquire both antibiotic resistance genes and novel virulence genes together on a large plasmid<sup>309</sup> and, in some cases, additional chromosomal elements as well. The biomarkers on the virulence plasmid differentiate hypervirulent from classical *K. pneumoniae*. Hypervirulent *K. pneumoniae* has the ability to infect healthy individuals and frequently causes invasive infections that further distinguish it from classical *K. pneumoniae*. Thus, clinical isolates of this superbug show a worrisome confluence of drug resistance and virulence determinants that threaten a medical crisis, including hypermucoviscous capsule, lipopolysaccharide (LPS), siderophores, and fimbriae.<sup>324,367</sup> Other factors also play a role in the virulence of *K. pneumoniae*: the OM permeability properties of its porins, IM efflux pumps, and systems involved in allantoin metabolism. In many cases, the contributions of these factors to pathogenesis are not yet fully understood.<sup>367</sup>



### 5.2.1. Overview of TonB-Dependent Iron Uptake by *K. pneumoniae*.—

Relative to wild-type strains, TonB-deficient *K. pneumoniae* are attenuated in murine infection models.<sup>95</sup> *K. pneumoniae* chromosomally encodes biosynthesis of four different siderophores: Ent, GEnt, Abn, and Ybt. The production of multiple iron acquisition systems counteracts host neutralization of any individual one of them, and different siderophores may promote colonization of different tissues in the host,<sup>264,368</sup> in both cases increasing the survival of the pathogen. Among four siderophores secreted by classical *K. pneumoniae*, Ent has the highest affinity for Fe<sup>3+</sup> ( $K_A = 10^{52} \text{ M}^{-1}$ )<sup>58</sup> and Abn has the lowest ( $K_A = 10^{23} \text{ M}^{-1}$ ),<sup>59</sup> but this Ent/GEnt/Abn example illustrates, as discussed above (section 4.2), that avidity for iron is not always the factor that determines the contributions of a particular iron uptake process to virulence, invasiveness, or pathogenesis.<sup>369</sup> Ent production is ubiquitous among both classical and hypervirulent *K. pneumoniae* that utilize ferric catecholates in both the wild and host environments. As in *E. coli*, the genes encoding the Ent biosynthetic enzymes of *K. pneumoniae* reside in the chromosomal *entABCDEFG* gene cluster, while genes encoding FeEnt transport are in the chromosomal *fepABCDEG* gene cluster. Both Ent production and FepA expression are upregulated during infection by *K. pneumoniae*, which enhances colonization of the lungs.<sup>370,371</sup>

**5.2.2. GEnt.**—Production of SCN by neutrophils and on mucosal surfaces opposes the actions of Ent/FeEnt by competing with KpnFepA for binding of the apo- and ferric siderophore.<sup>326,367</sup> Consequently, SCN minimizes iron uptake, which retards growth of bacterial pathogens in host fluids and tissues.<sup>122,326,367,372</sup> Increased production of SCN also causes acute inflammatory effects, resulting in secretion of IL-8 that recruits neutrophils to the infection site.<sup>122</sup> Host production of SCN illustrates the active role of innate immunity in combating bacterial iron uptake, but like other bacterial pathogens, *K. pneumoniae* responds by glucosylating Ent. The chromosomal- or plasmid-encoded *iroA* gene cluster (*iroBCDEN*) contains the genes for enzymes involved in GEnt biosynthesis<sup>319</sup> as well as for the OM FeGEnt receptor, IroN.<sup>367</sup> *KpnIroN* is only 53.2% identical to EcoFepA, considerably less than normally seen between LGP orthologues (the identity between KpnFepA and EcoFepA is ~80%). This lower extent of identity still infers the same structural fold, and may rationalize the different ligand selectivities of the two proteins: *KpnIroN* recognizes both FeEnt and FeGEnt, but EcoFepA only binds FeEnt and not FeGEnt.<sup>285</sup> Because SCN does not adsorb GEnt/FeGEnt, neither does the glucosylated siderophore induce inflammation at the infection site. Thus, concomitant glucosylation of Ent and expression of IroN combine as a virulence determinant in both classical and hypervirulent *K. pneumoniae* that supersedes the host innate immune response. GEnt producers are more virulent than Ent producers in an SCN-sufficient host. For instance, GEnt expression enhances colonization of the nasopharynx by classical *K. pneumoniae*.<sup>122</sup> Although only 2–4% of the hospital-acquired classical *K. pneumoniae* strains carry the *iroA* gene cluster, more than 90% of hypervirulent strains isolated from pyogenic liver abscesses carry the genes and produce GEnt.<sup>122</sup>

**5.2.3. Ybt.**—SCN does not recognize the mixed chelation siderophore Ybt that was originally identified in a pathogenicity island of *Yersinia enterocolitica*.<sup>329,373</sup> 18% of classical *K. pneumoniae* and 90% of hypervirulent clinical isolates produce Ybt.<sup>122,367,372</sup>

Ybt has robust affinity for  $\text{Fe}^{3+}$  ( $K_A = 10^{36.6} \text{ M}^{-1}$ )<sup>374</sup> but significantly lower than Ent/GEnt. FyuA binds and transports FeYbt; it is also a receptor for pesticin.<sup>375,376</sup> The IM ABC-transporter YbtPQ conveys FeYbt into the cytoplasm.<sup>367</sup> Because SCN does not bind FeYbt,<sup>280,326</sup> *K. pneumoniae* strains that produce it create increased bacterial loads during lung infections. TF antagonizes Ybt in plasma, but as a result of its lower affinity for  $\text{Fe}^{3+}$ , at equivalent concentrations the equilibrium favors the ferric siderophore. *K. pneumoniae* strains that only produce Ybt are unable to infect immunocompetent individuals,<sup>326</sup> but elaboration of Ybt is a virulence determinant for classical *K. pneumoniae* strains in mouse infection models.<sup>122,367</sup>

**5.2.4. Abn.**—The citrate-based hydroxamate siderophore Abn was originally isolated from *Aerobacter aerogenes*.<sup>377</sup> It has the lowest affinity for iron<sup>59</sup> of the siderophores secreted by *K. pneumoniae*, but Abn rapidly removes iron from TF,<sup>277</sup> and unlike the catecholate chelators, neither SCN nor serum albumin remove it from circulation.<sup>318</sup> Hence, Abn-mediated iron acquisition is unexpectedly efficacious in the host. Furthermore, 90% of hypervirulent *K. pneumoniae* strains excrete Abn, compared to only 6% of classical strains,<sup>378,379</sup> directly linking Abn to bacterial pathogenesis. In *K. pneumoniae*, as in virulent *E. coli* strains that make Abn and transport FeAbn,<sup>49,380</sup> the biosynthetic *iucABCD* enzyme system utilizes L-lysine and citrate to produce the hydroxamate siderophore. The sequential activities include a hydroxylase (IucD), an acetyltransferase (IucB) and the Abn synthetase (IucA), that stereospecifically adds  $N^6$ -acetyl- $N^6$ -hydroxylysine to the primary carboxylate of citrate.<sup>381</sup> Transfer of a plasmid carrying the *IucABCD* genes of hypervirulent *K. pneumoniae* to laboratory *E. coli* led to production of Abn,<sup>324</sup> confirming this pathway. The structural gene of the FeAbn receptor, *iutA*,<sup>308,382</sup> usually resides on the same plasmid as the Abn biosynthetic loci. Furthermore, in hypervirulent *K. pneumoniae*, the *rmpA* gene, that increases capsule production, is on the same plasmid.<sup>264,367</sup> Consequently, Abn-mediated iron acquisition and hypermucoviscous capsule are often linked in hypervirulent strains. Elevated levels of both Abn production (6–10-fold) and hypermucoviscous capsule are defining characteristics of these strains, relative to classical *K. pneumoniae*. Among the four siderophores that hypervirulent *K. pneumoniae* secretes, Abn accounts for more than 90% of iron transport activity,<sup>383</sup> is a critical factor for growth and survival in human ascites or *ex vivo* serum and confers virulence in murine systemic or pulmonary infection models.<sup>284</sup> This role as a primary virulence factor likely derives from a combination of Abn's indifference to SCN and its enhanced production by hypervirulent *K. pneumoniae*. Although hypervirulent *K. pneumoniae* normally also produces Ent/GEnt, the contributions of the glucosylated catecholate to systemic infections are not fully defined.<sup>284,323</sup> In the absence of Abn, otherwise wild-type classical *K. pneumoniae*, that still excrete Ent, GEnt, and Ybt, showed higher bacterial load in the lungs of mice, relative to an isogenic *entB ybtS* strain that did not produce either catecholate siderophore. All three siderophores were required for the dissemination of classical *K. pneumoniae* to the spleen and induction of proinflammatory cytokines.<sup>265</sup> These data support both the primary importance of Abn during pathogenesis by *K. pneumoniae*, as well as the ability of particular siderophore iron acquisition pathways to allow bacterial proliferation in specific host tissues.

**5.2.5. FepB.**—In *K. pneumoniae*, FepB participates in the uptake of FeEnt/FeGEnt; a *fepB* strain was attenuated in lung colonization and tissue dissemination *in vivo*. However, the reductions in virulence engendered by *fepB* were distinct from the FeEnt/FeGEnt uptake defects alone and unrelated to acquisition of FeYbt.<sup>253</sup> Studies of the transcriptional regulator RamA in another member of Enterobacterales, *S. enterica*, coincidentally revealed that the periplasmic FeEnt/FeGEnt binding protein FepB contributes to the survival of *S. enterica* in RAW 264.7 macrophages and to its virulence in BALB/c mice.<sup>253</sup>

### 5.3. *A. baumannii*

*A. baumannii* is a short, nonmotile, rod-shaped, oxidase-negative, Gram (–) coccobacillus in the Family Moraxcellaceae. In 2019, *A. baumannii* constituted over 20% of all hospital-acquired infections; nearly half of these isolates were carbapenem-resistant *Acinetobacter*<sup>384</sup> that are recognized as an urgent threat to human health from their propensity to cause pneumonia, wound, bloodstream, and urinary tract infections. The rapidly increasing resistance of this bacterium to most antibiotics is a concern for healthcare systems around the globe.<sup>20</sup> Additionally, *A. baumannii* has an abnormally high mortality rate compared to other Gram (–) pathogens (up to 70% from extreme drug resistant (XDR) strains).<sup>385</sup> *A. baumannii* further illustrates the impact of iron acquisition on pathogenesis, in that it overcomes the iron-limiting conditions of the host by secreting atypical siderophores and altering its OM protein composition to optimize the uptake of its own and other ferric siderophores.<sup>386-390</sup>

**5.3.1. Fur-Mediated Regulation of Iron Acquisition.**—Iron deficiency affects the virulence of *A. baumannii*, which responds by upregulating genes involved in iron acquisition and other processes like respiration, biofilm formation, and motility.<sup>391-393</sup> As in all Gram (–) bacteria, the ferric uptake regulator (Fur) controls expression of the iron transport systems of *A. baumannii*. Fur negatively controls expression by binding to the “Fur box,” a conserved DNA sequence upstream of iron-related biosynthetic and transport genes. The primary structure of Fur from *A. baumannii* strain BM2580 is 63% identical to that of Fur from *E. coli* K-12.<sup>387</sup> Fur boxes were also identified in the genomes of other *A. baumannii* strains.<sup>391,394</sup> The iron uptake systems of *A. baumannii* are also upregulated during growth at 28 °C compared to 37 °C,<sup>395</sup> and during growth in serum, supporting their role the organism’s virulence *in vivo*.<sup>396</sup> Additionally, at lower temperatures the BLUF-type photoreceptor BlsA interacts with Fur to photoregulate genes involved in Acn biosynthesis and FeAcn uptake.<sup>397</sup> In the dark at 23 °C, BlsA antagonizes the actions of Fur to upregulate the production of both biosynthetic and transport genes; growth in blue light or at 37 °C eliminates this effect.

**5.3.2. Siderophores: Acn, Bfn, Fbn.**—The native, chromosomally encoded siderophores of *A. baumannii* are the mixed chelate Acn,<sup>390</sup> the hydroxymates BfnA and BfnB,<sup>398</sup> and the mixed chelation compounds Fbn.<sup>399</sup> Other putative siderophores biosynthetic gene clusters exist among particular isolates of *A. baumannii* that are as yet uncharacterized.<sup>388,400-403</sup>

**5.3.2.1. Acn.:** The most-studied *A. baumannii* siderophore gene cluster encodes Acn<sup>390</sup>, that contains catecholate, hydroxamate, and imidazole groups. The Acn gene cluster occurs in the majority of clinical isolates and sequenced genomes, with the exception of *A. baumannii* SDF.<sup>391,400,404</sup> Fur boxes control transcription of the structural genes for the enzymes involved in Acn biosynthesis and for FeAcn transport, in response to extracellular iron levels.<sup>394</sup> Bioinformatic analyses identified three putative systems within the Acn cluster: *basA-J* for acinetobactin synthesis, *bauA-F* for *A. baumannii* acinetobactin utilization, and *barAB* for *A. baumannii* acinetobactin release to the environment.<sup>394,405</sup> Acn belongs to the nonribosomal peptide synthetase (NRPS) class of siderophores<sup>406</sup> and consists of 2,3-DHBA, threonine, and *N*-hydroxyhistamine.<sup>406</sup> The *entA* gene, that encodes production of DHBA, resides elsewhere in the genome, away from the acinetobactin gene cluster.<sup>394,407</sup> Acn exists in two forms: preacinetobactin (pAcn) contains an isooxazolidinone ring system that undergoes a pH-dependent isomerization to an oxazoline ring in Acn<sup>408</sup> (Figure 3). This response to the acidic conditions typically found at sites of acute infection makes pAcn/Acn virulence factors.<sup>409</sup> Both siderophore isomers bind iron as a 2:1 complex, and both enable *A. baumannii* growth in low iron conditions.<sup>408,410-412</sup> BauA, the pertinent OM receptor, was crystallized in complex with FepAcn.<sup>413</sup> However, the exact selectivity of BauA for iron complexes of pAcn and Acn is uncertain because both compounds promote growth. Furthermore, the next entity in the transport pathway, the periplasmic binding protein BauB, was crystallized in complex with FeAcn. BauB binds both FepAcn and FeAcn with nanomolar affinity.<sup>410,411</sup> The fact that the crystallized BauA protein originates from *A. baumannii* ATCC 19606,<sup>413</sup> whereas *bauA* was originally annotated in strain ATCC 17978, within the classic Acn biosynthesis and transport gene cluster,<sup>391</sup> further confuses the issue. The 19606 and 17978 BauA primary structures are only 56.6% identical, suggesting that they are functionally different receptors. Although it lacks the ability to produce Ent or Fc, *A. baumannii* assimilates both ferric siderophores through LGP encoded in its genome.<sup>264,272,285,414</sup>

Similar to hypervirulent *K. pneumoniae*, the presence or absence of genes for biosynthesis and uptake of various siderophores in the *A. baumannii* genome often affects the extent of its virulence. Acn synthesis is required for *A. baumannii* pathogenesis: the biosynthetic and transport proteins BasD and BauA, respectively, are virulence determinants for *A. baumannii* ATCC 19606<sup>T</sup> in the *Galleria mellonella* larvae infection model<sup>415,416</sup> and in a murine model of systemic infection.<sup>415</sup> BasD was required for full virulence of *A. baumannii* ATCC 19606<sup>T</sup> in a murine model of wound infections,<sup>417</sup> and Acn biosynthesis enabled persistence of *A. baumannii* ATCC 19606<sup>T</sup> in human alveolar epithelial cells, ultimately resulting in apoptosis.<sup>415,418</sup> Siderophores, especially Acn, promote survival of *A. baumannii* in serum, where they strip iron from TF and LF.<sup>176,419</sup>

**5.3.2.2. Bfn.:** A second siderophore biosynthetic cluster exists in *A. baumannii* AYE and other strains, that encodes the hydroxamates Bfn A and B.<sup>398</sup> The genetic and biochemical details of Bfn biosynthesis are less well-defined. *A. baumannii* AYE does not have a functional *entA* locus and therefore does not produce Acn.<sup>398,407</sup> The Bfn biosynthetic and transport gene cluster consists of *bfmA-L* and exists in the majority of sequenced strains.<sup>398</sup> Bfn compounds are nonribosomal peptide synthetase-independent (NIS) siderophores, based

on their production by BfnA and BfnD synthetases.<sup>398</sup> BfnH is the LGP that recognizes Bfn.<sup>398</sup> Bfn A and B are chemically similar to acinetoferrin, another hydroxamate from *Acinetobacter hemolyticus* ATCC 17906<sup>T</sup>.<sup>420</sup> The role of Bfn A and B in pathogenesis are not yet known.

**5.3.2.3. Fbn.:** *A. baumannii* produces a third unique iron acquisition system, based on the mixed chelation (catecholhydroxamate) siderophores Fbn A-F, that were found in *Acinetobacter baylyi* ADP1 and four other sequenced strains including *A. baumannii* ATCC 17978.<sup>391,399,400,411</sup> FbnA is the predominant siderophore in this group (~85% of total mass); FbnB-F are likely biosynthetic intermediates or shunt byproducts.<sup>399</sup> Like Acn, Fbn classify as NRPS siderophores, but unlike Acn, they contain a single hydroxamate and two catecholate groups that together create a 1:1 complex with Fe<sup>3+</sup>.<sup>411</sup> *A. baumannii* ATCC 17978 excretes less Fbn than Acn,<sup>411</sup> and the role of Fbn in pathogenesis is currently undefined. Regarding their transport, FeFbnA initially binds to FbsN,<sup>399</sup> then to BauB (the FeAcn periplasmic binding protein) with nanomolar affinity. The *fbn* gene cluster does not encode a periplasmic binding protein; broad recognition specificity is common in periplasmic siderophore binding proteins, as occurs in FhuD<sup>421</sup> and FepB<sup>248,421,422</sup> of *E. coli*. Consequently, FeFbnA transport competitively antagonizes FeAcn uptake.<sup>411</sup>

**5.3.3. Hn Utilization.**—Like many bacterial pathogens, *A. baumannii* displays hemolytic activity when grown in iron-deficient conditions<sup>423</sup> that releases Hn from erythrocyte hemoglobin as an iron source. The genomes of numerous sequenced strains and clinical isolates of *A. baumannii* contain *plc1* and *plc2* that encode phospholipase C enzymes with the capability of lysing host red blood cells.<sup>400,404,423,424</sup> Plc1 and Plc2 are upregulated and hemolytic to horse and human erythrocytes in low-iron conditions, suggesting a role in iron acquisition from Hn found in erythrocytes.<sup>423</sup> The former enzyme, but not the latter, is critical for the virulence of *A. baumannii* ATCC 19606 in the *G. mellonella* infection model.<sup>423</sup> Three different phospholipase D enzymes in *A. baumannii* also impact its virulence,<sup>404,425,426</sup> but their role in iron acquisition is not yet defined.

Once inserted into protoporphyrin IX by ferrochelatase, iron is stable in Hn unless the porphyrin ring system is compromised. Bacterial pathogens, including *A. baumannii*, liberate iron from Hn by the actions of oxidases. Although *A. baumannii* generally uses Hn as an iron source, different strains show variability in Hn utilization.<sup>427-430</sup> Separate gene clusters encode Hn uptake systems and a Hn oxygenase (HemO) that cleaves the porphyrin and releases iron.<sup>400,428,430</sup> For example, the highly virulent *A. baumannii* LAC-4 contains a cell envelope Hn uptake system, that acquires Hn at sites of infection, and it produces HemO, that degrades Hn to release iron.<sup>428,429</sup> On the other hand, *A. baumannii* ATCC 17978 encodes the Hn uptake loci but lacks *hemO*. Consequently, it does not grow well with Hn as a sole iron source, underscoring the importance of Hn degradation to its pathogenesis.<sup>428,429</sup>

**5.3.4. LGP.**—TonB-dependent ferric siderophore transport into *A. baumannii* encompasses as many as 21 predicted LGP, although at present only a few are biochemically characterized.<sup>400</sup> As noted above, AbaBauA recognizes FeAcn, while AbaBfnH<sup>398</sup> and AbaFbsN<sup>399</sup> are the predicted receptors for FeBfn and FeFbn, respectively. The latter

two designations are not yet experimentally verified. Besides the three siderophores of its own creation, *A. baumannii* utilizes other xenosiderophores, including FeEnt,<sup>272,431</sup> via the orthologue AbaFepA. Accordingly, *A. baumannii* apparently also acquires iron from monocatecholate compounds, catalyzed by AbaPiuA and AbaPirA, that confer sensitivity of *A. baumannii* ATCC 19606<sup>T</sup> to siderophore–monobactam antibiotic conjugates.<sup>432</sup> Despite the solution of crystal structures for PiuA and PirA from both *A. baumannii* and *P. aeruginosa*,<sup>432</sup> their biochemical roles in siderophore uptake, bacterial physiology and infection are currently undefined. *A. baumannii* utilizes iron from ferrichrome but not from ferrichrome A.<sup>272</sup> Other proteins were implicated in iron transport by *A. baumannii*, including homologues of OmpW and OprD.<sup>433</sup> Lastly, AbaFepA is a virulence determinant of *A. baumannii* ATCC 17978 in a mouse sepsis infection model, showing the importance of xenosiderophore utilization *in vivo*.<sup>431</sup>

**5.3.5. TonB/ExbBD.**—All sequenced *A. baumannii* genomes contain three separate *tonB* gene clusters that were likely horizontally acquired from different sources.<sup>434</sup> In *A. baumannii* ATCC 19606<sup>T</sup>, the three systems are *tonB*<sub>1</sub>/*exbB*<sub>1</sub>/*exbD*<sub>1.1</sub>/*exbD*<sub>1</sub>, *tonB*<sub>2</sub>, and *tonB*<sub>3</sub>/*exbB*<sub>3</sub>/*exbD*<sub>3</sub>. The genes in these loci are variably expressed, but only *tonB*<sub>3</sub> contains an upstream Fur box, and iron deprivation only upregulates *tonB*<sub>3</sub>, implicating it in iron homeostasis.<sup>393,434</sup> The analyses of individual mutants in these loci were inconclusive,<sup>393,434</sup> but both AbaTonB<sub>2</sub> and AbaTonB<sub>3</sub> functionally complement the absence of EcoTonB during iron-limited growth of *E. coli*.<sup>434</sup> AbaTonB<sub>1</sub> and AbaTonB<sub>2</sub> are both required, but neither are individually sufficient, for full virulence of *A. baumannii* ATCC 19606<sup>T</sup> in the *G. mellonella* infection model, nor in a mouse sepsis model. In the latter case, Runci *et al.*<sup>393</sup> inoculated mice with wild-type *A. baumannii* ATCC 19606<sup>T</sup>, and a second group with a *tonB*<sub>3</sub> derivative of the same strain. After 24 h, none of the mice infected with the wild-type survived, whereas all the mice inoculated with the *tonB*<sub>3</sub>-deficient strain survived. These data indicated that TonB<sub>3</sub> is essential to the virulence of *A. baumannii* ATCC 19606<sup>T</sup>. Overall, AbaTonB<sub>3</sub> was both necessary and sufficient for virulence in either experimental model.<sup>393,434</sup> Together these studies suggest that *tonB*<sub>3</sub>/*exbB*<sub>3</sub>/*exbD*<sub>3</sub> is the major system that facilitates iron acquisition by *A. baumannii*.

**5.3.6. Uptake of Fe<sup>2+</sup>.**—Like *E. coli*, *S. typhimurium* and other Gram (–) bacteria, *A. baumannii* utilizes the ferrous iron transport system, FeoAB, regulated by FeoC, during growth in reducing environments where ferrous iron may predominate.<sup>400</sup> The eukaryotic intracellular environment is one such situation. An *feoA* mutant of *A. baumannii* ATCC 17978 was deficient in iron-limiting conditions with regard to growth, biofilm formation, adhesion, and virulence.<sup>435</sup> Two *feoB* homologues exist in some *A. baumannii* strains, including ATCC 17978, that contains both chromosomal and plasmid (pAB3) loci.<sup>435</sup> In *A. baumannii* ATCC 19606<sup>T</sup>, *feoAB* is controlled by Fur, via an upstream Fur box.<sup>393</sup> The FeoAB system is a virulence determinant in both Gram (–)<sup>88</sup> and (+)<sup>436</sup> bacteria. However, a *feoB* derivative of *A. baumannii* ATCC 19606<sup>T</sup> was not impaired in low-iron media, nor in the *G. mellonella* nor mouse infection models. Conversely, its growth was restricted in human serum,<sup>393</sup> and *feoB* was required for full virulence in a mouse sepsis model.<sup>414</sup> On balance, despite some conflicting data, the FeoAB system is an important contributor to iron acquisition by many prokaryotes, including *A. baumannii*, in the host environment.

## 5.4. *P. aeruginosa*

*P. aeruginosa* is an encapsulated, catalase- and oxidase-positive Gram (–) bacillus in the Family Pseudomonadaceae that forms biofilms and causes disease in plants, animals, and humans. It is an opportunistic pathogen that thrives in numerous host environments, infects a variety of tissues, and causes particularly serious disease in patients with cystic fibrosis. Their lungs and digestive pathways accumulate copious sticky mucus, creating an environment that *P. aeruginosa* readily colonizes with biofilms that correlate with its virulence.<sup>437</sup> *P. aeruginosa* also infects the urinary tract and burn wounds, often resulting in septicemia. Like other pathogens it faces the reduced accessibility of iron in animal tissues, as a result of TF, LF, and FTN.<sup>44</sup> However, depending on the infection (acute vs chronic), *P. aeruginosa* adjusts its preferred iron source to minimize the metabolic input needed to obtain it,<sup>438</sup> and it employs diverse mechanisms of iron acquisition.

**5.4.1. Elaboration of Siderophores.**—*P. aeruginosa* synthesizes Pch<sup>211</sup> and Pvd,<sup>212</sup> that are atypical siderophores (Figure 3). The former is similar to Ybt, in that it contains a hydroxyphenyl and two thiazolidine rings (Ybt contains three thiazolidines), but Pch (324 Da) is smaller than Ybt (482 Da). Pch has considerably lower affinity for Fe<sup>3+</sup> ( $K_A = 10^5 \text{ M}^{-1}$ )<sup>439</sup> than most siderophores, it binds iron with a 2:1 stoichiometry and may form mixed iron complexes with other ligands.<sup>209</sup> Its biosynthesis requires expression of fewer genes than Pvd, so when environmental iron levels drop below micromolar levels, *P. aeruginosa* produces Pch first.<sup>440</sup> The larger, mixed chelation siderophore Pvd (1365 Da) has an uncommon structure, that includes a dihydroxyquinoline complexation moiety and 6–14 L- or D-amino acids, in some cases cyclized, that provide additional hydroxamate or carboxylate ligands to the hexadentate iron center. Its more typical high affinity for Fe<sup>3+</sup> ( $K_A = 10^{32} \text{ M}^{-1}$ )<sup>441,442</sup> allows Pvd to remove iron from TF/LF,<sup>443,444</sup> and it is not recognized and removed from circulation by SCN (see below). Pseudomonads in the biosphere produce over 60 chemical variants of pyoverdine (also called pseudobactins<sup>445,446</sup>). Strains that do not produce pyoverdine are less virulent in murine<sup>443</sup> and in rabbit<sup>447</sup> infection models, comparable to the reduction in virulence seen for TonB-deficient mutants.<sup>448</sup> The role of Pvd in pathogenesis goes beyond its ability to capture iron, because it regulates its own synthesis, as well as the production of two extracellular virulence factors, the protease Prp and exotoxin A.<sup>73,449</sup> Besides Pch and Pvd, studies on the effect of airway mucus secretions on the growth of *P. aeruginosa* revealed another siderophore biosynthesis and transport system.<sup>450</sup> A mutant strain devoid of Pch and Pvd survived iron deficiency by obtaining iron with a previously unknown, alternative mechanism. Using transposon-mutagenesis, Gi *et al.*<sup>450</sup> identified a multigene locus encoding the synthesis and uptake of nicotianamine, a tricarboxylate iron chelator formed from *S*-adenosyl methionine, that was originally described in plants.<sup>451,452</sup> Nicotianamine may play a role in the survival and fitness of *P. aeruginosa* in human lungs.<sup>450</sup>

**5.4.2. Uptake of Xenosiderophores.**—The genome of *P. aeruginosa* encodes more than 30 putative LGP, many of which bind and transport ferric siderophores that originated from other bacteria and fungi. PfeA and PirA bind and transport FeEnt, produced by Enterobacterales;<sup>453–455</sup> FoxA transports ferrioxamine B,<sup>456</sup> a siderophore from *Streptomyces*; FiuA transports the fungal siderophore ferrichrome;<sup>457,458</sup> FemA utilizes iron

complexes of mycobactin and carboxymycobactin;<sup>459</sup> FecA transports FeCit;<sup>460</sup> ChtA acts as receptor for iron complexes of rhizobactin, Abn, and schizokinen;<sup>461</sup> FvbA for the uptake of FeVbn.<sup>462</sup> The role of these ferric xenosiderophores in the mammalian pathogenesis of *P. aeruginosa* is not yet fully known, but *P. aeruginosa* has an ability to sense its environment, as illustrated by the fact that some strains stop making their own siderophores when grown together with *Streptomyces ambofaciens* and instead up-regulate the expression of FoxA to profit from the presence of ferrioxamine B.<sup>463</sup> Similar accommodations may occur during infection of mammalian hosts, depending on other microorganism that may be present.

**5.4.3. Hn Utilization.**—*P. aeruginosa* uses two distinct TonB-dependent systems for acquisition of Hn from proteins like hemoglobin or hemopexin.<sup>464</sup> *Pseudomonas* haem uptake (Phu) and haem assimilation system (Has). The Phu system involves an LGP, designated PhuR, that recognizes and directly extracts Hn from the target proteins, while the Has system encompasses an additional, secreted hemophore (HasAp) that binds Hn and then adsorbs to the LGP HasR.<sup>465-467</sup> Single mutants in either systems still utilize Hn as sole iron source, but a double mutant is unable to do so.<sup>464</sup> Experiments suggest that PhuR is the primary Hn receptor, whereas the Has system is centered on sensing Hn in the environment.<sup>468,469</sup> A third system, Hxu, was identified by proteomics.<sup>470</sup> Like Has, it may play a prominent role in sensing Hn but only a minor role in Hn uptake. However, in the absence of HasR, *P. aeruginosa* upregulates the OM receptor HxuA, suggesting its participation in Hn uptake.

**5.4.4. Extraction of Iron from FTN.**—Roughly 25% of all the iron in the human body resides in cytoplasmic FTN. Each molecule holds as many as 4000 iron atoms, which makes it a potentially useful source of iron for invading pathogens. However, the iron within FTN exists as a ferrihydrite that has only marginal solubility. To further complicate utilization of its iron, FTN is present in miniscule amounts in circulation: the plasma FTN concentration is 1.5–30 ng/mL; TF, by comparison, is present at 100-fold higher concentrations.<sup>471</sup> However, the lungs of CF patients contain a 70-fold higher extracellular concentration of FTN,<sup>472</sup> suggesting that it may act as an iron source for growth of strains adapted to thrive in that environment. It is relevant that both catecholate and hydroxamate siderophores readily remove iron from FTN.<sup>278</sup> Careful measurements with wild-type and siderophore-deficient strains implied that Pch and Pvd acquired iron from FTN to support growth of *P. aeruginosa*, even without any proteolytic degradation of the multimeric protein cage. FTN also supported growth of siderophore-deficient *P. aeruginosa* strains, but only in the presence of extraneous proteases.<sup>473</sup> In this case, after degradation of the protein framework, the actions of extracellular reducing agents (*e.g.*, phenazines like PCA) presumably produce Fe<sup>2+</sup>, allowing iron uptake by the FeoAB system.

**5.4.5. Cell Surface Signaling during Iron Uptake.**—As originally described for *E. coli* FecA,<sup>474</sup> certain LGP accomplish signal transduction through the cell envelope to the cytoplasm in response to recognition and binding of a cognate ligand on the cell surface. Binding of FeCit by EcoFecA positively upregulates transcription of its structural gene, ultimately increasing the rate of FeCit uptake. In *P. aeruginosa*, numerous LGP have the ability to regulate gene expression.<sup>475</sup> This phenomenon, now called cell-surface signaling



(CSS), was first shown in *P. aeruginosa* for the self-regulated uptake of FePvd by FpvA, but it was later observed for receptors of Hn and citrate, that act as xenosiderophores. CSS LGP like FecA and FpvA contain a 70–80 residue N-terminal extension that contains two  $\alpha$ -helices sandwiched between two  $\beta$ -sheets.<sup>476,477</sup> In the well-studied case of FpvA, binding of FePvd activates the alternate sigma factors PvdS and FpvI, leading to enhanced expression of the Pvd biosynthetic genes and *fpvA* itself.<sup>478,479</sup> In the absence of FePvd the activities of PvdS and FpvI are inhibited by an antisigma factor, FpvR, that spans the cytoplasmic membrane.<sup>480,449,481</sup> When Pvd captures iron and associates with FpvA, the binding reaction stimulates proteolytic degradation of FpvR, releasing the alternate sigma factors to act on RNA polymerase, which improves recognition of promoters and up-regulates both the synthesis of pyoverdine, FpvA, and virulence factors.

**5.4.6. Iron Uptake in Biofilms.**—The biofilms of *P. aeruginosa* are complex structures that may contain additional different microorganisms, all of which are surrounded by extracellular polysaccharides, DNA, and polypeptides.<sup>482-484</sup> Biofilm formation facilitates evasion of host immune recognition, phagocytosis, and bacteriocidal actions by the host.<sup>485</sup> Although Pch is not needed for biofilm production, Pvd biosynthesis is required,<sup>486,487</sup> indicating a need for iron uptake during biofilm formation. In the absence of Pvd, supplementation of media with FeCit restores biofilm formation, supporting this conclusion. High-throughput genetic screens using Pvd fluorescence as an assay of its production revealed 55 genes that affect Pvd production: their absence decreased Pvd biosynthesis.<sup>484</sup> The loci fell into a few classes; several genes related to biofilm production affected Pvd biosynthesis, including genes for flagellin biosynthesis, chemotaxis, type IV pili assembly, cup fimbriae biogenesis, and exopolysaccharide synthesis.<sup>484</sup> A direct correlation exists between Pvd production and biofilm formation, leading to the conclusion that FePvd provides the iron needed for biofilm biosynthesis in iron-deficient conditions. Nevertheless, Pvd biosynthesis is not needed for biofilm formation in iron-replete conditions.

**5.4.7. Extracellular Reduction of Iron.**—Production of siderophores combats the low solubility of ferric iron in aerobic aqueous environments but also create a dilemma for Gram (–) bacteria because ferric siderophore complexes are often too large and bulky to penetrate the 10 Å channels of general porins. LGP solve this OM transport problem, but at an energetic cost (in the case of EcoFepA, ~4 ATP per molecule of FeEnt internalized<sup>62</sup>). Ferrous iron, on the other hand, is soluble and predominates in partially anaerobic, acidic environments.<sup>488</sup> This setting may exist in the lungs of CF patients, due to the disproportionate amount of mucus that accumulates on their epithelial surfaces, where the bacterium forms biofilms. In that context, *P. aeruginosa* secretes PCA, a secondary metabolite with reducing potential. PCA is present in large amounts in the mucus of patients with advanced *P. aeruginosa* infections,<sup>489,490</sup> portending a role for this uptake system in virulence. Once reduced to Fe<sup>2+</sup>, iron may diffuse through OM general porin<sup>491</sup> channels to the periplasm, where the FeoAB transporter passes it to the cytoplasm. The human protein calprotectin targets PCA-mediated iron uptake by *P. aeruginosa*. Calprotectin sequesters Mn(II), Zn(II), and Fe(II),<sup>492</sup> and it inhibits phenazine biosynthesis in *P. aeruginosa*, resulting in iron-deprivation. Hence, its activity resembles the

sequestration of ferric catecholates by SCN, as a nutritional immunity defense mechanism against the pathogen<sup>493,494</sup>

**5.4.8. Periplasmic Transport of Pvd.**—FePvd is bound and transported to the periplasm by the TonB-dependent OM receptors FpvAI and FpvB.<sup>442,495</sup> In Gram (–) bacteria, ferric siderophores generally remain intact, even when bound to periplasmic binding proteins, until their internalization through the IM into the cytoplasm. In *P. aeruginosa*, however, it was suggested that reduction of iron occurs in the periplasm and that both Fe<sup>2+</sup> and the aposiderophore traverse the IM into the bacterial cytoplasm. For example, after OM transport through TonB-dependent LGP FpvAI or FpvB, FePvd is bound by periplasmic FpvC or FpvF,<sup>496</sup> after which the IM FpvG reduces the iron complex, releasing Fe<sup>2+</sup> for binding by periplasmic FpvC. According to this mechanism, the ABC-type transporter FpvDE ultimately transports ferrous iron into the cytoplasm. An overview of experiments concerning the fascinating path of pyoverdines from outside to inside the bacterial cell is found in Vigoroux *et al.*<sup>497</sup>

**5.4.9. Mitochondrial Toxicity of Pvd.**—Besides the well-known the role of Pvd in the virulence of *P. aeruginosa*, it directly contributes to cytotoxicity. When Pvd enters *Caenorhabditis elegans*<sup>498</sup> or mammalian cells,<sup>483</sup> it fatally disrupts mitochondrial homeostasis. Cells that suffer this type of damage destroy and recycle their mitochondria, in a process known as autophagy, which may be viewed as an arm of innate immunity against pathogens like *P. aeruginosa*.

## 5.5. *Y. pestis*

*Y. pestis* is a nonmotile, facultative anaerobic, rod-shaped, Gram (–) coccobacillus in the Family Yersiniaceae, that does not produce spores. It causes potentially fatal diseases: bubonic, pneumonic, and septicemic plague.<sup>499-502</sup> In *Y. pestis*, as in many pathogens, the ability to infect humans and animals hinges on the activation of virulence determinants, some of which acquire nutrients in the host. Iron uptake systems are required for intracellular growth of *Y. pestis* so they are tightly regulated during its colonization of humans and animals.<sup>503-506</sup> The *Y. pestis* genome encodes multiple iron or Hn transporters, including TonB-dependent OM systems, IM ABC- and non-ABC transporters. “Ironomic” studies of *Y. pestis* identified 16 iron uptake systems, but only two of them, the LGP FyuA, that internalizes FeYbt, and the IM ABC-transporter Yfe, that transports iron or manganese, correlate with its virulence.<sup>505,507-515</sup>

**5.5.1. The High Pathogenicity Island.**—The TonB-dependent uptake system for FeYbt is encoded in a high pathogenicity island termed *pgm*, that includes the biosynthetic *ybtPQXS* operon, the *irp12ybtUTE* loci, and the OM transport locus, *psn*.<sup>516</sup> The entire *pgm* region may be deleted by recombination, creating a strain with attenuated virulence.<sup>517-520</sup> In light of its high affinity for Fe<sup>3+</sup> ( $K_A = 4 \times 10^{36} \text{ M}^{-1}$ ),<sup>374</sup> Ybt readily extracts iron from LF and TF.<sup>502,521</sup> Ybt biosynthesis requires so-called “high molecular weight proteins” (HMWP), including the iron-regulated proteins (Irp), YbtU, YbtS, YbtT, and YbtE.<sup>516</sup> After secretion of Ybt to the extracellular host environment, where it complexes iron, FeYbt encounters the LGP YpePsn (99.4% identical to KpnFyuA), that binds and transports it to

the periplasm. The YbtPQ ABC-transporter passes FeYbt to the cytoplasm.<sup>522-524</sup> *ybtX*, in the same operon, is not required for iron uptake; the growth of a YbtX-deficient strain was not impaired in iron-deficient conditions. YbtX was essential, however, for Zn uptake,<sup>524</sup> suggesting that the same system transports two different metals. This conclusion faces some conceptual problems because the chemical attributes of FeYbt and uncomplexed Zn<sup>2+</sup> are significantly different.

**5.5.2. Iron Acquisition As a Determinant of Plague.**—The Ybt system is a virulence factor for *Y. pestis* in the early progression of bubonic plague. Loss of any gene that compromises the overall iron uptake system (*i.e.*, siderophore biosynthesis or ferric siderophore transport) renders *Y. pestis* avirulent in mice after subcutaneous inoculation, although virulence of the same strains was not reduced upon intravenous inoculation.<sup>502,525</sup> In a pneumonic plague model, the biosynthesis-deficient *irp* strain showed greater loss of virulence than a transport-deficient *psn* strain. These results suggest either redundancy in the FeYbt uptake process, or secondary functions of Ybt, distinct from its role in iron acquisition, during the progression of pneumonic plague.<sup>502,525</sup> For example, the presence of Ybt may activate transcription of relevant genes or other virulence factors in *Y. pestis*.<sup>502,525</sup> In avian pathogenic *E. coli*, that also synthesize Ybt and transport FeYbt, *irp2* and *fyuA* are virulence determinants: inactivation of either *irp2* or *fyuA* on its high-pathogenicity island impaired cell adhesion, inhibited transcription of other virulence genes and reduced pathogenicity.<sup>526</sup>

**5.5.3. OM LGP and IM Transporters.**—The OM receptor for FeYbt is a 651 residue protein, termed Psn in *Y. pestis* and FyuA in *K. pneumoniae*. YpePsn and KpnFyuA are 99.4% identical, with only four amino acid differences between the two proteins. Like all LGP, they contain a 22-stranded  $\beta$ -barrel that wraps around an N-terminal globular domain.<sup>527</sup> The two proteins function equivalently in *Y. pestis* and *K. pneumoniae*, as evidenced by their recognition of both FeYbt and pesticin in the two organisms.<sup>527-529</sup> Furthermore, an engineered hybrid toxin that contains the receptor binding domain of pesticin, and the N-terminus of T4 lysozyme, that degrades peptidoglycan (PG), killed both *Y. pestis* and pathogenic *E. coli*. The hybrid toxin crossed the OM and was unaffected by Pim, a protein that inhibits degradation of PG in some *Yersinia* pathogens. Such hybrid toxins or siderophores may target bacterial pathogens expressing particular receptor proteins that correlate with virulence.<sup>527</sup>

The cryo-EM structure of a predicted IM ABC transporter of FeYbt, YbtPQ from uropathogenic *E. coli*, unexpectedly revealed the conformation of a type IV exporter.<sup>530</sup> Furthermore, a transmembrane helix within YbtP unwinds upon release of substrate, while the nucleotide binding domain remains tightly packed even in the absence of a bound nucleotide. These findings suggest a different mechanism of ferric siderophore uptake by YbtPQ,<sup>530</sup> relative to other ABC-transporters, like the BtuCD complex that acquires B<sub>12</sub>.<sup>531,532</sup> The YbtPQ IM ABC-transporter, that contributes to the virulence of *Y. pestis*, spans a 5.6 kb region of the *Y. pestis* genome and contains the *yfeABCD* operon and the *yfeE* locus.<sup>509,511,521</sup> *yfeABCD* is regulated by iron availability, mediated by Fur; *yfeE* is tightly linked to *yfeABCD*, transcribed in the opposite direction, and expressed

independently of Fur.<sup>281</sup> Deletion of *yfeE* inhibited growth in iron-deficient conditions, indicating that YfeE participates in iron transport despite the fact that its expression is not iron-regulated. Although the exact function of the 184 residue Yfe protein is unknown, it contributes to the pathogenesis of bubonic plague:<sup>509,533</sup> a *ybt*, *yfe* double mutant was avirulent in mice after intravenous inoculation, suggesting that *yfe* is essential for its virulence during the later stage of the disease. By the subcutaneous route, a *ybt*<sup>+</sup>*yfe* strain had reduced virulence relative to its *ybt*<sup>+</sup>*yfe*<sup>+</sup> parent. These data suggested that Yfe participates early in the progression of bubonic plague but may not be absolutely essential.<sup>509</sup> On the other hand, the TonB-dependent Ybt system was essential for the virulence in the early stage of bubonic stage but not in the later stage. Hence, Ybt and Yfe system may act together to drive the progression of bubonic plague through different stages.<sup>509,533,534</sup> Regarding other components, YfeA resembles a periplasmic substrate binding protein. Its crystal structures<sup>535</sup> classified YfeA as a cluster A-1 substrate binding protein, whose other members directly bind metal ions, including zinc, manganese, and iron. YfeA contains two metal binding sites: site 1 shows polyspecificity for Zn<sup>2+</sup>, Mn<sup>2+</sup>, and Fe<sup>2+</sup> ions and alters its substrate binding specificity in response to environmental conditions. Binding site 1 in YfeA tightly binds metal ions because incubation with EDTA does not remove metals ions from it. Site 2 binds Zn<sup>2+</sup> and Mn<sup>2+</sup>, but not Fe<sup>2+</sup>, and its biological contributions are undefined.<sup>536</sup>

## 6. ADSORPTION OF APO- AND FERRIC SIDEROPHORES BY SCN

The innate immune system produces TF, LF, and FTN, that antagonize bacteria by scavenging, sequestering, and storing iron,<sup>537-540</sup> whereas SCN adsorbs both apo- and ferric siderophores in body fluids, eliminating them from circulation and thereby reducing their availability to the bacteria that produced them. Before the discovery of this activity,<sup>55</sup> SCN was known as neutrophil gelatinase-associated lipocalin (NGAL), a 25 kDa protein that was found covalently bound to matrix metalloproteinase 9 from human neutrophils.<sup>541</sup> The same protein was also discovered by the increase of its mRNA in mouse kidney cells infected by SV40 virus and named lipocalin 2 (LCN2).<sup>542</sup> Lipocalins were known as acute phase proteins from myelocytes that were stored in neutrophil granules and overexpressed in epithelial cells during inflammation.<sup>543</sup> Experiments suggested that LCN2 was an alternative means of delivering iron to epithelial cells during development, especially in the absence of TF,<sup>55</sup> although the form of delivered iron was unknown.<sup>544</sup> A so-called “mammalian siderophore” (2,5-DHB) was found bound to LCN2, implicating it in the delivery of iron to cells.<sup>545</sup> Consistent with these postulates, animals responded to infection by suppressing production of 2,5-DHB and upregulating LCN2.<sup>546</sup> Another member of the lipocalin superfamily, 24p3/NGAL, delivers iron to the cytoplasm of cells by endocytosis.<sup>544</sup> Goetz *et al.*<sup>55</sup> subsequently observed that FeEnt adsorbed to NGAL/LCN2, creating a red-colored complex and appropriately renamed the protein as SCN.

### 6.1. Specificity

Characterization of the SCN-FeEnt binding reaction by tryptophan fluorescence quenching analysis showed high affinity binding of the ferric siderophore to purified SCN ( $K_D = 0.4$  nM), which led to the conclusion that SCN competed with the bacterial receptor FepA to

capture FeEnt during bacterial infections. SCN also bound the apo-siderophore with about 10-fold lower affinity ( $K_D = 3.5 \mu\text{M}$ ). Structural delineation of the SCN–FeEnt complex found a binding interaction mediated by ionic and cation– $\pi$  interactions between anionic FeEnt ( $3^-$ ) and the cationic side chains of residues R81, K125, and K134 in the SCN calyx.<sup>547</sup> Additional experiments revealed broad recognition of siderophores (Figure 2) by SCN: it adsorbs tricatecholates, carboxylates, hydroxamates,<sup>547</sup> the monocatecholate breakdown products of Ent (DHBA, DHBS),<sup>548</sup> and carboxymycobactins.<sup>549</sup> Epithelial cells secrete another lipocalin, LCN1, in tears and respiratory secretions,<sup>550</sup> that binds an array of siderophores, including hydroxamates, but with lesser affinity, so its role in innate immunity may be secondary to the more efficient SCN.<sup>547</sup> Transcriptional microarrays that monitor host gene expression demonstrated that colonization of nasal passages by *Streptococcus pneumoniae* or *H. influenzae* induced expression of host SCN to higher levels.<sup>551</sup> Neither of these pathogens produces their own siderophores, but they utilize xenosiderophores of other microorganisms, so enhanced production of SCN naturally counteracts their infectivity. Similarly, the presence of bacteria in bronchial epithelium induces the influx of myeloid cells, resulting in increased SCN production. Consistent with these inferences, SCN-deficient mice were more susceptible to intraperitoneal or intratracheal infection with *E. coli*,<sup>552</sup> and more bacteria were found in their lungs. The protective effects of SCN were counteracted by administration of high doses of Fc.<sup>553</sup> These data all supported a major role for SCN in counteracting bacterial pathogenesis.

## 6.2. Glycosylated Catecholates: GEnt/FeGEnt

Despite the efficacy of SCN in neutralizing microbial siderophores, bacterial pathogens adapt to escape SCN-mediated defenses. As noted above, they synthesize and/or utilize GEnt/FeGEnt (see also below, section 5.2.2), that SCN does not efficiently bind.<sup>124</sup> The micromolar affinities of SCN for GEnt/FeGEnt are a thousand-fold lower than for Ent/FeEnt,<sup>124</sup> so the protein does not clear the glucosylated catecholates from blood, serum, lymph, or other fluids.<sup>554-556</sup>

## 6.3. Mixed Chelation Siderophores

Other noncatecholate siderophores also evade inhibition by SCN, including Abn, Ybt, and Pvd and Pch from *P. aeruginosa*. In part because of their SCN-resistance, Abn enhances the hypervirulent phenotype of *K. pneumoniae* in lung infections,<sup>324</sup> and Ybt increases the virulence of *Y. pestis* in the manifestations of bubonic plague.<sup>332</sup> Molecular modeling of the binding interactions between Ent or Pvd to SCN concluded that SCN readily adsorbs the former but not the latter.<sup>438</sup> Although Pvd docked to SCN in nine potential positions, none of them occurred in the binding cleft that adsorbs other siderophores. These data rationalize the finding that Pvd promotes colonization of *P. aeruginosa* in patients with cystic fibrotic lungs.<sup>438</sup> SCN also acts in the microbial ecology of the gut. Nonpathogenic *E. coli* that produce GEnt (*e.g.*, Nissle 1917) outcompete and reduce the numbers of pathogenic *S. typhimurium* in the intestines of normal mice that were used as a model of acute colitis and chronically persistent infections. In SCN-deficient mice, however, Nissle 1917 did not outcompete *S. typhimurium*.<sup>305</sup> *Bacillus anthracis* similarly evolved mechanisms to escape SCN-mediated iron deprivation. It produces two siderophores, Crn and petrobactin (Pbn); SCN adsorbs the former but not the latter. However, a combinatorial, genetically engineered

version of SCN selectively bound Pbn instead of Cbn, with even higher affinity ( $K_D = 20$  pM). The novel binding protein, called “petrocalin” was crystallographically solved, and when administered together with SCN it suppressed growth of *Bacillus cereus* under iron-limiting conditions. The reprogrammed SCN, petrocalin, may offer new treatment options for serious infections caused by *B. anthracis*.<sup>557</sup> Similar reshaping of SCN improved its binding of siderophores from *P. aeruginosa*.<sup>558</sup>

## 7. SIDEROPHORE–ANTIBIOTIC CONJUGATES (TROJAN HORSE ANTIBIOTICS)

### 7.1. Uptake of Trojan Horse Antibiotics by *E. coli*

The potential clinical applications of siderophores were hypothesized and realized soon after their discovery.<sup>56</sup> The first example was the ability of apoferritoxamine B (Figure 3, also called desferrioxamine B, desferal),<sup>559–561</sup> to combat hemochromatosis and reduce iron overload by excretion of ferrioxamine B in the urine.<sup>559</sup> Coulton *et al.*<sup>562</sup> subsequently discovered that even when conjugated to a large polymer, Fc was capable of TonB-dependent iron supply to *E. coli*, and Rogers *et al.*<sup>563,564</sup> showed that transition metal complexes of Ent had bacteriostatic effects on pathogenic bacteria. Soon thereafter,  $\beta$ -lactams conjugated to catecholates and related moieties were found active against *E. coli*, other members of *Enterobacterales*, and *P. aeruginosa*.<sup>565–570</sup> Furthermore, uptake of the catechol-containing cephalosporin E0702 (Figure 4) was TonB-dependent,<sup>571</sup> and it produced spontaneously resistant, 100- to 1000-fold less susceptible mutants of *E. coli* that mapped to the *tonB* locus.<sup>571</sup> Lastly, the antibacterial potency of E0702 was enhanced in iron-deficient conditions but lost in iron-replete and reduced in anaerobic conditions,<sup>119</sup> where TonB-independent pathways facilitate uptake of soluble  $\text{Fe}^{2+}$ , leading to downregulation of LGP expression.<sup>572</sup> These studies provided the key evidence that Gram (–) bacteria actively transport catechol-containing antibiotic compounds with iron-regulated LGP. Miller *et al.*<sup>573</sup> designated siderophore–antibiotic conjugates as Trojan Horse antibiotics.

To further characterize the uptake pathways, Curtis *et al.*<sup>574</sup> studied catechol–cephalosporins and evaluated their antibacterial activity against mutants with disruptions in one or more TonB-related genes. Single mutants in *tonB*, *exbB*, *exbD*, and *cir* had significantly elevated minimal inhibitory concentrations (MIC) for catechol-conjugated cephalosporins, but only mutant strains lacking both *fiu* and *cir* had elevated MIC values (as much as 1000-fold), which was comparable to *tonB* mutants.<sup>574</sup> The double *fiu-cir* mutant also exhibited dramatic MIC shifts for the catechol–cephalosporin E0702 and the hydroxypyridinone–monobactam, pirazmonam (Figure 4).<sup>204</sup> Uptake of the <sup>55</sup>Fe-chelate of a catechol–cephalosporin confirmed that both TonB and Fiu/Cir participate in transport of the ferric catechol–cephalosporin complex, consistent with the MIC shifts observed for the mutants.<sup>574</sup> Wild-type cells transported both the unliganded and ferric E0702 at equivalent rates, but uptake of both forms was lost in the *fiu-cir* double mutant.<sup>204</sup>

Trojan Horse antibiotics involve, mimic, or capitalize on the native iron acquisition systems and siderophores of the target bacteria. Consequently, the chemistry and biology of the

iron acquisition pathways are essential to the design of antibiotic compounds against them. *A priori*, it is difficult to evaluate the contributions of the various potential catecholate iron complexes in the microenvironment of a bacterium that is producing and excreting Ent/GEnt. The efficacy of the degradation products (such as mono- and dicatecholates) in complexing and supplying iron may depend on whether other, potentially more avid siderophores are present. However, members of Enterobacterales and other Gram (–) Families produce TonB-dependent uptake systems for ferric monocatecholates. Nikaido *et al.*<sup>204</sup> suggested that the natural ligands of Fiu and Cir are the monocatechol hydrolytic products of Ent: DHBS and/or DHBA. The latter is most relevant as a biosynthetic byproduct, rather than a degradation byproduct. Besides the prokaryotic monocatechols, the eukaryotic catecholamine stress hormones epinephrine, norepinephrine, and dopamine are relevant to this phenomenon.<sup>575-577</sup> They are proposed to release iron from TF/LF, making it available to support bacterial growth, mediated by the scavenging actions of bacterial siderophores or the catecholamine iron complexes themselves.<sup>577</sup> Even in the absence of TF/LF, dopamine promoted *S. enterica* growth and increased iron uptake from the medium.<sup>575</sup> *Bordetella bronchiseptica* utilizes ferric-norepinephrine to support growth of a siderophore-deficient mutant due to the presence of three TonB-dependent catecholamine transporters.<sup>576</sup> These receptors can also recognize the Ent component DHBA.<sup>576</sup> It is noteworthy that in the presence of equivalent concentrations of tricatecholate siderophores like Ent, GEnt or Vbn, monocatecholates are not thought to significantly contribute to extracellular iron scavenging. The intact tricatecholates will monopolize Fe<sup>3+</sup> because of their much higher affinity. Nevertheless, as discussed above (section 4.4), the affinity of a chelate for iron is not the only consideration that determines its overall importance to iron utilization. Siderophores complex Fe<sup>3+</sup> over a broad range of affinities;<sup>59,60</sup> lower affinity siderophores like Pch<sup>439</sup> and Abn<sup>59</sup> still effectively bind iron, and their cognate LGP internalize the iron complexes *via* TonB-dependent reactions. Gram (–) bacteria also efficiently transport monocatecholate ferric complexes supplied at appropriate external concentrations.<sup>578-580</sup> Analogously, LGP (*e.g.*, EcoFiu and EcoCir) actively transport catecholate siderophore–antibiotics (such as those in Figure 4) by virtue of their chemical similarity to native monocatecholate compounds. In contrast to most natural siderophores, and like the degradation products of Ent/GEnt, synthetic siderophore  $\beta$ -lactam conjugates (*S* $\beta$ LC) have a single bidentate Fe<sup>3+</sup> chelation ligand (Figure 4) and show orders of magnitude lower affinity for Fe<sup>3+</sup><sup>581</sup> than Ent/GEnt<sup>58</sup> or other relevant siderophores (*e.g.*, Pvd<sup>582</sup>). Iron-regulated LGP are expressed at higher levels in iron-deficient conditions,<sup>119,204,574,583</sup> so the antibacterial activity of Trojan Horse conjugates increases in low-iron media<sup>119,204,574,583</sup> despite the fact that Fe<sup>3+</sup> levels are below the  $K_D$  of Fe*S* $\beta$ LC binding to their OM receptors and further decrease as bacteria secrete high-affinity siderophores.<sup>583</sup> This situation suggests the possibility that the relevant LGP also recognize and transport apo-*S* $\beta$ LC. Some ferric siderophore receptors bind the corresponding aposiderophore (*e.g.*, Ent/FepA; Pvd/FpvA<sup>584</sup>), but this association has minimal biological significance because LGP optimally recognize the metal center of ferric siderophores, often stereospecifically.<sup>585-589</sup> Ferric siderophores always adsorb to their receptors with higher affinity than the corresponding aposiderophores. Consequently, in a binding equilibrium involving both forms, the ferric siderophore predominates. It is plausible that both apo- and ferric complexes of *S* $\beta$ LC may be recognized and transported

by LGP, but uptake of an aposiderophore is intuitively counterproductive and has not been demonstrated. Besides the apo- and ferric complexes of  $S\beta LC$ ,<sup>204</sup>  $S\beta LC$  may form complexes with alternative divalent cations ( $Zn^{2+}$ ,  $Ca^{2+}$ , or  $Mg^{2+}$ ) that are present in culture media or host tissues, and may also form mixed, “piggyback” complexes with ferric siderophores (e.g., pAcn or Pvd) to gain entry through the cell envelope.<sup>590</sup>

## 7.2. Spectrum of Trojan Horse Antibiotic Activity

Besides the susceptibility of *E. coli* to siderophore–antibiotics,  $S\beta LC$  are potent and effective against other Gram (–) bacteria, including *P. aeruginosa* and *A. baumannii*.<sup>119,591-593</sup> The repertoire of iron-regulated LGP varies among Gram (–) pathogens, but orthologues of *E. coli* Fiu, FepA, and Cir exist across the Family Enterobacterales<sup>432</sup> and other Families as well, although these relationships are mostly bioinformatically defined and not yet experimentally validated. In *P. aeruginosa*<sup>432,592,594-597</sup> and *A. baumannii*,<sup>432</sup> for example, the OM proteins PiuA/D and PirA were implicated in  $S\beta LC$  uptake. Disruption of one or both of the genes encoding these proteins, in both organisms, reduced susceptibility to  $S\beta LC$ .<sup>432,592,594-596</sup> PiuA is most homologous to Fiu; PirA is most homologous to FepA.<sup>432</sup> Expression of both proteins is regulated by Fur<sup>598,599</sup> in response to extracellular iron availability and potentially by iron uptake through other pathways. The *P. aeruginosa* genome encodes 34 different LGP, whose specificities and natural ligands are mostly undefined. Iron deprivation leads to >2-fold upregulation for nearly half of the *P. aeruginosa* LGP; expression of FptA, the receptor for FePch,<sup>594</sup> increases as much as 120-fold. The expression levels of these proteins during infection is not known, but in a *P. aeruginosa* *piuA* mutant as many as 7 LGP significantly affected susceptibility to  $S\beta LC$ ,<sup>594</sup> suggesting that multiple OM proteins may actively transport  $S\beta LC$  via TonB-dependent pathways. In each target organism,  $S\beta LC$  potency is a function of the relevant LGP expression level, its affinity for the siderophore–antibiotic, potential competition with other natural iron-binding ligands, and overall uptake efficiency.

## 7.3. Cefiderocol, The First FDA-Approved Trojan Horse Antibiotic

The first and only FDA-approved Trojan Horse antibiotic is the catechol–cephalosporin conjugate cefiderocol (Fetroja; FDC, Figure 4), that was authorized for treatment of complicated urinary tract infections, including pyelonephritis.<sup>592,600-602</sup> FDC is potent against critical Gram (–) pathogens including carbapenem-resistant *P. aeruginosa* and *A. baumannii*, due to the combination of uptake via LGP, good stability against all classes of carbapenemases, and its covalent inhibition of target PBPs.<sup>581,592,594,602</sup> The branded name of FDC, Fetroja, reflects its transport through iron (Fe) siderophore uptake like a Trojan Horse (troja). Because of the enhanced uptake of FDC by LGP and *in vivo* pharmacokinetic/pharmacodynamics (PK/PD) correlations to MIC, the standard medium for FDC susceptibility testing is iron-depleted, cation-adjusted Mueller–Hinton broth (final [Fe] < 0.10 mg/L, [Ca] = 22.5 mg/L, [Mg] = 11.25 mg/L, [Zn] = 0.65 mg/L).<sup>583</sup> FDC utilizes the typical pathogen-specific LGP identified for other  $S\beta LC$  (e.g., Fiu-Cir or PiuA-PirA),<sup>592,594,596</sup> but an alternative uptake pathway for FDC uptake through FptA may exist in a pyochelin-dependent manner.<sup>590</sup>



Earlier  $S\beta LC$ , such as MB-1 (Figure 4) and SMC-3176, failed to show efficacy in animal infection models and suffered from “adaptive resistance” *in vitro*.<sup>596,603,604</sup> FDC avoids the adaptive resistance liability compared to MC-1, MB-1, and SMC-3176.<sup>604,605</sup> In the case of *P. aeruginosa*, increased levels of Pvd were implicated in adaptive resistance to MB-1.<sup>603,606</sup> Higher Pvd levels would be expected to result in more efficient  $Fe^{3+}$  uptake, higher cytosolic Fe levels, and downregulation of the preferred  $S\beta LC$  LGP. Although FDC seems to avoid the adaptive resistance liability of other  $S\beta LC$ , *in vivo* efficacy studies with humanized exposures of FDC identified clinical isolates of both *P. aeruginosa* and *A. baumannii* against which FDC underperformed or did not demonstrate expected efficacy.<sup>605</sup> A significant 10–20% of these isolates did not achieve bacterial stasis or  $1\text{-log}_{10}\text{-CFU}$  reduction despite having MIC values that predicted susceptibility. The results with many isolates also showed high variability due to inconsistent responses to FDC among the replicates.<sup>605</sup> Whether these issues relate to adaptive resistance is not known. While FDC has potent antibacterial activity against Gram (–) pathogens, as a cephalosporin, it is still hydrolyzed by clinically relevant  $\beta$ -lactamases.<sup>602</sup> It is worth noting that  $S\beta LC$  that show adaptive resistance liability (*e.g.*, MC-1, MB-1, and SMC-3176) all contain hydroxypyridinone chelation groups, whereas FDC is based on chelation by a catecholate (Figure 4).<sup>596</sup> Another catechol-containing  $\beta$ -lactamase inhibitor LN-1-255 (a substituted penicillin sulfone) was reported, though nothing was known about whether it promotes adaptive resistance or is transported by an LGP.<sup>607</sup> The only other  $S\beta LC$  to enter clinical trials, BAL30072, was also a hydroxypyridinone siderophore (Figure 4). It did not show adaptive resistance,<sup>432,594,595</sup> but its development was suspended in phase 1.<sup>608</sup>

#### 7.4. Non- $\beta$ -Lactam Siderophore Conjugates

Decades before FDA approval of FDC, a diverse group of non- $\beta$ -lactam siderophore–antibiotic conjugates were described and studied. The research began with natural sideromycins, albomycins,<sup>609–613</sup> and salmycins;<sup>614</sup> the former showed broad spectrum antibacterial activity against Gram (+) and Gram (–) bacteria in a murine infection model,<sup>615</sup> but the latter were less effective, likely as a result of its chemical lability. Synthetic siderophore–antibiotic conjugates were subsequently developed that required some form of cleavage for full activity.<sup>616–619</sup> While the targets of  $\beta$ -lactam antibiotics, penicillin-binding proteins, reside in the periplasm, many other systems or pathways that are susceptible to antibiotic action reside in the cytoplasm. So although LGP may deliver siderophore–antibiotics into the periplasm, the IM poses a second permeability barrier, especially to charged/polar compounds.<sup>620</sup> However, appropriate IM ABC transporters may recognize and internalize the ferric siderophore moiety of Trojan Horse compounds, with concomitant uptake of the attached antibiotic. Nolan and co-workers created Ent-antibiotic conjugates, beginning with Ent- $\beta$ -lactam conjugates that are active in the periplasm.<sup>618</sup> The uptake of the conjugate depended on FepA and provided 1000-fold lower MIC than the  $\beta$ -lactam alone.<sup>618</sup> They later conjugated Ent to ciprofloxacin (CIP), whose targets (DNA gyrase and topoisomerase IV) reside in the cytoplasm.<sup>617</sup> In the latter case, the Ent-CIP conjugate crossed the OM *via* FepA-TonB/ExbBD and then crossed the IM by FepCDG.<sup>617</sup> Ent-CIP was inactive unless hydrolyzed by the salmochelin esterase IroD in the cytoplasm to release the DHBS-CIP monomer.<sup>617</sup> An alternative strategy for cytoplasmic release of CIP employs

a disulfide linker in the Ent-CIP conjugate that may be cleaved by the cytoplasmic low-molecular-weight thiols like glutathione.<sup>617</sup>

Miller and co-workers used other siderophores and cleavage strategies for cytoplasmic antibiotic delivery and release.<sup>616,619</sup> They first conjugated desferrioxamine B to CIP with potential esterase- and phosphatase-susceptible linkers.<sup>621</sup> The esterase-triggered conjugate had weaker activity than that of the parent CIP, while the phosphatase-triggered conjugate was inactive.<sup>619</sup> These results revealed the extent of optimization needed when considering all the uptake and implementation variables: OM and IM transport, enzymatic cleavage, and target engagement. The Gram (–) OM creates a potentially insurmountable permeability barrier<sup>27,28</sup> to many antibiotics that are active against Gram (+) cells. For example, oxazolidinones target the ribosome but are limited to Gram-positive pathogens, even though their ribosomal target is conserved in Gram (–) bacteria like *E. coli*. Consequently, Miller and co-workers designed a clever siderophore–cephalosporin–oxazolidinone conjugate,<sup>616</sup> whose cleavage depended on periplasmic hydrolysis by cephalosporinases, releasing the free oxazolidinone.<sup>616</sup> This conjugate, that contains a bis-catechol siderophore, boosted cephalosporin activity against periplasmic PBP. Although expression of the cephalosporinase impacted the potency of the cephalosporin core, the consequent release of the oxazolidinone provided a significant boost in antibacterial potency.<sup>622</sup> Another study conjugated bis-catechol or bis-catechol-monohydroxamate to teicoplanin, which normally targets the PG D-Ala-D-Ala termini of only Gram-positive bacteria because it cannot penetrate the OM of Gram (–) bacteria.<sup>623</sup> Interestingly, the siderophore–teichoplanin conjugates demonstrated potent activity in *A. baumannii* but not *E. coli* or *P. aeruginosa*, despite the fact that their PG targets are identical.<sup>623</sup> These data suggest differences in the LGP-mediated uptake pathways among the different bacteria. Compared to SβLC, the challenges to synthesize, characterize, and develop synthetic sideromycins are daunting. Nevertheless, antimicrobial resistance is inevitable for every new drug, so the development of all types of Trojan Horse antibacterials remains a desirable long-term goal.

## 8. MECHANISTIC INSIGHT FROM BIOINFORMATIC ANALYSES OF TONB-DEPENDENT SYSTEMS

As a consequence of their high rate of antibiotic resistance, the Gram (–) CRE/ESKAPE pathogens<sup>33,34</sup> cause a large fraction of nosocomial infections, and clinical options against them are limited.<sup>31,32,36</sup> Both strategic design of antibiotics and large scale screening of chemical libraries for compounds that may block iron acquisition in these organisms hinge on the understanding of LGP transport biochemistry. The bacteria under discussion in this analysis represent four phylogenetic Families: Enterobacterales, Moraxellaceae, Pseudomonadaceae, and Yersiniaceae. Together, they inhabit different natural environments, but each one has adapted to infect humans and animals, in part from OM permeability properties that differ from those of *E. coli*, the prototype of Enterobacterales. For example, clinical isolates of *K. pneumoniae*, in the same Family, have much lower overall OM permeability from the absence of certain porins<sup>624-627</sup> and higher serum resistance from enhanced capsule formation.<sup>628,629</sup> The latter trait was maximized in the highly virulent,

hypermucoviscous form that also manifests more efficient iron acquisition.<sup>630,631</sup> Both *P. aeruginosa*<sup>632-635</sup> and *A. baumannii*,<sup>636-638</sup> in the Families Pseudomonadaceae and Moraxellaceae, respectively, have similarly low OM permeability, and their iron-regulated formation of biofilms<sup>639-641</sup> constitutes an additional virulence determinant. Lastly, Ybt, the primary siderophore of *Y. pestis*, was co-opted by members of the other families in ways that augment their virulence.<sup>326,358,376</sup> Such adaptations illustrate the connections between cell envelope architecture, the mechanisms of TonB-dependent iron acquisition, and pathogenic virulence.

### 8.1. Sequence Diversity in TonB

TonB action encompasses a number of biochemical activities that are potential targets for chemical inhibition: binding to the TonB-box of LGP,<sup>239,240</sup> physical interactions with ExbBD,<sup>232,233</sup> and associations with PG<sup>238</sup> that may involve monomer–dimer conversions<sup>91,241</sup> and other currently un-delineated aspects of the transport process. Besides their microbiological and ecological diversity, each ESKAPE bacterium acquires multiple ferric siderophores, some of which correlate with their invasiveness, tissue tropism, or overall virulence (*K. pneumoniae*, FeAbn; *P. aeruginosa*, FePvd; *A. baumannii*, FeAcn; *Y. pestis*, FeYbt). Consequently, their TonB proteins must physically interact with multiple iron-transporting LGP. The primary structures of these TonB orthologues are unusually variable. The extent of EcoTonB (NCBI: NP\_415768.1) sequence identity to KpnTonB (CAA48498.1), PaeTonB (Q51368.2), and AbaTonB (AHB92731.1) is 75%, 37%, and 25%, respectively; a CLUSTALW2 alignment of the four TonB proteins showed only 11% identity (26 of 239 residues). This divergence among TonB proteins indicates that the component proteins of the individual OM iron transport systems are uniquely adapted to one another in each species and explains why the LGP from one species do not necessarily function in other species. Structural data is only available for the C-terminal domain of EcoTonB, but both bioinformatic predictions and biochemical data suggest that the 239 aa EcoTonB encompasses a hydrophobic N-terminal helix in the IM,<sup>238,642</sup> a central rigid region that spans the periplasm,<sup>236,643,644</sup> and a globular, periplasmic C-terminal domain (CTD) that associates with the LGP in the OM.<sup>239-241,645,646</sup> Most of the conserved residues among the four noted TonB proteins reside in the central, ~75-residue rigid region (9 Pro, 4 Lys and 2 Glu), whereas the ~75-residue CTD, that recruits TonB-box peptides of LGP into a four-stranded  $\beta$ -sheet, contains only six conserved identical residues (5 Val, 1 Phe). This structural variability suggests that it is unlikely to find a generic, broad-spectrum inhibitor of TonB activity that functions across distantly related bacterial pathogens. Yet, an HTS screen against EcoTonB discovered numerous compounds that also inhibited the activity of AbaTonB,<sup>272</sup> so despite *a priori* skepticism, a broad-spectrum anti-TonB antibiotic is conceivable.

The conserved identical residues in the CTD of ESKAPE TonB proteins localize to internal regions of both the dimeric<sup>241</sup> and monomeric<sup>239,240,647</sup> forms. The hydrophobic nature of the conserved residues and their internal localization infer that they stabilize the domain's tertiary structure. Since the completion of the crystal structures of the TonB CTD in different forms, including its association with the TonB-box of LGP,<sup>241,645-647</sup> few experiments reflected on the functional relationships between its monomeric and dimeric forms. Yet, the

crystallographic demonstration of interactions between the monomeric TonB CTD and LGP N-termini validated the relevance of the monomer, and the interactions of the dimer with PG in the bacterial periplasm had implications on the potential mechanism of TonB action.<sup>91,238</sup>

## 8.2. Commonality of FeEnt Transport by Prototypic FepA Proteins

Each of the four CRE/ESKAPE organisms secretes different siderophores and utilizes different ferric xenosiderophores by the actions of unique LGP, but they all also efficiently transport FeEnt<sup>120,285</sup> with orthologues of EcoFepA. The *E. coli* protein is an accessible prototype of both active OM transport and biochemical interactions with TonB. The comparative bioinformatic analysis of EcoFepA orthologues (see below) reveals unexpected aspects about the capture of ferric catecholates by Gram (–) bacterial pathogens.

**8.2.1. EcoFepA.**—Laboratory *E. coli* K-12 strains produce Ent and transport FeEnt through EcoFepA, but pathogenic *E. coli* (UPEC, EHEC; Table 1) also glucosylate the siderophore and transport FeGEnt through orthologues of Iron. The primary structures of EcoFepA and EcoIron are only 52% identical, intimating a potentially significant divergence of specificity and function.

**8.2.2. KpnFepA.**—*K. pneumoniae* encodes four apparent orthologues of EcoFepA in its genome: three in the chromosome [*loci* 1658 (KpnFepA1), 2380 (KpnFepA2), 4984 (KpnFepA4)] and one (*locus* 0027: *KpnIron*) from an endogenous plasmid. The resulting four FeEnt receptors are 82%, 53%, 73%, and 53% identical to EcoFepA, respectively.

**8.2.3. AbaFepA.**—*A. baumannii* produces a single LGP (AbaFepA) that catalyzes FeEnt uptake, and has 46% sequence identity with EcoFepA. Despite being the most distant orthologue to EcoFepA in the CRE/ESKAPE group, AbaFepA still retains sufficient identity (*i.e.*, >30%<sup>648,649</sup>) to predict a conserved tertiary structure.<sup>648</sup>

**8.2.4. PaeFepA.**—Like *K. pneumoniae*, *P. aeruginosa* strain PAO1 contains the structural genes for 3 FepA orthologues, as well as Iron, all in its chromosome. PaeFepA1, PaeFepA2, and PaePfeA share 71%, 81%, and 61% identity with EcoFepA; the sequence of PaeIron is 60% identical to that of EcoIron.

When grown to low-iron stress in iron-deficient MOPS media,<sup>650</sup> the four CRE/ESKAPE pathogens comparably transport FeEnt like *E. coli* K-12.<sup>285</sup> Despite their sequence divergence, the ESKAPE FepA orthologues all have sufficient identity to predict a nearly identical overall structural fold as EcoFepA (1FEP<sup>196</sup>), but like TonB, their primary structures have evolved in *K. pneumoniae*, *A. baumannii*, and *P. aeruginosa* such that they are not generally interchangeable among the four species. Closely related KpnFepA transports FeEnt when expressed in *E. coli*, but more distant PaeFepA and AbaFepA do not partner with EcoTonB to catalyze FeEnt uptake in *E. coli* (Nairn, Newton, Kumar and Chakravorty, unpublished data). This situation reinforces the notion that TonB and LGP concomitantly evolved in the different species. Therefore, compounds that inhibit TonB-dependent Fe<sup>3+</sup> uptake in *E. coli* may not similarly block iron uptake in *K. pneumoniae*, and even less so in *P. aeruginosa* or *A. baumannii*. Hence, each CRE/ESKAPE pathogen will likely exhibit different susceptibilities to compounds in chemical libraries, and potential

inhibitors of TonB-dependent processes may require species-specific evaluation and/or optimization to attain appropriate efficacy.

### 8.3. Other Ferric Catecholate Transporters

At least six LGP participate in uptake of ferric siderophores in *E. coli* K-12: Fiu, FecA, FepA, FhuE, FhuA, and Cir. Expanding the scope to pathogenic *E. coli* adds IutA, IroN, ChuA, and FyuA;<sup>651</sup> consideration of vitamin B<sub>12</sub> (cyanocobalamin) includes BtuB.<sup>652</sup> The fact that among 11 *E. coli* LGP, five (FepA, IroN, Fiu, FecA, Cir) function in the uptake of ferric catecholates underscores the importance of this class of siderophore to bacterial iron acquisition. With the exception of IroN, the structures of these ferric catecholate transporters were independently crystallographically determined. However, the scope of their recognition specificities and binding preferences are only now becoming fully known.<sup>285</sup> Orthologues of EcoFepA are broadly distributed among members of Enterobacteriales and other Families, to selectively recognize and transport FeEnt, but the chemical lability of the catecholate trilactone siderophore makes its degradation products, that include mono-catecholates (Figure 3), also relevant to iron acquisition by the spectrum of Gram (–) bacteria. Within a few days of forming and purifying FeEnt,<sup>66</sup> its visible absorbance spectrum begins to change, even if the ferric siderophore is stored on ice or frozen. Chromatography over Sephadex LH20 reveals a rapidly mobile, purple peak of oxidized FeEnt (FeEnt\*) that separates from the crimsoncolored authentic FeEnt.<sup>214</sup> These changes primarily derive from oxidation of the catechol groups at the metal center to quinones. Furthermore, the lactone backbone is susceptible to cleavage by acid, base, and esterases. Consequently, the monomeric iron–catecholate complexes, formed by the degradation products of FeEnt, inhabit the environments that bacteria experience in the host. Cir<sup>574</sup> and Fiu<sup>204</sup> participate in the transport of monocatecholate iron complexes [*e.g.*, Fe(DHBS)<sub>3</sub>] and catechol-containing antibiotics.<sup>653,654</sup> GEnt is secreted by uropathogenic *E. coli*, *S. enterica*, and *K. pneumoniae*, whereas Crn<sup>267,655,656</sup> is a similar but distinct catecholate from Gram (+) bacteria. Collectively, the catecholate siderophores create a myriad of possible iron complexes that bacterial pathogens may utilize to different extents and priorities.

The approximately one dozen iron-transporting LGP in *E. coli* expand into a plethora of LGP in some other organisms. The genomes of *C. crescentus* and *P. aeruginosa* encode 66 and 34 LGP, respectively. Besides a similar cadre of iron-regulated LGP,<sup>194</sup> one of the *C. crescentus* receptors performs TonB-dependent transport of maltodextrins,<sup>658,659</sup> and others are predicted to transport a variety of substrates besides metal complexes. The primary, secondary, and tertiary structures of proteins in the LGP superfamily create a consistent structure/function paradigm. The external hydrophobic surfaces of their amphiphilic transmembrane  $\beta$ -barrels interact with OM lipids, while their internal hydrophilic surfaces circumscribe an aqueous channel and envelop the N-terminal, 150-residue globular domain that interacts with TonB/ExbBD to regulate ligand movement through the pore. Large surface loops that selectively bind ligands and short reverse  $\beta$ -turns between the  $\beta$ -strands of the barrel complete LGP architecture. Despite this conserved format, variability of their surface loops results in a relatively low overall sequence identity in the superfamily. The *E. coli* LGP only average about 20% overall identity between any

two individual proteins despite much higher levels of identity in the strands of their  $\beta$ -barrels. The highest degree of conservation of primary structure among *E. coli* LGP is the 52% identity that occurs between FepA and IroN, the receptors for FeEnt and FeGEnt. The low overall sequence identity among EcoLGP is somewhat unexpected because they all physically interact with EcoTonB and likely function by the same general mechanism. However, sequence divergence in the surface loops confers unique ligand recognition specificity to each individual LGP. Furthermore, this ligand selectivity occurs in the context of antigenic variation in the same external loops to evade the vertebrate immune response. The biochemical selectivity created by the external loops impacts the actions of Trojan Horse antibiotics. For instance, both mono- or di- glucosylated Ent (GEnt) derivatized with ampicillin or amoxicillin showed improved antibacterial activity and evaded scavenging by SCN from the host. Both siderophore-antibiotics had a narrow application range that selectively killed pathogenic *E. coli* (expressing IroN) but not nonpathogenic *E. coli* (lacking IroN).<sup>660</sup> These findings suggest that the recognition of particular iron complexes by LGP may be exploited with Trojan Horse compounds to only target pathogens that produce those siderophores and/or utilize their iron complexes. These are significant advantages over wide-spectrum antibiotics and potentially superior for clinical applications.

#### 8.4. Biphasic Ligand Adsorption

The initial stage of ligand adsorption is a mechanistically well-defined aspect of LGP-mediated iron transport. Payne *et al.*<sup>661</sup> demonstrated biphasic binding kinetics for the interactions of both FeEnt and ColB with EcoFepA. Subsequent studies refined this conclusion for EcoFepA<sup>219</sup> and EcoFecA,<sup>197</sup> in the former case with chemical cross-linking studies and in the latter case by crystallographic depictions that showed conspicuous motion of surface loop 7 (L7) in the transition from the ligand-free to the FeCit-bound form of the receptor. Crystallographic characterizations and simulations of PaePfeA found potential FeEnt binding sites in both its surface loops and within its external vestibule, supporting the two-stage nature of FeEnt binding.<sup>662</sup> Furthermore, fluoresceination of individual Cys substitutions in EcoFepA<sup>220</sup> allowed descriptions of the loop motion that LGP undergo during ligand adsorption: stopped-flow measurements of fluorescence quenching showed that they move at different rates, individually and independently, as they capture FeEnt from the environment. The two-stage kinetic process thus resolves into rapid initial interactions of the ligand with surface loop residues that engender a slower second stage of conformational motion as loops coalesce around the metal complex by induced fit, creating a high-affinity form at equilibrium. The process of ligand acquisition by the surface loops of FepA is analogous to a hand catching a ball from the air: the ball collides with the open hand, and then the fingers individually move to close around it.<sup>220</sup> In that sense, in iron-deficient conditions the Gram (-) bacterial cell surface becomes infused with thousands of molecular hands, each adapted to catch a particular type of iron complex for subsequent translocation into the cell.

As noted for FepA, biphasic binding kinetics correlate with a structural transition from a form with open, extended loops to a form with contracted loops that surround the bound ligand.<sup>219</sup> Crystal structures of EcoFiu reiterated this conclusion.<sup>663</sup> Like other TonB-dependent transporters, Fiu contains a 22-stranded  $\beta$ -barrel, covered by extracellular

loops. Crystallography revealed two distinct structural states of Fiu: a conformation with disordered extracellular loops that form an open cavity to the extracellular environment, and a conformation with ordered, closed loops.<sup>663</sup> By opening and closing in this manner during ligand transport the dynamic actions of LGP maintain the natural permeability barrier of the OM. They allow ligand recognition and uptake while still excluding deleterious compounds like bile salts and antibiotics that may compromise the integrity of the IM bilayer, PG biosynthesis, or other processes in the periplasm.<sup>663</sup> As Dick van der Helm described it, the FepA channel functions like an air-lock: the external loops close before the internal domain opens.

### 8.5. Evolutionary Covariance and Conserved Sites of Mechanistic Importance

Despite 50 years of research on TonB-dependent membrane transport, the underlying molecular mechanism of metal internalization remains incompletely defined. Nevertheless, the mountain of available genomic information, mined by bioinformatic algorithms, yields insight into this conundrum. We aligned and analyzed 79 LGP sequences (Table 1) by CLUSTALΩ<sup>664</sup> (Figure S1) and BIS<sup>2,665</sup> which identified sequence conservation that reflects on the biochemical transport mechanisms of ferric siderophore and Hn receptors. The analyses also described the phylogenetic relationships of the proteins (Supporting Information, Figure S2). The collection of 79 proteins, that transport at least 16 different metal complexes, exposed an unexpected characteristic of LGP N-domains: the most significantly conserved and simultaneously covariant amino acids in the LGP N-termini are glycines (Figure 5). Among seven highly conserved residues (>90% identity) in the N-domains of 79 LGPs of bacterial pathogens, five were Gly. The other two conserved amino acids have basic side chains (R75, R126 in EcoFepA), that map adjacent to and pair with conserved acidic amino acids on the interior of the C-terminal  $\beta$ -barrel (E511, E567 in EcoFepA). In the full length primary structures of the 79 proteins, a total of 16 residues exhibited extensive identity, or evolutionary covariance, or both. Together they defined a charge cluster in LGP infrastructure,<sup>90</sup> situated among a group of conserved glycines (Figure 5). These data suggest two attributes of LGP ligand transport: an electrostatic channel-gating mechanism and conformational flexibility that promotes uptake functionality. The association of R75-E511 and R126-E567 in an ionic cluster on the channel wall, directly above the TonB-box and across the pore from the N-domain- $\beta$ -barrel junction, strongly suggests a protonation-based trigger to the ligand internalization process. Protonation of E511 and E567 is a key to unlocking this electrostatically closed channel because it will free the N-domain to movement. As in the case of LacY, the protein environment surrounding the R75-E511 and R126-E567 pairings may significantly change the  $pK_a$  values of the acidic side chains.<sup>666,667</sup> This inference concurs with the PMF-dependence of LGP-mediated transport,<sup>62,668</sup> but in an unexpected way that raises the question, does this biochemistry precede, coincide with, or follow the interaction of the TonB-box of LGP with the C-terminus of TonB? Second, five conserved Gly surrounding the charge cluster in the N-domain minimizes  $\phi/\psi$  steric hindrance to conformational motion, which reinforces conclusions from site-directed disulfide bonds within EcoFepA: disulfide links in the N-domain that precluded conformational motion also prevented FeEnt transport.<sup>669</sup> Thus, both bioinformatic and experimental results point to structural rearrangements within

the N-terminal globule, while resident in the transmembrane channel, allowing passage of FeEnt into the periplasm.

## 9. INTERVENTION AGAINST GRAM (–) BACTERIAL PATHOGENS

The indispensability of iron in aerobic metabolism, combined with the uniqueness of prokaryotic cell envelope iron acquisition systems, makes TonB-dependent transport activity a potentially susceptible target in the Gram (–) cell envelope. It is conceivable to either block uptake of iron complexes by immunochemical inhibition, or to chemically target the mechanisms of LGP biochemistry.

### 9.1. Immunological Approaches

Certain anti-LGP antibodies prevent the recognition and binding of ferric siderophores by adsorbing to loops that participate in the recognition process,<sup>670-674</sup> and these immunogenic epitopes are the basis of vaccines.<sup>675-677</sup> However, rough *E. coli* K-12 strains were used for many of the immunochemical analyses of these phenomena, which raises questions about their application to unattenuated, wild bacterial pathogens that are usually encapsulated and produce complete lipopolysaccharide (LPS) O-antigens. Full-length LPS shields Omp surface epitopes from antibody binding,<sup>678,679</sup> capsule accentuates this effect, and the cell envelopes of CRE/ESKAPE pathogens encompass both of these traits. Consequently, efficacious human vaccines against CRE/ESKAPE organisms from Gram (–) bacterial LGP are an uncertain prospect, and existing data substantiate these concerns.<sup>680</sup> Therapeutic monoclonal antibodies, that react with single or multiple epitopes of specific iron transporters, face similar obstacles to recognition of surface proteins in pathogenic bacteria and are costly to produce for clinical use. It is fair to say that the conceptual promise of immunological intervention against TonB-dependent iron uptake systems faces practical problems that will be difficult to circumvent or supersede.

### 9.2. Biochemical Targets of Antibiotic Action

The overall biochemistry of Gram (–) bacterial iron acquisition offers both specific and general molecular targets that are vulnerable to chemical inhibition. The former, specific category includes cell surface ligand binding reactions, intrinsic LGP mechanisms, and the activities of periplasmic binding proteins, ABC transporters, and ferric reductases that function during iron uptake. The latter, general category focuses on TonB: physical interactions between LGP and TonB, intrinsic TonB/ExbBD mechanisms, and interactions between TonB and ExbBD. The latter category is more desirable, but the notion of compounds that broadly inhibit TonB/ExbBD in a group of diverse pathogens is undercut by the known sequence diversity in the target proteins of these bacteria. The diversity originates from coevolution of LGP and TonB together in the unique cell envelopes of the ESKAPE organisms, as they propagate in different wild and host environments (see following). From the current understanding of TonB/ExbBD physiology,<sup>91,237</sup> inhibitors may block iron uptake by adsorbing to TonB's C-terminal domain (CTD), that interacts with PG<sup>238</sup> and with ligand-bound iron transporters,<sup>239,240,681</sup> or to the regions of TonB that interact with ExbBD.<sup>232,233</sup> The sequence diversity that was noted in the TonB proteins of the ESKAPE organisms (see section 8.1, above) also occurs in their FepA orthologues: the



extent of EcoFepA (NP\_415116.1) sequence identity to KpnFepA (EYB77073.1), PaeFepA (NP\_251378.1), and AbaFepA (KFG14278.1) is 81%, 61%, and 46%, respectively. Hence, in each individual bacterium, the LGP is adapted to the properties and components of its own cell envelope, including the nuances of the TonB/ExbBD complex. Hypothetically, chemicals that block TonB-dependent iron uptake in *E. coli* may not inhibit, or may have less efficacy against, *K. pneumoniae*, *P. aeruginosa*, and *A. baumannii*. Thus a search for broad-spectrum inhibitors of TonB action that are efficacious against all Gram (–) cells may not succeed. Specific inhibitors of TonB systems in each individual CRE/ESKAPE organism are a potentially realistic goal for HTS of chemical libraries. Because the activities of TonB/ExbBD occur in the periplasm or IM, potential antibiotics against TonB-dependent activity must also overcome the size and hydrophobicity barriers of the Gram (–) bacterial OM.<sup>28</sup> Efficacy depends in part on the cell envelope permeability properties of the individual target organisms, so it is most apt to directly screen chemical libraries against the pathogen of interest and subsequently assess whether specific hits that inhibit TonB-dependent processes may have generic activity. Alternatively, one may seek compounds that target and block specific iron transporters instead of TonB/ExbBD, for example, specific inhibitors of FeEnt uptake in *E. coli*, *K. pneumoniae*, or *A. baumannii*, or of FePvd uptake in *P. aeruginosa*. However, this approach is potentially compromised by the numerous, redundant iron uptake systems that exist in bacterial pathogens.

### 9.3. Fluorescent High-Throughput Screening (FLHTS)

A search for therapeutic chemicals requires an assay that identifies them. Kaback and colleagues extensively explored Cys scanning mutagenesis of the lactose permease of the *E. coli* cell envelope<sup>682-684</sup> and extended the approach to alkylation of single Cys residues<sup>685-688</sup> with fluorescent<sup>686,689-692</sup> or paramagnetic<sup>693-696</sup> probes. These biophysical modifications allowed determinations of internal distances, conformational change, sugar binding, and other parameters. Their studies with the lactose permease required preliminary mutagenesis to eliminate seven native Cys residues, followed by site-directed introduction of Cys at positions of interest into the so-called “Cys-less” LacY. However, Cys is often conveniently absent from Gram (–) bacterial OM proteins or involved in stable disulfide bonds when it is present. EcoFepA, for example, contains a single pair of Cys residues in L7 that are unreactive unless reduced.<sup>697</sup> Many porins, including most LGP, are devoid of Cys. Cao *et al.*<sup>698</sup> took advantage of this fact and employed site-directed fluoresceination to create a spectroscopic assay of FeEnt uptake by EcoFepA in living bacterial cells.<sup>698</sup> This methodology observes TonB-dependent FeEnt uptake by monitoring fluorescence quenching as bacterial transport the ferric siderophore. The *in vivo* approach surmounts our current inability to reconstitute TonB-dependent systems *in vitro* and confers the advantages of living cell-based assays: convenience, predictability, miniaturization, automation, and multiplexing.<sup>699</sup>

**9.3.1. Specific Fluoresceination of Heterologous Proteins.**—Once modified with a fluorophore in its surface loops, an LGP becomes a sensitive biophysical sensor for the detection, quantification, and flux of a particular metal complex in the environment. Fluoresceination usually does not impair either the specificity or affinity of an LGP for its ligand.<sup>220,285</sup> Hence, it is feasible to design and create fluorescent LGP sensors in the

individual pathogens of interest. Each CRE/ESKAPE bacterium poses challenges from their particular cell envelope architecture and biochemistry, which complicates the interpretation of HTS data and makes it advantageous to directly screen chemical libraries against the individual pathogens of interest. Lastly, each bacterium may transport specific ferric siderophores that correlate with their virulence (*K. pneumoniae*, FeAbn; *P. aeruginosa*, FePvd, FePch; *A. baumannii*, FeAcn); FLHTS methods have the ability to modify and analyze virtually any LGP in a living bacterium. The structural folds of approximately 20 LGP are crystallographically solved (Table 1), which simplifies the identification of optimal sites for localization of fluorescent probes.<sup>220,285,700</sup> Unsolved proteins may be modeled from the structures of solved orthologues. For example, AbaFepA in *A. baumannii* ATCC 17978 shares 46% sequence identity with EcoFepA in *E. coli* MG1655, resulting in a nearly conserved predicted tertiary structure<sup>196</sup> that accurately suggested good locations for fluoresceination.<sup>272</sup> However, caution is advised, because modeling of an orthologue/parologue with lower identity (*e.g.*, EcoFiu, 20% identical to EcoFepA) may significantly err in the delineation and disposition of LGP secondary structures and surface loop regions.

**9.3.2. Universal Fluorescent Sensors.**—Further development of the FLHTS concept revealed another approach that obviates the need to genetically engineer the LGP of individual pathogens for site-directed fluoresceination. Production of EcoFepA-FM in a *tonB E. coli* host creates a “sensor strain” that detects [FeEnt] and sensitively reports FeEnt depletion from solution. The *E. coli* sensor strain binds but cannot transport FeEnt because of its TonB-deficiency. By monitoring FeEnt-mediated quenching, the sensor strain observes FeEnt uptake by other bacteria in the same solution. This method creates a “universal” fluorescence assay of FeEnt uptake by any organism and readily adapts to uptake of any iron complex by any bacterium.<sup>285</sup> Both species-specific<sup>272,701</sup> and universal<sup>285</sup> FLHTS assays effectively function in microtiter plate format.

#### 9.4. Summary of Antibiotic Discovery

Several small-scale HTS studies conceived assays that targeted TonB-dependent uptake systems. Yep *et al.*<sup>273</sup> employed a whole-cell growth-based high throughput screen of 149 243 compounds against UPEC under iron-limiting conditions and found 16 compounds that arrested bacterial growth only under iron-limiting conditions, that were all bacteriostatic, and that did not inhibit proton motive force. Two of the compounds lost inhibitory activity against a TonB-deficient strain. Nairn *et al.*<sup>272</sup> used FLHTS to identify inhibitors of TonB function in *E. coli* K-12 and *A. baumannii*. In a screen of 17 441 compounds, 165 primary hits inhibited TonB-dependent FeEnt uptake at a level of at least 30%. Among 20 of the primary hits that were further analyzed with respect to TonB-dependent ferrichrome uptake, colicin killing, and proton-motive force-dependent lactose transport, six of the compounds blocked TonB activity in all tests without affecting lactose uptake. Lastly, Bailey *et al.*<sup>702</sup> conducted HTS of 110 000 compounds for inhibitors of Abn biosynthesis<sup>324</sup> in hypervirulent *K. pneumoniae*. As noted above, Abn is a virulence factor for Hv *Kpn*. The HTS system utilized a sensitive malachite green-based assay, in which an inorganic pyrophosphatase cleaved the byproduct pyrophosphate to produce inorganic phosphate. The screening assay identified potent inhibitors of IucA, but these compounds also showed undesirable attributes, especially inhibition of unrelated enzymes.

## 10. CONCLUSIONS AND FUTURE DIRECTIONS

As this overview illustrates, the correlations between prokaryotic iron acquisition and the pathogenesis of humans and animals are diverse, numerous, and well supported by extensive data. Bacterial pathogens secrete siderophores that capture iron from host cells or proteins and facilitate bacterial tropism or invasiveness to particular tissues. Additionally, a multitude of unique LGP of different specificities populate the outer membranes of Gram (–) bacteria, allowing recognition and transport the many ferric xenosiderophores that they may encounter in wild or host environments. The various examples of these phenomena spotlight the potential for chemical therapeutics that block prokaryotic iron uptake. The redundancy and complexity of these systems, and the relative inaccessibility of TonB in the periplasm, created skepticism about LGP systems as targets for antibiotic discovery. However, opportunity exists for the identification of efficacious compounds against TonB-dependent uptake systems. Random high-throughput screening of chemical libraries, and rational design of novel compounds that target iron transport biochemistry or related cell envelope processes are viable approaches. Both will profit from additional findings that better explain the mechanisms of TonB-dependent transport.

### 10.1. Antibiotic Development

Although cefiderocol is now available for clinical applications against Gram (–) bacterial infections, numerous questions remain about it and related Trojan Horse antibiotics. For example, which among the four or five ferric catecholate receptors in each ESKAPE pathogen act to receive and transport ferric monocatecholate–antibiotic conjugates? This query highlights the fact that for many LGP, the full scope of their ligand recognition attributes are not well-defined. What are their natural ligands (human or bacterial), do they include catecholamine stress hormones, and what are the affinities of their binding interactions and the rates of their iron transport reactions? Little experimental data exists to illuminate the uptake of monocatecholate iron complexes. Presumably the Trojan Horse catecholate conjugates follow the entry same routes as iron complexes of the hydrolytic and/or oxidized degradation products of Ent, but which LGP participate in these transport events in the various CRE/ESKAPE organisms? Once through the OM into the bacterial periplasm, FeS $\beta$ LC complexes enter a biochemical no-man’s land that is difficult to experimentally characterize or observe. What periplasmic binding proteins recognize these complexes, does the AcrAB-TolC export pathway counteract their OM uptake,<sup>62</sup> and how do such large molecules gain entry into bacterial cells through IM membrane permeases? The answers to these questions may explain the molecular mechanisms of adaptive resistance that are major obstacles to continuing use of antibiotics like Fetroja.

### 10.2. HTS of Chemical Libraries

Once an HTS assay method, like FLHTS,<sup>703</sup> is developed and optimized for the primary screening of a chemical library, the main impediments to antibiotic discovery within the library derive from the secondary screening process. For example, primary hits against EcoTonB by FLHTS were subject to a funnel of criteria that attempted to exclude nonrelevant inhibition. In the FeEnt uptake FLHTS assay, besides authentic inhibitors of TonB action, primary hits may include: (i) specific antagonists of FeEnt uptake,

(ii) nonspecific fluorescence quenchers, (iii) metabolic poisons that interfere with active transport, (iv) membrane disruptors that compromise cellular integrity, and (v) pan assay interference compounds (PAINS<sup>704-706</sup>). Secondary screens on candidate compounds are laborious and time-consuming. Whereas primary HTS of a chemical library only requires a few weeks of experiments, the ensuing secondary screens are much slower because they usually involve biochemical characterizations of each individual candidate inhibitor. Analysis of only 20 or 30 compounds may involve months of work. Nairn *et al.*<sup>272</sup> screened a small chemical scaffold library of 17 500 compounds and found 165 primary hits. Applications of the same method, that yielded a 1% hit rate to a more typical library of 500 000 chemicals will produce ~5000 primary hits that are unmanageable except by HTS methods. Hence, the expansion and optimization of secondary assays to HTS formats is an important aspect of antibiotic discovery in chemical libraries. It is likely that the novel antibiotics we seek are present in those chemical collections, but it will take cleverness and technical innovations to find them.

## Supplementary Material

Refer to Web version on PubMed Central for supplementary material.

## ACKNOWLEDGMENTS

This work was supported by NIH grant R21AI115187 to P. E. Klebba and S. M. Newton. D.A. Six was supported in whole or in part with Federal funds from the Defense Threat Reduction Agency (DTRA) under Contract No. HDTRA117C0070 and the National Institutes of Health/National Institute of Allergy and Infectious Diseases (NIH/NIAID) under Contract No. 75N93020C00016.

## Biography

Phillip E. Klebba is a Distinguished Professor of Biochemistry and Molecular Biophysics at Kansas State University. He received his doctorate in biochemistry with J.B. Neilands at UC Berkeley, and completed postdoctoral study in microbiology and immunology with L.T. Rosenberg at Stanford Medical School, and with Hiroshi Nikaido at UC Berkeley, studying the immunology and transport biochemistry of bacterial porins. Relevant to this review, he was a Professor of Medical Microbiology at the Medical College of Wisconsin, a visiting scientist with M. Hofnung at Institut Pasteur, and with A. Charbit at Institut Necker Enfants Malades, and a visiting professor with H.R. Kaback at the UCLA David Geffen School of Medicine. His current research involves the development of fluorescent sensors to monitor membrane transport, toward the understanding of TonB-dependent iron acquisition and development of new antibiotics.

Salette M. Newton is a Research Professor of Biochemistry and Molecular Biophysics at Kansas State University. She received her doctorate in biochemistry with Sergio Olavo Pinto da Costa at Universidade de Sao Paulo and performed research with B.A.D. Stocker at Stanford University, studying the biotechnology of vaccines. She was a visiting scientist with M. Hofnung at Institut Pasteur and with A. Charbit at Institut Necker Enfants Malades and a visiting professor with H.R. Kaback at the UCLA David Geffen School of Medicine. Her current research focuses on the biochemistry of bacterial iron acquisition.

David A. Six is a Principal Scientist in Biology at Venatorx Pharmaceuticals. He obtained his M.S. and doctorate in Chemistry with E.A. Dennis at UC San Diego, working on the enzymology of cytosolic phospholipase A<sub>2</sub>. After postdoctoral work on lipopolysaccharide with C.R.H. Raetz at Duke University, he led antibacterial drug discovery programs at Novartis Institutes for BioMedical Research in Infectious Diseases, where he developed assays to measure bacterial compound accumulation. His work at Venatorx supports the clinical-stage cefepime–taniborbactam combination and novel non- $\beta$ -lactam inhibitors of penicillin-binding proteins.

Ashish Kumar is a predoctoral researcher in Biochemistry and Molecular Biophysics with P.E. Klebba and S.M. Newton at Kansas State University. His research addresses the development of fluorescent sensors to detect infectious bacteria in blood, tissue, and food samples.

Taihao Yang is a predoctoral researcher in Biochemistry and Molecular Biophysics with P.E. Klebba and S.M. Newton at Kansas State University. His current research focuses on iron transporters of Gram-negative bacteria, with the objective of developing next generation antibiotics against bacterial pathogens.

Brittany L. Nairn (formerly Mortensen) is an Assistant Professor of Biology at Bethel University in St. Paul, MN. She completed her doctorate in microbiology and immunology with T. Kawula at UNC Chapel Hill and performed postdoctoral study with E.P. Skaar at Vanderbilt and with P.E. Klebba and S.M. Newton at Kansas State University and with M.C. Herzberg at the University of Minnesota. Her research interests include biofilm formation, metal acquisition, and pathogenesis of bacteria, focusing on *Acinetobacter baumannii* and *Streptococcus gordonii*.

Colton Munger is an undergraduate researcher in Biochemistry and Molecular Biophysics with P.E. Klebba and S.M. Newton at Kansas State University.

Somnath Chakravorty is a postdoctoral scientist at the University of Buffalo Medical School. He received his doctorate in Microbiology with R. Gachhui at Jadavpur University, India, and performed postdoctoral research with P.E. Klebba and S.M. Newton at Kansas State University, working on iron uptake by ESKAPE pathogens. His current work with T.A. Russo at UB includes study of virulence factors in Hypervirulent *Klebsiella pneumoniae* and XDR *Acinetobacter baumannii*, and the role of iron acquisition in pathogenesis of *K. pneumoniae*.

## ABBREVIATIONS

Siderophore or Porphyrin

<b>Ent*</b>	degraded enterobactin
<b>GEnt</b>	glucosylated enterobactin
<b>DHBA</b>	2,3-dihydroxybenzoic acid
<b>DHBS</b>	2,3-dihydroxybenzoyl serine

<b>Crn</b>	corynebactin (= bacillibactin)
<b>Pbn</b>	petrobactin
<b>Vbn</b>	vibriobactin
<b>Fc</b>	ferrichrome
<b>FcA</b>	ferrichrome A
<b>FxB</b>	ferrioxamine B (apoFxB: desferal)
<b>Abn</b>	aerobactin
<b>Acn</b>	acinetobactin
<b>Fbn</b>	fimsbactin
<b>Bfn</b>	baumannoferrin
<b>Ybt</b>	yersiniabactin
<b>Pvd</b>	pyoverdin
<b>Pch</b>	pyochelin
<b>Nti</b>	nicotianamine
<b>Mbn</b>	mycobactin
<b>Hn</b>	heme
<b>B<sub>12</sub></b>	cyanocobalamin (vitamin B <sub>12</sub> )
<b>Cit</b>	citrate
<b>TF</b>	transferrin
<b>LF</b>	lactoferrin
<b>FTN</b>	ferritin
<b>NGAL</b>	neutrophil gelatinase-associated lipocalin
<b>LCN2</b>	lipocalin 2
<b>SCN</b>	siderocalin (= NGAL, LCN2)
<b>FDC</b>	Fetroja (= cefidericol)
<b>CIP</b>	ciprofloxacin

Phrase or Series of Words

<b>CRE</b>	carbapenem-resistant Enterobacterales
------------	---------------------------------------

<b>ESKAPE</b>	<i>Enterococcus, Staphylococcus, Klebsiella, Acinetobacter, Pseudomonas, Enterobacter</i>
<b>OM</b>	outer membrane
<b>IM</b>	inner membrane
<b>PG</b>	peptidoglycan
<b>IRMP</b>	iron-related or -regulated membrane proteins
<b>IROMP</b>	iron-regulated outer membrane proteins
<b>LGP</b>	ligand-gated porin
<b>TBDT</b>	TonB-dependent transporter
<b>PMF</b>	proton-motive force
<b>CTD</b>	C-terminal domain
<b>ABC</b>	ATP-binding cassette
<b>HPI</b>	high pathogenicity island
<b>UTI</b>	urinary tract infection
<b>ExPEC</b>	extra-intestinal pathogenic <i>E. coli</i>
<b>ETEC</b>	entero-toxigenic <i>E. coli</i>
<b>EHEC</b>	entero-hemorrhagic <i>E. coli</i>
<b>EPEC</b>	entero-pathogenic <i>E. coli</i>
<b>EAEC</b>	entero-aggregative <i>E. coli</i>
<b>AIEC</b>	adherent-invasive <i>E. coli</i>
<b>UPEC</b>	uropathogenic <i>E. coli</i>
<b>ESBL</b>	extended spectrum $\beta$ -lactamase
<b>XDR</b>	extreme drug resistant
<b>CSS</b>	cell-surface signaling
<b>HMWP</b>	high molecular weight protein
<b>PK/PD</b>	pharmacokinetic/pharmacodynamic
<b>MIC</b>	minimum inhibitory concentration
<b>PAINS</b>	pan assay interference compounds

## REFERENCES

- (1). Pappenheimer AM Jr Diphtheria toxin; a reinvestigation of the effect of iron on toxin and porphyrin production. *J. Biol. Chem* 1947, 167, 251–9. [PubMed: 20281645]
- (2). Bullen JJ; Rogers HJ; Cushnie GH Abolition of passive immunity to bacterial infections by iron. *Nature* 1967, 214, 515–6. [PubMed: 4166352]
- (3). Bullen JJ Iron-binding proteins in milk and resistance to *Escherichia coli* infection in infants. *Postgrad Med. J* 1975, 51, 67–70.
- (4). Bullen JJ The significance of iron in infection. *Clin. Infect. Dis* 1981, 3, 1127–38.
- (5). Bullen JJ Iron and infection. *Eur. J. Clin. Microbiol* 1985, 4, 537–9. [PubMed: 4092698]
- (6). Bullen JJ; Rogers HJ Bacterial iron metabolism and resistance to infection. *J. Med. Microbiol* 1970, 3, P8–P9.
- (7). Bullen JJ; Rogers HJ; Griffiths E Role of iron in bacterial infection. *Curr. Top. Microbiol. Immunol* 1978, 80, 1–35. [PubMed: 352628]
- (8). Bullen JJ; Rogers HJ; Spalding PB; Ward CG Iron and infection: the heart of the matter. *FEMS Immunol. Med. Microbiol* 2005, 43, 325–30. [PubMed: 15708305]
- (9). Bullen JJ; Ward CG; Rogers HJ Iron, infection, and the role of bicarbonate. *FEMS Microbiol. Lett* 1990, 71, 27–29.
- (10). Bullen JJ; Ward CG; Rogers HJ The critical role of iron in some clinical infections. *Eur. J. Clin. Microbiol. Infect. Dis* 1991, 10, 613–7. [PubMed: 1748112]
- (11). Perez F; Van Duin D Carbapenem-resistant Enterobacteriaceae: a menace to our most vulnerable patients. *Cleve Clin J. Med* 2013, 80, 225–33. [PubMed: 23547093]
- (12). Smith HZ; Kendall B Carbapenem Resistant Enterobacteriaceae. In *Stat Pearls*; StatPearls: Treasure Island, FL, 2020.
- (13). Adeolu M; Alnajjar S; Naushad S; Gupta RS Genome-based phylogeny and taxonomy of the ‘Enterobacteriales’: proposal for Enterobacterales ord. nov. divided into the families Enterobacteriaceae, Erwiniaceae fam. nov., Pectobacteriaceae fam. nov., Yersiniaceae fam. nov., Hafniaceae fam. nov., Morganellaceae fam. nov., and Budviciaceae fam. nov. *Int. J. Syst. Evol. Microbiol* 2016, 66, 5575–5599. [PubMed: 27620848]
- (14). Lasko MJ; Nicolau DP Carbapenem-Resistant Enterobacterales: Considerations for Treatment in the Era of New Antimicrobials and Evolving Enzymology. *Curr. Infect Dis Rep* 2020, 22, 6. [PubMed: 32034524]
- (15). McAdam AJ Enterobacteriaceae? Enterobacterales? What Should We Call Enteric Gram-Negative Bacilli? A Micro-Comic Strip. *J. Clin. Microbiol* 2020, 58, 58.
- (16). Boucher HW; Talbot GH; Bradley JS; Edwards JE; Gilbert D; Rice LB; Scheld M; Spellberg B; Bartlett J Bad bugs, no drugs: no ESKAPE! An update from the Infectious Diseases Society of America. *Clin. Infect. Dis* 2009, 48, 1–12. [PubMed: 19035777]
- (17). Rice LB Federal funding for the study of antimicrobial resistance in nosocomial pathogens: no ESKAPE. *J. Infect. Dis* 2008, 197, 1079–81. [PubMed: 18419525]
- (18). Elemam A; Rahimian J; Mandell W Infection with panresistant *Klebsiella pneumoniae*: a report of 2 cases and a brief review of the literature. *Clin. Infect. Dis* 2009, 49, 271–4. [PubMed: 19527172]
- (19). Tacconelli E; Magrini N Global priority list of antibiotic-resistant bacteria to guide research, discovery, and development of new antibiotics World Health Organization 2017.
- (20). Antibiotic Resistance Threats in the United States; U.S. Department of Health and Human Services, Centers for Disease Control and Prevention, 2019; <https://www.cdc.gov/drugresistance/pdf/threats-report/2019-ar-threats-report-508.pdf>, DOI: DOI: 10.15620/cdc:82532.
- (21). Pollack A Rising Threat of Infections Unfazed by Antibiotics. *New York Times* 2 26, 2010.
- (22). Pollack A Deadly Germs Largely Ignored by Drug Firms. *New York Times*, 2 27 2010; p 1.
- (23). Ventola CL The antibiotic resistance crisis: part 1: causes and threats. *P & T* 2015, 40, 277–283. [PubMed: 25859123]
- (24). Hu C Pharmaceutical Companies Are Backing Away from a Growing Threat That Could Kill 10 Million People a Year by 2050. *Business Insider*, 2018.



- (25). Jacobs A Deadly Germs, Lost Cures: Crisis Looms in Antibiotics as Drug Makers Go Bankrupt. *New York Times*, 12 26, 2019.
- (26). Nikaido H Multiple antibiotic resistance and efflux. *Curr. Opin. Microbiol* 1998, 1, 516–523. [PubMed: 10066525]
- (27). Nikaido H Molecular basis of bacterial outer membrane permeability revisited. *Microbiol. Mol. Biol. Rev* 2003, 67, 593–656. [PubMed: 14665678]
- (28). Nikaido H; Vaara M Molecular basis of bacterial outer membrane permeability. *Microbiol. Rev* 1985, 49, 1–32. [PubMed: 2580220]
- (29). Yu EW; McDermott G; Zgurskaya HI; Nikaido H; Koshland DE Jr Structural basis of multiple drug-binding capacity of the AcrB multidrug efflux pump. *Science (Washington, DC, U. S.)* 2003, 300, 976–80.
- (30). Zgurskaya HI; Nikaido H Bypassing the periplasm: reconstitution of the AcrAB multidrug efflux pump of *Escherichia coli*. *Proc. Natl. Acad. Sci. U. S. A* 1999, 96, 7190–5. [PubMed: 10377390]
- (31). Khan SN; Khan AU Breaking the Spell: Combating Multidrug Resistant ‘Superbugs’. *Front. Microbiol* 2016, 7, 174. [PubMed: 26925046]
- (32). Yaneja N; Kaur H Insights into Newer Antimicrobial Agents Against Gram-negative Bacteria. *Microbiol. Insights* 2016, 9, 9–19. [PubMed: 27013887]
- (33). Bassetti M; Righi E Development of novel antibacterial drugs to combat multiple resistant organisms. *Langenbecks Arch Surg* 2015, 400, 153–65. [PubMed: 25667169]
- (34). Pogue JM; Kaye KS; Cohen DA; Marchaim D Appropriate antimicrobial therapy in the era of multidrug-resistant human pathogens. *Clin. Microbiol. Infect* 2015, 21, 302–12. [PubMed: 25743999]
- (35). Cornelissen CN; Sparling PF Iron piracy: acquisition of transferrin-bound iron by bacterial pathogens. *Mol. Microbiol* 1994, 14, 843–50. [PubMed: 7715446]
- (36). Li J; Nation RL; Milne RW; Turnidge JD; Coulthard K Evaluation of colistin as an agent against multi-resistant Gram-negative bacteria. *Int. J. Antimicrob. Agents* 2005, 25, 11–25. [PubMed: 15620821]
- (37). McGann P; Snesrud E; Maybank R; Corey B; Ong AC; Clifford R; Hinkle M; Whitman T; Lesho E; Schaecher KE *Escherichia coli* Harboring *mcr-1* and *blaCTX-M* on a Novel *IncF* Plasmid: First report of *mcr-1* in the USA. *Antimicrob. Agents Chemother* 2016, 60, 4420. [PubMed: 27230792]
- (38). Buckling A; Harrison F; Vos M; Brockhurst MA; Gardner A; West SA; Griffin A Siderophore-mediated cooperation and virulence in *Pseudomonas aeruginosa*. *FEMS Microbiol. Ecol* 2007, 62, 135–141. [PubMed: 17919300]
- (39). Dhople AM; Ibanez MA; Poirier TC Role of iron in the pathogenesis of *Mycobacterium avium* infection in mice. *Microbios* 1996, 87, 77–87. [PubMed: 9032957]
- (40). Payne SM; Neilands IB Iron and virulence in the family Enterobacteriaceae. *Critical Rev. Microbiol* 1988, 16, 81–111. [PubMed: 3067977]
- (41). Payne SM Iron and virulence in *Shigella*. *Mol. Microbiol* 1989, 3, 1301–6. [PubMed: 2677608]
- (42). Payne SM Iron acquisition in microbial pathogenesis. *Trends Microbiol.* 1993, 1, 66–9. [PubMed: 8044465]
- (43). Schoolnik GK Microarray analysis of bacterial pathogenicity. *Adv. Microb. Physiol* 2002, 46, 1–45. [PubMed: 12073651]
- (44). Smith KD Iron metabolism at the host pathogen interface: lipocalin 2 and the pathogen-associated *iroA* gene cluster. *Int. J. Biochem. Cell Biol* 2007, 39, 1776–80. [PubMed: 17714976]
- (45). Snyder JA; Haugen BJ; Buckles EL; Lockett CV; Johnson DE; Donnenberg MS; Welch RA; Mobley HL Transcriptome of uropathogenic *Escherichia coli* during urinary tract infection. *Infect. Immun* 2004, 72, 6373–81. [PubMed: 15501767]
- (46). Stojjkovic I; Hwa V; Saint Martin L; O’Gaora P; Nassif X; Heffron F; So M The *Neisseria meningitidis* haemoglobin receptor: its role in iron utilization and virulence. *Mol. Microbiol* 1995, 15, 531–541. [PubMed: 7783623]
- (47). Sturm AW Iron and virulence of *Haemophilus ducreyi* in a primate model. *Sex. Transm. Dis* 1997, 24, 64–8. [PubMed: 9111750]

- (48). Torres AG; Redford P; Welch RA; Payne SM TonB-dependent systems of uropathogenic *Escherichia coli*: aerobactin and heme transport and TonB are required for virulence in the mouse. *Infect. Immun* 2001, 69, 6179–85. [PubMed: 11553558]
- (49). Williams PH Novel iron uptake system specified by ColV plasmids: an important component in the virulence of invasive strains of *Escherichia coli*. *Infect. Immun* 1979, 26, 925–32. [PubMed: 160892]
- (50). Wong HC; Liu CC; Yu CM; Lee YS Utilization of iron sources and its possible roles in the pathogenesis of *Vibrio parahaemolyticus*. *Microbiol. Immunol* 1996, 40, 791–8. [PubMed: 8985934]
- (51). Zhou D; Hardt WD; Galan JE *Salmonella typhimurium* encodes a putative iron transport system within the centisome 63 pathogenicity island. *Infect. Immun* 1999, 67, 1974–81. [PubMed: 10085045]
- (52). Anderson CP; Shen M; Eisenstein RS; Leibold EA Mammalian iron metabolism and its control by iron regulatory proteins. *Biochim. Biophys. Acta, Mol. Cell Res* 2012, 1823, 1468–83.
- (53). Anderson GJ; Frazer DM Current understanding of iron homeostasis. *Am. J. Clin. Nutr* 2017, 106, 1559s–1566s. [PubMed: 29070551]
- (54). Cronin SJF; Woolf CJ; Weiss G; Penninger JM The Role of Iron Regulation in Immunometabolism and Immune-Related Disease. *Front Mol. Biosci* 2019, 6, 116. [PubMed: 31824960]
- (55). Goetz DH; Holmes MA; Borregaard N; Bluhm ME; Raymond KN; Strong RK The neutrophil lipocalin NGAL is a bacteriostatic agent that interferes with siderophore-mediated iron acquisition. *Mol. Cell* 2002, 10, 1033–43. [PubMed: 12453412]
- (56). Neilands JB A Crystalline Organo-iron Pigment from a Rust Fungus (*Ustilago sphaerogena*). *J. Am. Chem. Soc* 1952, 74, 4846–7.
- (57). Neilands JB Siderophores: structure and function of microbial iron transport compounds. *J. Biol. Chem* 1995, 270, 26723–6. [PubMed: 7592901]
- (58). Harris WR; Carrano CJ; Raymond KN Spectrophotometric determination of the proton-dependent stability constant of ferric enterobactin. *J. Am. Chem. Soc* 1979, 101, 2213–2214.
- (59). Neilands JB Microbial iron compounds. *Annu. Rev. Biochem* 1981, 50, 715–31. [PubMed: 6455965]
- (60). Hider RC; Kong X Chemistry and biology of siderophores. *Nat. Prod. Rep* 2010, 27, 637–57. [PubMed: 20376388]
- (61). Di Masi DR; White JC; Schnaitman CA; Bradbeer C Transport of vitamin B12 in *Escherichia coli*: common receptor sites for vitamin B12 and the E colicins on the outer membrane of the cell envelope. *J. Bacteriol* 1973, 115, 506–13. [PubMed: 4579869]
- (62). Newton SM; Trinh V; Pi H; Klebba PE Direct measurements of the outer membrane stage of ferric enterobactin transport: postuptake binding. *J. Biol. Chem* 2010, 285, 17488–97. [PubMed: 20335169]
- (63). McIntosh MA; Earhart CF Effect of iron of the relative abundance of two large polypeptides of the *Escherichia coli* outer membrane. *Biochem. Biophys. Res. Commun* 1976, 70, 315–22. [PubMed: 776187]
- (64). Pugsley AP; Reeves P The role of colicin receptors in the uptake of ferrienterochelin by *Escherichia coli* K-12. *Biochem. Biophys. Res. Commun* 1977, 74, 903–11. [PubMed: 139147]
- (65). Noinaj N; Guillier M; Barnard TJ; Buchanan SK TonB-dependent transporters: regulation, structure, and function. *Annu. Rev. Microbiol* 2010, 64, 43–60. [PubMed: 20420522]
- (66). Klebba PE; McIntosh MA; Neilands JB Kinetics of biosynthesis of iron-regulated membrane proteins in *Escherichia coli*. *J. Bacteriol* 1982, 149, 880–8. [PubMed: 6174499]
- (67). Morton DJ; Williams P Characterization of the outer-membrane proteins of *Haemophilus parainfluenzae* expressed under iron-sufficient and iron-restricted conditions. *Microbiology* 1989, 135, 445–51.
- (68). Rutz JM; Liu J; Lyons JA; Goranson J; Armstrong SK; McIntosh MA; Feix JB; Klebba PE Formation of a gated channel by a ligand-specific transport protein in the bacterial outer membrane. *Science (Washington, DC, U. S.)* 1992, 258, 471–5.

- (69). Schauer K; Rodionov DA; de Reuse H New substrates for TonB-dependent transport: do we only see the 'tip of the iceberg'? *Trends Biochem. Sci* 2008, 33, 330. [PubMed: 18539464]
- (70). Abbott GW KCNQs: Ligand- and Voltage-Gated Potassium Channels. *Front. Physiol* 2020, 11, 583. [PubMed: 32655402]
- (71). Moreira C; Calixto AR; Richard JP; Kamerlin SCL The role of ligand-gated conformational changes in enzyme catalysis. *Biochem. Soc. Trans* 2019, 47, 1449–1460. [PubMed: 31657438]
- (72). Vetter I; Carter D; Bassett J; Deuis JR; Tay B; Jami S; Robinson SD High-Throughput Fluorescence Assays for Ion Channels and GPCRs. *Adv. Exp. Med. Biol* 2020, 1131, 27–72. [PubMed: 31646506]
- (73). Cornelis P Iron uptake and metabolism in pseudomonads. *Appl. Microbiol. Biotechnol* 2010, 86, 1637–45. [PubMed: 20352420]
- (74). Guerinot ML Microbial iron transport. *Annu. Rev. Microbiol* 1994, 48, 743–72. [PubMed: 7826025]
- (75). Bullen J; Griffiths E; Rogers H; Ward G Sepsis: the critical role of iron. *Microbes Infect.* 2000, 2, 409–15. [PubMed: 10817643]
- (76). Griffiths E; Rogers HJ; Bullen JJ Iron, plasmids and infection. *Nature* 1980, 284, 508–9. [PubMed: 7366717]
- (77). Adams TJ; Vartivarian S; Cowart RE Iron acquisition systems of *Listeria monocytogenes*. *Infect. Immun* 1990, 58, 2715–8. [PubMed: 2115028]
- (78). Conte MP; Longhi C; Buonfiglio V; Polidoro M; Seganti L; Valenti P The effect of iron on the invasiveness of *Escherichia coli* carrying the *inv* gene of *Yersinia pseudotuberculosis*. *J. Med. Microbiol* 1994, 40, 236–40. [PubMed: 8151672]
- (79). Coulanges V; Andre P; Vidon DJ Effect of siderophores, catecholamines, and catechol compounds on *Listeria* spp. Growth in iron-complexed medium. *Biochem. Biophys. Res. Commun* 1998, 249, 526–30. [PubMed: 9712730]
- (80). Cowart RE; Foster BG Differential effects of iron on the growth of *Listeria monocytogenes*: minimum requirements and mechanism of acquisition. *J. Infect. Dis* 1985, 151, 721–30. [PubMed: 3919119]
- (81). Neilands JB Iron absorption and transport in microorganisms. *Annu. Rev. Nutr* 1981, 1, 27–46. [PubMed: 6226306]
- (82). Conte MP; Longhi C; Polidoro M; Petrone G; Buonfiglio V; Di Santo S; Papi E; Seganti L; Visca P; Valenti P Iron availability affects entry of *Listeria monocytogenes* into the enterocyte-like cell line Caco-2. *Infection and immunity* 1996, 64, 3925–9. [PubMed: 8751952]
- (83). Furman M; Fica A; Saxena M; Di Fabio JL; Cabello FC *Salmonella typhi* iron uptake mutants are attenuated in mice. *Infect. Immun* 1994, 62, 4091–4. [PubMed: 8063432]
- (84). Gregory EM; Yost FJ Jr; Fridovich I Superoxide dismutases of *Escherichia coli*: intracellular localization and functions. *J. Bacteriol* 1973, 115, 987–91. [PubMed: 4580575]
- (85). Rouquette C; Bolla JM; Berche P An iron-dependent mutant of *Listeria monocytogenes* of attenuated virulence. *FEMS Microbiol. Lett* 1995, 133, 77–83. [PubMed: 8566716]
- (86). Rozalska B; Lisiecki P; Sadowska B; Mikucki J; Rudnicka W The virulence of *Staphylococcus aureus* isolates differing by siderophore production. *Acta Microbiol. Pol* 1998, 47, 185–194. [PubMed: 9839377]
- (87). Tai SS; Lee CJ; Winter RE Hemin utilization is related to virulence of *Streptococcus pneumoniae*. *Infect. Immun* 1993, 61, 5401–5. [PubMed: 8225615]
- (88). Tsolis RM; Baumler AJ; Heffron F; Stojiljkovic I Contribution of TonB- and Feo-mediated iron uptake to growth of *Salmonella typhimurium* in the mouse. *Infection and immunity* 1996, 64, 4549–56. [PubMed: 8890205]
- (89). Ward CG; Bullen JJ; Rogers HJ Iron and infection: new developments and their implications. *J. Trauma* 1996, 41, 356–64. [PubMed: 8760553]
- (90). Klebba PE Three paradoxes of ferric enterobactin uptake. *Front. Biosci., Landmark Ed* 2003, 8, s1422–s1436.
- (91). Klebba PE ROSET Model of TonB Action in Gram-Negative Bacterial Iron Acquisition. *J. Bacteriol* 2016, 198, 1013–21. [PubMed: 26787763]

- (92). Abdelhamed H; Lawrence ML; Karsi A The Role of TonB Gene in *Edwardsiella ictaluri* Virulence. *Front. Physiol* 2017, 8, 1066. [PubMed: 29326601]
- (93). Beddek AJ; Sheehan BJ; Bosse JT; Rycroft AN; Kroll JS; Langford PR Two TonB systems in *Actinobacillus pleuropneumoniae*: their roles in iron acquisition and virulence. *Infect. Immun* 2004, 72, 701–8. [PubMed: 14742511]
- (94). Holden KM; Browning GF; Noormohammadi AH; Markham PF; Marenda MS TonB is essential for virulence in avian pathogenic *Escherichia coli*. *Comp Immunol Microbiol Infect Dis* 2012, 35, 129–38. [PubMed: 22237011]
- (95). Hsieh PF; Lin TL; Lee CZ; Tsai SF; Wang JT Serum-induced iron-acquisition systems and TonB contribute to virulence in *Klebsiella pneumoniae* causing primary pyogenic liver abscess. *J. Infect. Dis* 2008, 197, 1717–27. [PubMed: 18433330]
- (96). Lu F; Miao S; Tu J; Ni X; Xing L; Yu H; Pan L; Hu Q The role of TonB-dependent receptor TbdR1 in *Riemerella anatipestifer* in iron acquisition and virulence. *Vet. Microbiol* 2013, 167, 713–718. [PubMed: 24075356]
- (97). Morton DJ; Hempel RJ; Seale TW; Whitby PW; Stull TL A functional tonB gene is required for both virulence and competitive fitness in a chinchilla model of *Haemophilus influenzae* otitis media. *BMC Res. Notes* 2012, 5, 327. [PubMed: 22731867]
- (98). Stork M; Di Lorenzo M; Mourino S; Osorio CR; Lemos ML; Crosa JH Two tonB systems function in iron transport in *Vibrio anguillarum*, but only one is essential for virulence. *Infect. Immun* 2004, 72, 7326–9. [PubMed: 15557661]
- (99). Zhang SR; Zhang L; Sun L Identification and analysis of three virulence-associated TonB-dependent outer membrane receptors of *Pseudomonas fluorescens*. *Dis. Aquat. Org* 2014, 110, 181–91.
- (100). Carver PL Metal ions and infectious diseases. An overview from the clinic. *Met. Ions Life Sci* 2013, 13, 1–28. [PubMed: 24470087]
- (101). Cowart RE Reduction of iron by extracellular iron reductases: implications for microbial iron acquisition. *Arch. Biochem. Biophys* 2002, 400, 273–81. [PubMed: 12054438]
- (102). Elkins C; Chen CJ; Thomas CE Characterization of the hgbA locus encoding a hemoglobin receptor from *Haemophilus ducreyi*. *Infection and immunity* 1995, 63, 2194–200. [PubMed: 7768598]
- (103). Henderson DP; Payne SM *Vibrio cholerae* iron transport systems: roles of heme and siderophore iron transport in virulence and identification of a gene associated with multiple iron transport systems. *Infect. Immun* 1994, 62, 5120–5. [PubMed: 7927795]
- (104). Seliger SS; Mey AR; Valle AM; Payne SM The two TonB systems of *Vibrio cholerae*: redundant and specific functions. *Mol. Microbiol* 2001, 39, 801–12. [PubMed: 11169119]
- (105). Bjarnason J; Southward CM; Surette MG Genomic profiling of iron-responsive genes in *Salmonella enterica* serovar typhimurium by high-throughput screening of a random promoter library. *J. Bacteriol* 2003, 185, 4973–82. [PubMed: 12897017]
- (106). Bruske AK; Anton M; Heller KJ Cloning and sequencing of the *Klebsiella pneumoniae* tonB gene and characterization of *Escherichia coli*-*K. pneumoniae* TonB hybrid proteins. *Gene* 1993, 131, 9–16. [PubMed: 8370545]
- (107). Kingsley RA; Reissbrodt R; Rabsch W; Ketley JM; Tsolis RM; Everest P; Dougan G; Baumler AJ; Roberts M; Williams PH Ferrioxamine-mediated Iron(III) utilization by *Salmonella enterica*. *Appl. Environ. Microbiol* 1999, 65, 1610–8. [PubMed: 10103258]
- (108). Angerer A; Klupp B; Braun V Iron transport systems of *Serratia marcescens*. *J. Bacteriol* 1992, 174, 1378–1387. [PubMed: 1531225]
- (109). Benevides-Matos N; Biville F The Hem and Has haem uptake systems in *Serratia marcescens*. *Microbiology* 2010, 156, 1749–1757. [PubMed: 20299406]
- (110). Cobessi D; Meksem A; Brillet K Structure of the heme/hemoglobin outer membrane receptor ShuA from *Shigella dysenteriae*: heme binding by an induced fit mechanism. *Proteins: Struct., Funct., Genet* 2010, 78, 286–94. [PubMed: 19731368]
- (111). Paquelin A; Ghigo JM; Bertin S; Wandersman C Characterization of HasB, a *Serratia marcescens* TonB-like protein specifically involved in the haemophore-dependent haem acquisition system. *Mol. Microbiol* 2001, 42, 995–1005. [PubMed: 11737642]

- (112). Turner PC; Thomas CE; Stojiljkovic I; Elkins C; Kizel G; Ala'Aldeen DA; Sparling PF Neisserial TonB-dependent outer-membrane proteins: detection, regulation and distribution of three putative candidates identified from the genome sequences. *Microbiology* 2001, 147, 1277–90. [PubMed: 11320131]
- (113). Bitter W; Marugg JD; de Weger LA; Tommassen J; Weisbeek PJ The ferric-pseudobactin receptor PupA of *Pseudomonas putida* WCS358: homology to TonB-dependent *Escherichia coli* receptors and specificity of the protein. *Mol. Microbiol* 1991, 5, 647–655. [PubMed: 1646376]
- (114). Poole K; Zhao Q; Neshat S; Heinrichs DE; Dean CR The *Pseudomonas aeruginosa* tonB gene encodes a novel TonB protein. *Microbiology* 1996, 142, 1449–58. [PubMed: 8704984]
- (115). Perry RD; Shah J; Bearden SW; Thompson JM; Fetherston JD *Yersinia pestis* TonB: role in iron, heme, and hemoprotein utilization. *Infect. Immun* 2003, 71, 4159–62. [PubMed: 12819108]
- (116). Stojiljkovic I; Hantke K Hemin uptake system of *Yersinia enterocolitica*: similarities with other TonB-dependent systems in gram-negative bacteria. *EMBO J.* 1992, 11, 4359–67. [PubMed: 1425573]
- (117). Thompson JM; Jones HA; Perry RD Molecular characterization of the hemin uptake locus (hmu) from *Yersinia pestis* and analysis of hmu mutants for hemin and hemoprotein utilization. *Infect. Immun* 1999, 67, 3879–92. [PubMed: 10417152]
- (118). Torres AG; Payne SM Haem iron-transport system in enterohaemorrhagic *Escherichia coli* O157:H7. *Mol. Microbiol* 1997, 23, 825–33. [PubMed: 9157252]
- (119). Fung-Tomc J; Bush K; Minassian B; Kolek B; Flamm R; Gradeliski E; Bonner D Antibacterial activity of BMS-180680, a new catechol-containing monobactam. *Antimicrob. Agents Chemother* 1997, 41, 1010–6. [PubMed: 9145861]
- (120). Rutz JM; Abdullah T; Singh SP; Kalve VI; Klebba PE Evolution of the ferric enterobactin receptor in gram-negative bacteria. *J. Bacteriol* 1991, 173, 5964–74. [PubMed: 1717434]
- (121). Bullen JJ Proceedings: Iron and infection. *Br. J. Haematol* 1974, 28, 139–140. [PubMed: 4415278]
- (122). Bachman MA; Miller VL; Weiser JN Mucosal lipocalin 2 has pro-inflammatory and iron-sequestering effects in response to bacterial enterobactin. *PLoS Pathog.* 2009, 5, No. e1000622. [PubMed: 19834550]
- (123). Collins HL Withholding iron as a cellular defence mechanism—friend or foe? *Eur. J. Immunol* 2008, 38, 1803–6. [PubMed: 18546145]
- (124). Fischbach MA; Lin H; Liu DR; Walsh CT How pathogenic bacteria evade mammalian sabotage in the battle for iron. *Nat. Chem. Biol* 2006, 2, 132–8. [PubMed: 16485005]
- (125). Haley KP; Skaar EP A battle for iron: host sequestration and *Staphylococcus aureus* acquisition. *Microbes Infect.* 2012, 14, 217–27. [PubMed: 22123296]
- (126). Kim H; Sandaruwan Elvitigala DA; Lee Y; Lee S; Whang I; Lee J Ferritin H-like subunit from Manila clam (*Ruditapes philippinarum*): molecular insights as a potent player in host antibacterial defense. *Fish Shellfish Immunol.* 2012, 33, 926–936. [PubMed: 23198293]
- (127). McLaughlin HP; Hill C; Gahan CG The impact of iron on *Listeria monocytogenes*; inside and outside the host. *Curr. Opin. Biotechnol* 2011, 22, 194–199. [PubMed: 21093251]
- (128). Parrow NL; Fleming RE; Minnick MF Sequestration and scavenging of iron in infection. *Infect. Immun* 2013, 81, 3503–3514. [PubMed: 23836822]
- (129). Pieracci FM; Barie PS Iron and the risk of infection. *Surg Infect (Larchmt).* 2005, 6, S41–S46. [PubMed: 19284357]
- (130). Radtke AL; O'Riordan MX Intracellular innate resistance to bacterial pathogens. *Cell. Microbiol* 2006, 8, 1720–9. [PubMed: 16939532]
- (131). Wakeman CA; Skaar EP Metalloregulation of Gram-positive pathogen physiology. *Curr. Opin. Microbiol* 2012, 15, 169–174. [PubMed: 22155062]
- (132). Allen CE; Burgos JM; Schmitt MP Analysis of novel iron-regulated, surface-anchored hemin-binding proteins in *Corynebacterium diphtheriae*. *J. Bacteriol* 2013, 195, 2852–63. [PubMed: 23585541]
- (133). Cadieux B; Lian T; Hu G; Wang J; Biondo C; Teti G; Liu V; Murphy ME; Creagh AL; Kronstad JW The Mannoprotein Cig1 supports iron acquisition from heme and virulence in the pathogenic fungus *Cryptococcus neoformans*. *J. Infect. Dis* 2013, 207, 1339–47. [PubMed: 23322859]

- (134). Caza M; Kronstad JW Shared and distinct mechanisms of iron acquisition by bacterial and fungal pathogens of humans. *Front. Cell. Infect. Microbiol* 2013, 3, 80. [PubMed: 24312900]
- (135). Cornelis P; Dingemans J *Pseudomonas aeruginosa* adapts its iron uptake strategies in function of the type of infections. *Front. Cell. Infect. Microbiol* 2013, 3, 75. [PubMed: 24294593]
- (136). Erac B; Yilmaz FF; Hosgor Limoncu M; Ozturk I; Aydemir S [Investigation of the virulence factors of multidrug-resistant *Acinetobacter baumannii* isolates]. *Mikrobiyol Bul.* 2014, 48, 70–81. [PubMed: 24506717]
- (137). Jung WH; Do E Iron acquisition in the human fungal pathogen *Cryptococcus neoformans*. *Curr. Opin. Microbiol* 2013, 16, 686–91. [PubMed: 23927895]
- (138). Konings AF; Martin LW; Sharples KJ; Roddam LF; Latham R; Reid DW; Lamont IL *Pseudomonas aeruginosa* uses multiple pathways to acquire iron during chronic infection in cystic fibrosis lungs. *Infect. Immun* 2013, 81, 2697–704. [PubMed: 23690396]
- (139). Mortensen BL; Skaar EP The contribution of nutrient metal acquisition and metabolism to *Acinetobacter baumannii* survival within the host. *Front. Cell. Infect. Microbiol* 2013, 3, 95. [PubMed: 24377089]
- (140). Nagy TA; Moreland SM; Andrews-Polymenis H; Detweiler CS The ferric enterobactin transporter Fep is required for persistent *Salmonella enterica* serovar typhimurium infection. *Infect. Immun* 2013, 81, 4063–70. [PubMed: 23959718]
- (141). Pandey SD; Choudhury M; Yousuf S; Wheeler PR; Gordon SV; Ranjan A; Sritharan M Iron-regulated protein HupB of *Mycobacterium tuberculosis* positively regulates siderophore biosynthesis and is essential for growth in macrophages. *J. Bacteriol* 2014, 196, 1853–65. [PubMed: 24610707]
- (142). Alonzo F 3rd; Benson MA; Chen J; Novick RP; Shopsis B; Torres VJ *Staphylococcus aureus* leucocidin ED contributes to systemic infection by targeting neutrophils and promoting bacterial growth in vivo. *Mol. Microbiol* 2012, 83, 423–35. [PubMed: 22142035]
- (143). Pich OQ; Merrell DS The ferric uptake regulator of *Helicobacter pylori*: a critical player in the battle for iron and colonization of the stomach. *Future Microbiol.* 2013, 8, 725–38. [PubMed: 23701330]
- (144). Runyen-Janecky LJ Role and regulation of heme iron acquisition in gram-negative pathogens. *Front. Cell. Infect. Microbiol* 2013, 3, 55. [PubMed: 24116354]
- (145). Wells RM; Jones CM; Xi Z; Speer A; Danilchanka O; Doornbos KS; Sun P; Wu F; Tian C; Niederweis M Discovery of a siderophore export system essential for virulence of *Mycobacterium tuberculosis*. *PLoS Pathog.* 2013, 9, No. e1003120. [PubMed: 23431276]
- (146). Wilks A; Ikeda-Saito M Heme Utilization by Pathogenic Bacteria: Not All Pathways Lead to Biliverdin. *Acc. Chem. Res* 2014, 47, 2291. [PubMed: 24873177]
- (147). Zapotoczna M; Jevnikar Z; Miajlovic H; Kos J; Foster TJ Iron-regulated surface determinant B (IsdB) promotes *Staphylococcus aureus* adherence to and internalization by non-phagocytic human cells. *Cell. Microbiol* 2013, 15, 1026–41. [PubMed: 23279065]
- (148). Cassat JE; Skaar EP Iron in infection and immunity. *Cell Host Microbe* 2013, 13, 509–19. [PubMed: 23684303]
- (149). Silva-Gomes S; Vale-Costa S; Appelberg R; Gomes MS Iron in intracellular infection: to provide or to deprive? *Front. Cell. Infect. Microbiol* 2013, 3, 96. [PubMed: 24367768]
- (150). Larrie-Bagha SM; Rasooli I; Mousavi-Gargari SL; Rasooli Z; Nazarian S Passive immunization by recombinant ferric enterobactin protein (FepA) from *Escherichia coli* O157. *Iran J. Microbiol* 2013, 5, 113–119. [PubMed: 23825727]
- (151). Abergel C; Rigal A; Chenivresse S; Lazdunski C; Claverie JM; Bouveret E; Benedetti H Crystallization and preliminary crystallographic study of a component of the *Escherichia coli* tol system: TolB. *Acta Crystallogr., Sect. D: Biol. Crystallogr* 1998, 54, 102–4. [PubMed: 9761825]
- (152). Ons E; Bleyen N; Tuntufye HN; Vandemaele F; Goddeeris BM High prevalence iron receptor genes of avian pathogenic *Escherichia coli*. *Avian Pathol.* 2007, 36, 411–414. [PubMed: 17899466]
- (153). Abergel RJ; Clifton MC; Pizarro JC; Warner JA; Shuh DK; Strong RK; Raymond KN The siderocalin/enterobactin interaction: a link between mammalian immunity and bacterial iron transport. *J. Am. Chem. Soc* 2008, 130, 11524–11534. [PubMed: 18680288]

- (154). Baghal SM; Gargari SL; Rasooli I Production and immunogenicity of recombinant ferric enterobactin protein (FepA). *Int. J. Infect. Dis* 2010, 14, e166–e170. [PubMed: 20418143]
- (155). Warner PJ; Williams PH; Bindereif A; Neilands JB ColV plasmid-specific aerobactin synthesis by invasive strains of *Escherichia coli*. *Infect. Immun* 1981, 33, 540–545. [PubMed: 6456229]
- (156). Abbott MB; Gaponenko V; Abusamhadneh E; Finley N; Li G; Dvoretzky A; Rance M; Solaro RJ; Rosevear PR Regulatory domain conformational exchange and linker region flexibility in cardiac troponin C bound to cardiac troponin I. *J. Biol. Chem* 2000, 275, 20610–7. [PubMed: 10801883]
- (157). Wolf SL; Hogan JS; Smith KL Iron uptake by *Escherichia coli* cultured with antibodies from cows immunized with high-affinity ferric receptors. *J. Dairy Sci* 2004, 87, 2103–7. [PubMed: 15328222]
- (158). Budzikiewicz H Siderophore-antibiotic conjugates used as trojan horses against *Pseudomonas aeruginosa*. *Curr. Top. Med. Chem* 2001, 1, 73–82. [PubMed: 11895295]
- (159). Kline T; Fromhold M; McKennon TE; Cai S; Treiberg J; Ihle N; Sherman D; Schwan W; Hickey MJ; Warrenner P; Witte PR; Brody LL; Goltry L; Barker LM; Anderson SU; Tanaka SK; Shawar RM; Nguyen LY; Langhorne M; Bigelow A; Embuscado L; Naeemi E Antimicrobial effects of novel siderophores linked to beta-lactam antibiotics. *Bioorg. Med. Chem* 2000, 8, 73–93. [PubMed: 10968267]
- (160). Miethke M; Marahiel MA Siderophore-based iron acquisition and pathogen control. *Microbiol. Mol. Biol. Rev* 2007, 71, 413–51. [PubMed: 17804665]
- (161). Dolence EK; Lin CE; Miller MJ; Payne SM Synthesis and siderophore activity of albomycin-like peptides derived from N5-acetyl-N5-hydroxy-L-ornithine. *J. Med. Chem* 1991, 34, 956–68. [PubMed: 1825849]
- (162). Mislin GL; Schalk IJ Siderophore-dependent iron uptake systems as gates for antibiotic Trojan horse strategies against *Pseudomonas aeruginosa*. *Metallomics*. 2014, 6, 408–420. [PubMed: 24481292]
- (163). Wenciewicz TA; Long TE; Mollmann U; Miller MJ Trihydroxamate siderophore-fluoroquinolone conjugates are selective sideromycin antibiotics that target *Staphylococcus aureus*. *Bioconjugate Chem*. 2013, 24, 473–486.
- (164). Pi H; Jones SA; Mercer LE; Meador JP; Caughron JE; Jordan L; Newton SM; Conway T; Klebba PE Role of catecholate siderophores in gram-negative bacterial colonization of the mouse gut. *PLoS One* 2012, 7, No. e50020. [PubMed: 23209633]
- (165). Zughair SM; Cornelis P Editorial: Role of Iron in Bacterial Pathogenesis. *Front. Cell. Infect. Microbiol* 2018, 8, 344. [PubMed: 30460202]
- (166). Ali MK; Kim RY; Karim R; Mayall JR; Martin KL; Shahandeh A; Abbasian F; Starkey MR; Loustaud-Ratti V; Johnstone D; Milward EA; Hansbro PM; Horvat JC Role of iron in the pathogenesis of respiratory disease. *Int. J. Biochem. Cell Biol* 2017, 88, 181–195. [PubMed: 28495571]
- (167). Tang F; Saier MH Jr Transport proteins promoting *Escherichia coli* pathogenesis. *Microb. Pathog* 2014, 71–72, 41–55.
- (168). Benjamin WH Jr; Turnbough CL Jr; Posey BS; Briles DE The ability of *Salmonella typhimurium* to produce the siderophore enterobactin is not a virulence factor in mouse typhoid. *Infect. Immun* 1985, 50, 392–7. [PubMed: 2932389]
- (169). Desai PJ; Garges E; Genco CA Pathogenic neisseriae can use hemoglobin, transferrin, and lactoferrin independently of the tonB locus. *J. Bacteriol* 2000, 182, 5586–91. [PubMed: 10986265]
- (170). Najimi M; Lemos ML; Osorio CR Identification of iron regulated genes in the fish pathogen *Aeromonas salmonicida* subsp. *salmonicida*: genetic diversity and evidence of conserved iron uptake systems. *Vet. Microbiol* 2009, 133, 377–382. [PubMed: 18774242]
- (171). Perry RD; Mier I Jr.; Fetherston JD Roles of the Yfe and Feo transporters of *Yersinia pestis* in iron uptake and intracellular growth. *BioMetals* 2007, 20, 699–703. [PubMed: 17206386]
- (172). Braun V Iron uptake by *Escherichia coli*. *Front. Biosci., Landmark Ed* 2003, 8, s1409–a1421.
- (173). Miller CE; Williams PH; Ketley JM Pumping iron: mechanisms for iron uptake by *Campylobacter*. *Microbiology* 2009, 155, 3157–4165. [PubMed: 19696110]

- (174). Nielubowicz GR; Mobley HL Host-pathogen interactions in urinary tract infection. *Nat. Rev. Urol* 2010, 7, 430–441. [PubMed: 20647992]
- (175). Neilands JB; Peterson T; Leong SA High affinity iron transport in microorganisms. In *Inorganic Chemistry in Biology and Medicine*; ACS Symposium Series 140; Martell AE, Ed.; American Chemical Society, 1980; Vol. 140, pp 263–278.
- (176). Sheldon JR; Skaar EP *Acinetobacter baumannii* can use multiple siderophores for iron acquisition, but only acinetobactin is required for virulence. *PLoS Pathog.* 2020, 16, No. e1008995. [PubMed: 33075115]
- (177). Baquero F; Levin BR Proximate and ultimate causes of the bactericidal action of antibiotics. *Nat. Rev. Microbiol* 2021, 19, 123–132. [PubMed: 33024310]
- (178). Brown AR; Gordon RA; Hyland SN; Siegrist MS; Grimes CL Chemical Biology Tools for Examining the Bacterial Cell Wall. *Cell Chem. Biol* 2020, 27, 1052–1062. [PubMed: 32822617]
- (179). Geisinger E; Huo W; Hernandez-Bird J; Isberg RR *Acinetobacter baumannii*: Envelope Determinants That Control Drug Resistance, Virulence, and Surface Variability. *Annu. Rev. Microbiol* 2019, 73, 481–506. [PubMed: 31206345]
- (180). Kuhn A The Bacterial Cell Wall and Membrane-A Treasure Chest for Antibiotic Targets. *Subcell. Biochem* 2019, 92, 1–5. [PubMed: 31214982]
- (181). Agarwal AK; Yee J Hepcidin. *Adv. Chronic Kidney Dis* 2019, 26, 298–305. [PubMed: 31477260]
- (182). Gao G; Li J; Zhang Y; Chang YZ Cellular Iron Metabolism and Regulation. *Adv. Exp. Med. Biol* 2019, 1173, 21–32. [PubMed: 31456203]
- (183). Testi C; Boffi A; Montemiglio LC Structural analysis of the transferrin receptor multifaceted ligand(s) interface. *Biophys. Chem* 2019, 254, 106242. [PubMed: 31419721]
- (184). Yanatori I; Kishi F DMT1 and iron transport. *Free Radical Biol. Med* 2019, 133, 55–63. [PubMed: 30055235]
- (185). Yeowell HN; White JR Iron requirement in the bactericidal mechanism of streptonigrin. *Antimicrob. Agents Chemother* 1982, 22, 961–8. [PubMed: 6218780]
- (186). Cohen MS; Chai Y; Britigan BE; McKenna W; Adams J; Svendsen T; Bean K; Hassett DJ; Sparling PF Role of extracellular iron in the action of the quinone antibiotic streptonigrin: mechanisms of killing and resistance of *Neisseria gonorrhoeae*. *Antimicrob. Agents Chemother* 1987, 31, 1507–13. [PubMed: 2829710]
- (187). Dyer DW; McKenna W; Woods JP; Sparling PF Isolation by streptonigrin enrichment and characterization of a transferrin-specific iron uptake mutant of *Neisseria meningitidis*. *Microb. Pathog* 1987, 3, 351–63. [PubMed: 3143887]
- (188). Holland J; Towner KJ; Williams P Isolation and characterisation of *Haemophilus influenzae* type b mutants defective in transferrin-binding and iron assimilation. *FEMS Microbiol. Lett* 1991, 77, 283–288.
- (189). Sato T; Yamawaki K Cefiderocol: Discovery, Chemistry, and In Vivo Profiles of a Novel Siderophore Cephalosporin. *Clin. Infect. Dis* 2019, 69, S538–s543. [PubMed: 31724047]
- (190). Simner PJ; Patel R Cefiderocol Antimicrobial Susceptibility Testing Considerations: the Achilles' Heel of the Trojan Horse? *J. Clin. Microbiol* 2020, 59, e951–20.
- (191). Zhanel GG; Golden AR; Zelenitsky S; Wiebe K; Lawrence CK; Adam HJ; Domalaon R; Schweizer F; Zhanel MA; Lagacé-Wiens PRS; Walkty AJ; Noreddin A; Lynch JP Iii; Karlowsky JA Cefiderocol: A Siderophore Cephalosporin with Activity Against Carbapenem-Resistant and Multidrug-Resistant Gram-Negative Bacilli. *Drugs* 2019, 79, 271–289. [PubMed: 30712199]
- (192). Anderson JE; Sparling PF; Cornelissen CN Gonococcal transferrin-binding protein 2 facilitates but is not essential for transferrin utilization. *J. Bacteriol* 1994, 176, 3162–70. [PubMed: 8195069]
- (193). Klebba PE *Transport Biochemistry of FepA*; ASM Press, 2004; pp 147–157.
- (194). Balhasteros H; Shipelskiy Y; Long NJ; Majumdar A; Katz BB; Santos NM; Leadon L; Newton SM; Marques MV; Klebba PE TonB-Dependent Heme/Hemoglobin Utilization by *Caulobacter crescentus* HutA. *J. Bacteriol* 2017, 199, e00723–16. [PubMed: 28031282]



- (195). Buchanan SK; Lukacik P; Grizot S; Ghirlando R; Ali MM; Barnard TJ; Jakes KS; Kienker PK; Esser L Structure of colicin I receptor bound to the R-domain of colicin Ia: implications for protein import. *EMBO J.* 2007, 26, 2594–604. [PubMed: 17464289]
- (196). Buchanan SK; Smith BS; Venkatramani L; Xia D; Esser L; Palnitkar M; Chakraborty R; van der Helm D; Deisenhofer J Crystal structure of the outer membrane active transporter FepA from *Escherichia coli* [see comments]. *Nat. Struct. Biol* 1999, 6, 56–63. [PubMed: 9886293]
- (197). Ferguson AD; Chakraborty R; Smith BS; Esser L; van der Helm D; Deisenhofer J Structural basis of gating by the outer membrane transporter FecA. *Science (Washington, DC, U. S.)* 2002, 295, 1715–1719.
- (198). Ferguson AD; Hofmann E; Coulton JW; Diederichs K; Welte W Siderophore-mediated iron transport: crystal structure of FhuA with bound lipopolysaccharide [see comments]. *Science (Washington, DC, U. S.)* 1998, 282, 2215–2220.
- (199). Locher KP; Rees B; Koebnik R; Mitschler A; Moulinier L; Rosenbusch JP; Moras D Transmembrane signaling across the ligand-gated FhuA receptor: crystal structures of free and ferrichrome-bound states reveal allosteric changes. *Cell* 1998, 95, 771–778. [PubMed: 9865695]
- (200). Saier MH Jr Families of proteins forming transmembrane channels. *J. Membr. Biol* 2000, 175, 165–180. [PubMed: 10833527]
- (201). Pugsley AP; Reeves P Iron uptake in colicin B-resistant mutants of *Escherichia coli* K-12. *J. Bacteriol* 1976, 126, 1052–62. [PubMed: 7543]
- (202). Wayne R; Frick K; Neilands JB Siderophore protection against colicins M, B, V, and Ia in *Escherichia coli*. *J. Bacteriol* 1976, 126, 7–12. [PubMed: 131121]
- (203). Rabsch W; Ma L; Wiley G; Najjar FZ; Kaserer W; Schuerch DW; Klebba JE; Roe BA; Laverde Gomez JA; Schallmey M; Newton SM; Klebba PE FepA- and TonB-dependent Bacteriophage H8: Receptor Binding and Genomic Sequence. *J. Bacteriol* 2007, 189, 5568–5574.
- (204). Nikaido H; Rosenberg EY Cir and Fiu proteins in the outer membrane of *Escherichia coli* catalyze transport of monomeric catechols: study with beta-lactam antibiotics containing catechol and analogous groups. *J. Bacteriol* 1990, 172, 1361–1367. [PubMed: 2407721]
- (205). Hantke K Identification of an iron uptake system specific for coprogen and rhodotorulic acid in *Escherichia coli* K12. *Mol. Gen. Genet* 1983, 191, 301–6. [PubMed: 6353165]
- (206). Bindereif A; Neilands JB Cloning of the aerobactin-mediated iron assimilation system of plasmid ColV. *J. Bacteriol* 1983, 153, 1111–3. [PubMed: 6296043]
- (207). Chimento DP; Mohanty AK; Kadner RJ; Wiener MC Substrate-induced transmembrane signaling in the cobalamin transporter BtuB. *Nat. Struct. Mol. Biol* 2003, 10, 394–401.
- (208). Cobessi D; Celia H; Folschweiller N; Schalk IJ; Abdallah MA; Pattus F The crystal structure of the pyoverdine outer membrane receptor FpvA from *Pseudomonas aeruginosa* at 3.6 angstroms resolution. *J. Mol. Biol* 2005, 347, 121–134. [PubMed: 15733922]
- (209). Cobessi D; Celia H; Pattus F Crystal structure at high resolution of ferric-pyochelin and its membrane receptor FptA from *Pseudomonas aeruginosa*. *J. Mol. Biol* 2005, 352, 893–904. [PubMed: 16139844]
- (210). Cox CD Iron uptake with ferripyochelin and ferric citrate by *Pseudomonas aeruginosa*. *J. Bacteriol* 1980, 142, 581–587. [PubMed: 6769903]
- (211). Liu PV; Shokrani F Biological activities of pyochelins: iron-chelating agents of *Pseudomonas aeruginosa*. *Infect. Immun* 1978, 22, 878–90. [PubMed: 103839]
- (212). Elliott RP Some properties of pyoverdine, the water-soluble fluorescent pigment of the pseudomonads. *Appl. Microbiol.* 1958, 6, 241–6. [PubMed: 13559972]
- (213). Philson SB; Llinás M Siderochromes from *Pseudomonas fluorescens*. I. Isolation and characterization. *J. Biol. Chem* 1982, 257, 8081–8085. [PubMed: 6211450]
- (214). Wayne R; Neilands JB Evidence for common binding sites for ferrichrome compounds and bacteriophage phi 80 in the cell envelope of *Escherichia coli*. *J. Bacteriol* 1975, 121, 497–503. [PubMed: 803957]
- (215). Weiss MS; Wacker T; Weckesser J; Weite W; Schulz GE The three-dimensional structure of porin from *Rhodobacter capsulatus* at 3 Å resolution. *FEBS Lett.* 1990, 267, 268–272. [PubMed: 2165921]

- (216). Cowan SW; Schirmer T; Rummel G; Steiert M; Ghosh R; Pauptit RA; Jansonius JN; Rosenbusch JP Crystal structures explain functional properties of two *E. coli* porins. *Nature* 1992, 358, 727–733. [PubMed: 1380671]
- (217). Guterman SK; Dann L Excretion of enterochelin by *exbA* and *exbB* mutants of *Escherichia coli*. *J. Bacteriol* 1973, 114, 1225–1230. [PubMed: 4576403]
- (218). Kadner RJ Vitamin B12 transport in *Escherichia coli*: energy coupling between membranes. *Mol. Microbiol* 1990, 4, 2027–33. [PubMed: 2089218]
- (219). Scott DC; Newton SM; Klebba PE Surface loop motion in FepA. *J. Bacteriol* 2002, 184, 4906–4911. [PubMed: 12169616]
- (220). Smallwood CR; Jordan L; Trinh V; Schuerch DW; Gala A; Hanson M; Shipelskiy Y; Majumdar A; Newton SM; Klebba PE Concerted loop motion triggers induced fit of FepA to ferric enterobactin. *J. Gen. Physiol* 2014, 144, 71–80. [PubMed: 24981231]
- (221). Kreuzsch A; Neubuser A; Schiltz E; Weckesser J; Schulz GE Structure of the membrane channel porin from *Rhodospseudomonas blastica* at 2.0 Å resolution. *Protein Sci.* 1994, 3, 58–63. [PubMed: 8142898]
- (222). Meyer JE; Hofnung M; Schulz GE Structure of maltoporin from *Salmonella typhimurium* ligated with a nitrophenylmaltotrioxide. *J. Mol. Biol* 1997, 266, 761–75. [PubMed: 9102468]
- (223). Schirmer T; Keller TA; Wang YF; Rosenbusch JP Structural basis for sugar translocation through maltoporin channels at 3.1 Å resolution [see comments]. *Science (Washington, DC, U. S.)* 1995, 267, 512–514.
- (224). Davies JK; Reeves P Genetics of resistance to colicins in *Escherichia coli* K-12: cross-resistance among colicins of group B. *J. Bacteriol* 1975, 123, 96–101. [PubMed: 124727]
- (225). Guterman SK Colicin B: mode of action and inhibition by enterochelin. *J. Bacteriol* 1973, 114, 1217–24. [PubMed: 4576402]
- (226). Pugsley AP; Reeves P Characterization of group B colicin-resistant mutants of *Escherichia coli* K-12: colicin resistance and the role of enterochelin. *J. Bacteriol* 1976, 127, 218–28. [PubMed: 6433]
- (227). Wang CC; Newton A An additional step in the transport of iron defined by the *tonB* locus of *Escherichia coli*. *J. Biol. Chem* 1971, 246, 2147–51. [PubMed: 4929287]
- (228). Fischer E; Gunter K; Braun V Involvement of *ExbB* and *TonB* in transport across the outer membrane of *Escherichia coli*: phenotypic complementation of *exb* mutants by overexpressed *tonB* and physical stabilization of *TonB* by *ExbB*. *J. Bacteriol* 1989, 171, 5127–34. [PubMed: 2670904]
- (229). Braun V The structurally related *exbB* and *tolQ* genes are interchangeable in conferring *tonB*-dependent colicin, bacteriophage, and albomycin sensitivity. *J. Bacteriol* 1989, 171, 6387–90. [PubMed: 2553680]
- (230). Braun V; Herrmann C Evolutionary relationship of uptake systems for biopolymers in *Escherichia coli*: cross-complementation between the *TonB-ExbB-ExbD* and the *TolA-TolQ-TolR* proteins. *Mol. Microbiol* 1993, 8, 261–8. [PubMed: 8316079]
- (231). Ollis AA; Manning M; Held KG; Postle K Cytoplasmic membrane protonmotive force energizes periplasmic interactions between *ExbD* and *TonB*. *Mol. Microbiol* 2009, 73, 466–81. [PubMed: 19627500]
- (232). Celia H; Botos I; Ni X; Fox T; De Val N; Lloubes R; Jiang J; Buchanan SK Cryo-EM structure of the bacterial *Ton* motor subcomplex *ExbB-ExbD* provides information on structure and stoichiometry. *Commun. Biol* 2019, 2, 358. [PubMed: 31602407]
- (233). Celia H; Noinaj N; Zakharov SD; Bordignon E; Botos I; Santamaria M; Barnard TJ; Cramer WA; Lloubes R; Buchanan SK Structural insight into the role of the *Ton* complex in energy transduction. *Nature* 2016, 538, 60. [PubMed: 27654919]
- (234). Bassford PJ Jr; Bradbeer C; Kadner RJ; Schnaitman CA Transport of vitamin B12 in *tonB* mutants of *Escherichia coli*. *J. Bacteriol* 1976, 128, 242–7. [PubMed: 135755]
- (235). Cadieux N; Phan PG; Cafiso DS; Kadner RJ Differential substrate-induced signaling through the *TonB*-dependent transporter *BtuB*. *Proc. Natl. Acad. Sci. U. S. A* 2003, 100, 10688–10693. [PubMed: 12958215]

- (236). Evans JS; Levine BA; Trayer IP; Dorman CJ; Higgins CF Sequence-imposed structural constraints in the TonB protein of *E. coli*. *FEBS Lett.* 1986, 208, 211–6. [PubMed: 3023135]
- (237). Jordan LD; Zhou Y; Smallwood CR; Lill Y; Ritchie K; Yip WT; Newton SM; Klebba PE Energy-dependent motion of TonB in the Gram-negative bacterial inner membrane. *Proc. Natl. Acad. Sci. U. S. A* 2013, 110, 11553–8. [PubMed: 23798405]
- (238). Kaserer WA; Jiang X; Xiao Q; Scott DC; Bauler M; Copeland D; Newton SM; Klebba PE Insight from TonB hybrid proteins into the mechanism of iron transport through the outer membrane. *J. Bacteriol* 2008, 190, 4001–16. [PubMed: 18390658]
- (239). Pawelek PD; Croteau N; Ng-Thow-Hing C; Khursigara CM; Moiseeva N; Allaire M; Coulton JW Structure of TonB in complex with FhuA, *E. coli* outer membrane receptor. *Science* 2006, 312, 1399–402. [PubMed: 16741125]
- (240). Shultis DD; Purdy MD; Banchs CN; Wiener MC Outer membrane active transport: structure of the BtuB:TonB complex. *Science* 2006, 312, 1396–9. [PubMed: 16741124]
- (241). Chang C; Mooser A; Pluckthun A; Wlodawer A Crystal structure of the dimeric C-terminal domain of TonB reveals a novel fold. *J. Biol. Chem* 2001, 276, 27535–40. [PubMed: 11328822]
- (242). Zhai YF; Heijne W; Saier MH Jr Molecular modeling of the bacterial outer membrane receptor energizer, ExbBD/TonB, based on homology with the flagellar motor, MotAB. *Biochim. Biophys. Acta, Biomembr* 2003, 1614, 201–10.
- (243). Bradbeer C; Woodrow ML Transport of vitamin B12 in *Escherichia coli*: energy dependence. *J. Bacteriol* 1976, 128, 99–104. [PubMed: 135757]
- (244). Wang CC; Newton A Iron transport in *Escherichia coli*: relationship between chromium sensitivity and high iron requirement in mutants of *Escherichia coli*. *J. Bacteriol* 1969, 98, 1135–41. [PubMed: 4892367]
- (245). Chu BCH; Vogel HJ A structural and functional analysis of type III periplasmic and substrate binding proteins: their role in bacterial siderophore and heme transport. *Biol. Chem* 2011, 392, 39–52. [PubMed: 21194366]
- (246). Fukamizo T; Kitaoku Y; Suginta W Periplasmic solute-binding proteins: Structure classification and chitooligosaccharide recognition. *Int. J. Biol. Macromol* 2019, 128, 985–993. [PubMed: 30771387]
- (247). Chu BC; Otten R; Krewulak KD; Mulder FA; Vogel HJ The solution structure, binding properties, and dynamics of the bacterial siderophore-binding protein FepB. *J. Biol. Chem* 2014, 289, 29219–34. [PubMed: 25173704]
- (248). Sprencel C; Cao Z; Qi Z; Scott DC; Montague MA; Ivanoff N; Xu J; Raymond KM; Newton SM; Klebba PE Binding of ferric enterobactin by the *Escherichia coli* periplasmic protein fepB. *J. Bacteriol* 2000, 182, 5359–64. [PubMed: 10986237]
- (249). Delepelaire P Bacterial ABC transporters of iron containing compounds. *Res. Microbiol* 2019, 170, 345–357. [PubMed: 31678562]
- (250). Ford RC; Beis K Learning the ABCs one at a time: structure and mechanism of ABC transporters. *Biochem. Soc. Trans* 2019, 47, 23–36. [PubMed: 30626703]
- (251). Holland IB Rise and rise of the ABC transporter families. *Res. Microbiol* 2019, 170, 304–320. [PubMed: 31442613]
- (252). Li B; Li N; Yue Y; Liu X; Huang Y; Gu L; Xu S An unusual crystal structure of ferric-enterobactin bound FepB suggests novel functions of FepB in microbial iron uptake. *Biochem. Biophys. Res. Commun* 2016, 478, 1049–53. [PubMed: 27539322]
- (253). Palacios M; Broberg CA; Walker KA; Miller VL A Serendipitous Mutation Reveals the Severe Virulence Defect of a *Klebsiella pneumoniae* fepB Mutant. *mSphere* 2017, 2, e00341–17. [PubMed: 28861522]
- (254). Shea CM; McIntosh MA Nucleotide sequence and genetic organization of the ferric enterobactin transport system: homology to other periplasmic binding protein-dependent systems in *Escherichia coli*. *Mol. Microbiol* 1991, 5, 1415–28. [PubMed: 1838574]
- (255). Abergel RJ; Warner JA; Shuh DK; Raymond KN Enterobactin protonation and iron release: structural characterization of the salicylate coordination shift in ferric enterobactin. *J. Am. Chem. Soc* 2006, 128, 8920–31. [PubMed: 16819888]

- (256). Cianciotto NP An update on iron acquisition by *Legionella pneumophila*: new pathways for siderophore uptake and ferric iron reduction. *Future Microbiol* 2015, 10, 841–51. [PubMed: 26000653]
- (257). Ecker DJ; Lancaster JR Jr; Emery T Siderophore iron transport followed by electron paramagnetic resonance spectroscopy. *J. Biol. Chem* 1982, 257, 8623–6. [PubMed: 6284739]
- (258). Kazmi SA; Shorter AL; McArdle JV; Ashiq U; Jamal RA Studies on the redox characteristics of ferrioxamine E. *Chem. Biodiversity* 2010, 7, 656–65.
- (259). Leong J; Neilands JB Mechanisms of siderophore iron transport in enteric bacteria. *J. Bacteriol* 1976, 126, 823–30. [PubMed: 131124]
- (260). Mies KA; Wirgau JI; Crumbliss AL Ternary complex formation facilitates a redox mechanism for iron release from a siderophore. *BioMetals* 2006, 19, 115–26. [PubMed: 16718598]
- (261). Schalk IJ; Guillon L Fate of ferrisiderophores after import across bacterial outer membranes: different iron release strategies are observed in the cytoplasm or periplasm depending on the siderophore pathways. *Amino Acids* 2013, 44, 1267–77. [PubMed: 23443998]
- (262). Francis J; Macturk HM; Madinaveitia J; Snow GA Mycobactin, a growth factor for *Mycobacterium johnei*. I. Isolation from *Mycobacterium phlei*. *Biochem. J* 1953, 55, 596–607. [PubMed: 13115341]
- (263). Raymond KN; Dertz EA; Kim SS Enterobactin: an archetype for microbial iron transport. *Proc. Natl. Acad. Sci. U. S. A* 2003, 100, 3584–3588. [PubMed: 12655062]
- (264). Holden VI; Bachman MA Diverging roles of bacterial siderophores during infection. *Metallomics: integrated biometal science* 2015, 7, 986–95. [PubMed: 25745886]
- (265). Holden VI; Breen P; Houle S; Dozois CM; Bachman MA *Klebsiella pneumoniae* Siderophores Induce Inflammation, Bacterial Dissemination, and HIF-1 $\alpha$  Stabilization during Pneumonia. *mBio* 2016, 7, e01397–16. [PubMed: 27624128]
- (266). Griffiths GL; Sigel SP; Payne SM; Neilands JB Vibriobactin, a siderophore from *Vibrio cholerae*. *J. Biol. Chem* 1984, 259, 383–5. [PubMed: 6706943]
- (267). Budzikiewicz H; Bössenkamp A; Taraz K; Pandey A; Meyer JM Corynebactin, a cyclic catecholate siderophore from *Corynebacterium glutamicum* ATCC14067 (*Brevibacterium* sp. DSM 20411). *Z. Naturforsch., C: J. Biosci* 1997, 52, 551–554.
- (268). Raymond KN; Isied SS; Brown LD; Fronczek FR; Nibert JH Coordination isomers of biological iron transport compounds. VI. Models of the enterobactin coordination site. A crystal field effect in the structure of potassium tris(catecholato)-chromate(III) and -ferrate(III) sesquihydrates, K<sub>3</sub>(M(O<sub>2</sub>C<sub>6</sub>H<sub>4</sub>)<sub>3</sub>)-1.5H<sub>2</sub>O, M = Cr, Fe1. *J. Am. Chem. Soc* 1976, 98, 1767–74. [PubMed: 130396]
- (269). Nairz M; Haschka D; Demetz E; Weiss G Iron at the interface of immunity and infection. *Front. Pharmacol* 2014, 5, 152. [PubMed: 25076907]
- (270). Nairz M; Dichtl S; Schroll A; Haschka D; Tymoszek P; Theurl I; Weiss G Iron and innate antimicrobial immunity-Depriving the pathogen, defending the host. *J. Trace Elem. Med. Biol* 2018, 48, 118–133. [PubMed: 29773170]
- (271). Silva-Gomes S; Vale-Costa S; Appelberg R; Gomes MS Iron in intracellular infection: to provide or to deprive? *Front. Cell. Infect. Microbiol* 2013, 3, 96. [PubMed: 24367768]
- (272). Nairn BL; Eliasson OS; Hyder DR; Long NJ; Majumdar A; Chakravorty S; McDonald P; Roy A; Newton SM; Klebba PE Fluorescence high-throughput screening for inhibitors of TonB action. *J. Bacteriol* 2017, 199, e00889–16. [PubMed: 28242720]
- (273). Yep A; McQuade T; Kirchoff P; Larsen M; Mobley HL Inhibitors of TonB function identified by a high-throughput screen for inhibitors of iron acquisition in uropathogenic *Escherichia coli* CFT073. *mBio* 2014, 5, No. e01089–13. [PubMed: 24570372]
- (274). Braun V Bacterial iron transport related to virulence. *Contrib Microbiol* 2004, 12, 210–33.
- (275). Cornelissen CN Subversion of nutritional immunity by the pathogenic *Neisseriae*. *Pathog. Dis* 2018, 76, ftx112.
- (276). Cornelissen CN; Hollander A TonB-Dependent Transporters Expressed by *Neisseria gonorrhoeae*. *Front. Microbiol* 2011, 2, 117. [PubMed: 21747812]
- (277). Konopka K; Bindereif A; Neilands JB Aerobactin-mediated utilization of transferrin iron. *Biochemistry* 1982, 21, 6503–8. [PubMed: 6295467]

- (278). Tidmarsh GF; Klebba PE; Rosenberg LT Rapid release of iron from ferritin by siderophores. *J. Inorg. Biochem* 1983, 18, 161–8. [PubMed: 6222161]
- (279). Aisen P; Leibman A; Zweier J Stoichiometric and site characteristics of the binding of iron to human transferrin. *J. Biol. Chem* 1978, 253, 1930–7. [PubMed: 204636]
- (280). Bachman MA; Lenio S; Schmidt L; Oyler JE; Weiser JN Interaction of lipocalin 2, transferrin, and siderophores determines the replicative niche of *Klebsiella pneumoniae* during pneumonia. *mBio* 2012, 3, e00224–11. [PubMed: 23169997]
- (281). Bearden SW; Staggs TM; Perry RD An ABC transporter system of *Yersinia pestis* allows utilization of chelated iron by *Escherichia coli* SAB11. *J. Bacteriol* 1998, 180, 1135–47. [PubMed: 9495751]
- (282). Caza M; Lepine F; Dozois CM Secretion, but not overall synthesis, of catecholate siderophores contributes to virulence of extraintestinal pathogenic *Escherichia coli*. *Mol. Microbiol* 2011, 80, 266–82. [PubMed: 21306443]
- (283). Russo TA; Olson R; Fang CT; Stoesser N; Miller M; MacDonald U; Hutson A; Barker JH; La Hoz RM; Johnson JR; et al. Identification of Biomarkers for Differentiation of Hypervirulent *Klebsiella pneumoniae* from Classical *K. pneumoniae*. *J. Clin. Microbiol* 2018, 56, 776–18.
- (284). Russo TA; Olson R; MacDonald U; Beanan J; Davidson BA Aerobactin, but not yersiniabactin, salmochelin, or enterobactin, enables the growth/survival of hypervirulent (hypermucoviscous) *Klebsiella pneumoniae* ex vivo and in vivo. *Infect. Immun* 2015, 83, 3325–33. [PubMed: 26056379]
- (285). Chakravorty S; Shipelskiy Y; Kumar A; Majumdar A; Yang T; Nairn BL; Newton SM; Klebba PE Universal fluorescent sensors of high-affinity iron transport, applied to ESKAPE pathogens. *J. Biol. Chem* 2019, 294, 4682–4692. [PubMed: 30679312]
- (286). Zhang Y; Sen S; Giedroc DP Iron Acquisition by Bacterial Pathogens: Beyond Tris-Catecholate Complexes. *ChemBioChem* 2020, 21, 1955. [PubMed: 32180318]
- (287). Guarner F; Malagelada JR Gut flora in health and disease. *Lancet* 2003, 361, 512–9. [PubMed: 12583961]
- (288). Lynch SV; Pedersen O The Human Intestinal Microbiome in Health and Disease. *N. Engl. J. Med* 2016, 375, 2369–2379. [PubMed: 27974040]
- (289). Shreiner AB; Kao JY; Young VB The gut microbiome in health and in disease. *Curr. Opin. Gastroenterol* 2015, 31, 69–75. [PubMed: 25394236]
- (290). Klebba PE; Charbit A; Xiao Q; Jiang X; Newton SM Mechanisms of iron and haem transport by *Listeria monocytogenes*. *Mol. Membr. Biol* 2012, 29, 69–86. [PubMed: 22703022]
- (291). Abergel RJ; Moore EG; Strong RK; Raymond KN Microbial evasion of the immune system: structural modifications of enterobactin impair siderocalin recognition. *J. Am. Chem. Soc* 2006, 128, 10998–9. [PubMed: 16925397]
- (292). Karlinsky JE; Stepien TA; Mayho M; Singletary LA; Bingham-Ramos LK; Brehm MA; Greiner DL; Shultz LD; Gallagher LA; Bawn M; Kingsley RA; Libby SJ; Fang FC Genome-wide Analysis of *Salmonella enterica* serovar Typhi in Humanized Mice Reveals Key Virulence Features. *Cell Host Microbe* 2019, 26, 426–434. [PubMed: 31447308]
- (293). Peigne C; Bidet P; Mahjoub-Messai F; Plainvert C; Barbe V; Médigue C; Frapy E; Nassif X; Denamur E; Bingen E; Bonacorsi S The plasmid of *Escherichia coli* strain S88 (O45:K1:H7) that causes neonatal meningitis is closely related to avian pathogenic *E. coli* plasmids and is associated with high-level bacteremia in a neonatal rat meningitis model. *Infect. Immun* 2009, 77, 2272–84. [PubMed: 19307211]
- (294). Sobieszka BM Distribution of genes encoding iron uptake systems among enteroaggregative *Escherichia coli* strains isolated from adults with irritable bowel syndrome. *Clin. Microbiol. Infect* 2008, 14, 1083–6. [PubMed: 19040481]
- (295). Matteoli FP; Passarelli-Araujo H; Pedrosa-Silva F; Olivares FL; Venancio TM Population structure and pangenome analysis of *Enterobacter bugandensis* uncover the presence of bla(CTX-M-55), bla(NDM-5) and bla(IMI-1), along with sophisticated iron acquisition strategies. *Genomics* 2020, 112, 1182–1191. [PubMed: 31279858]
- (296). Bäumlér AJ; Tsolis RM; Van Der Velden AW; Stojiljkovic I; Anic S; Heffron F Identification of a new iron regulated locus of *Salmonella typhi*. *Gene* 1996, 183, 207–213. [PubMed: 8996108]

- (297). Hantke K; Nicholson G; Rabsch W; Winkelmann G Salmochelins, siderophores of *Salmonella enterica* and uropathogenic *Escherichia coli* strains, are recognized by the outer membrane receptor IroN. *Proc. Natl. Acad. Sci. U. S. A* 2003, 100, 3677–3682. [PubMed: 12655053]
- (298). Bister B; Bischoff D; Nicholson GJ; Valdebenito M; Schneider K; Winkelmann G; Hantke K; Süßmuth RD The structure of salmochelins: C-glycosylated enterobactins of *Salmonella enterica* §. *BioMetals* 2004, 17, 471–481. [PubMed: 15259369]
- (299). Zhu M; Valdebenito M; Winkelmann G; Hantke K Functions of the siderophore esterases IroD and IroE in iron-salmochelin utilization. *Microbiology* 2005, 151, 2363–2372. [PubMed: 16000726]
- (300). Valax P; Georgiou G Molecular characterization of beta-lactamase inclusion bodies produced in *Escherichia coli*. 1. Composition. *Biotechnol. Prog* 1993, 9, 539–47. [PubMed: 7764166]
- (301). Sonnenborn U *Escherichia coli* strain Nissle 1917-from bench to bedside and back: history of a special *Escherichia coli* strain with probiotic properties. *FEMS microbiology letters* 2016, 363, fnw212. [PubMed: 27619890]
- (302). Goerg KJ; Schlörer E [Probiotic therapy of pseudomembranous colitis. Combination of intestinal lavage and oral administration of *Escherichia coli*]. *Dtsch. Med. Wochenschr* 1998, 123, 1274–8. [PubMed: 9817997]
- (303). Kruis W; Schütz E; Fric P; Fixa B; Judmaier G; Stolte M Double-blind comparison of an oral *Escherichia coli* preparation and mesalazine in maintaining remission of ulcerative colitis. *Aliment. Pharmacol. Ther* 1997, 11, 853–8. [PubMed: 9354192]
- (304). Rembacken BJ; Snelling AM; Hawkey PM; Chalmers DM; Axon AT Non-pathogenic *Escherichia coli* versus mesalazine for the treatment of ulcerative colitis: a randomised trial. *Lancet* 1999, 354, 635–9. [PubMed: 10466665]
- (305). Deriu E; Liu JZ; Pezeshki M; Edwards RA; Ochoa RJ; Contreras H; Libby SJ; Fang FC; Raffatellu M Probiotic bacteria reduce salmonella typhimurium intestinal colonization by competing for iron. *Cell Host Microbe* 2013, 14, 26–37. [PubMed: 23870311]
- (306). Massip C; Branchu P; Bossuet-Greif N; Chagneau CV; Gaillard D; Martin P; Boury M; Sécher T; Dubois D; Nougayrède JP; Oswald E Deciphering the interplay between the genotoxic and probiotic activities of *Escherichia coli* Nissle 1917. *PLoS Pathog.* 2019, 15, No. e1008029. [PubMed: 31545853]
- (307). Klebba PE Regulation of the biosynthesis of the iron-related membrane proteins in *Escherichia coli*, 1981.
- (308). Van Tiel-Menkveld GJ; Mentjox-Vervuurt JM; Oudega B; de Graaf FK Siderophore production by *Enterobacter cloacae* and a common receptor protein for the uptake of aerobactin and cloacin DF13. *J. Bacteriol* 1982, 150, 490–7. [PubMed: 6461633]
- (309). Struve C; Roe CC; Stegger M; Stahlhut SG; Hansen DS; Engelthaler DM; Andersen PS; Driebe EM; Keim P; Krogfelt KA Mapping the Evolution of Hypervirulent *Klebsiella pneumoniae*. *mBio* 2015, 6, No. e00630–15. [PubMed: 26199326]
- (310). Breurec S; Melot B; Hoen B; Passet V; Schepers K; Bastian S; Brisse S Liver Abscess Caused by Infection with Community-Acquired *Klebsiella quasipneumoniae* subsp. *quasipneumoniae*. *Emerging Infect. Dis* 2016, 22, 529–31.
- (311). Lee IR; Molton JS; Wyres KL; Gorrie C; Wong J; Hoh CH; Teo J; Kalimuddin S; Lye DC; Archuleta S; Holt KE; Gan YH Differential host susceptibility and bacterial virulence factors driving *Klebsiella* liver abscess in an ethnically diverse population. *Sci. Rep* 2016, 6, 29316. [PubMed: 27406977]
- (312). Cheng DL; Liu YC; Yen MY; Liu CY; Wang RS Septic metastatic lesions of pyogenic liver abscess. Their association with *Klebsiella pneumoniae* bacteremia in diabetic patients. *Arch. Intern. Med* 1991, 151, 1557–1559. [PubMed: 1872659]
- (313). Liu YC; Cheng DL; Lin CL *Klebsiella pneumoniae* liver abscess associated with septic endophthalmitis. *Arch. Intern. Med* 1986, 146, 1913–1916. [PubMed: 3532983]
- (314). Wang JH; Liu YC; Lee SS; Yen MY; Chen YS; Wang JH; Wann SR; Lin HH Primary liver abscess due to *Klebsiella pneumoniae* in Taiwan. *Clin. Infect. Dis* 1998, 26, 1434–1438. [PubMed: 9636876]

- (315). Wang YY; Lee FY; Chang FY; Lee SD; Fung CP A vanishing liver abscess complicated with *Klebsiella pneumoniae* chest wall abscess: a case report. *J. Microbiol Immunol Infect* 1998, 31, 249–252. [PubMed: 10496167]
- (316). Russo TA; Shon AS; Beanan JM; Olson R; MacDonald U; Pomakov AO; Visitacion MP Hypervirulent *K. pneumoniae* secretes more and more active iron-acquisition molecules than “classical” *K. pneumoniae* thereby enhancing its virulence. *PLoS One* 2011, 6, No. e26734. [PubMed: 22039542]
- (317). Lam MMC; Wyres KL; Judd LM; Wick RR; Jenney A; Brisse S; Holt KE Tracking key virulence loci encoding aerobactin and salmochelin siderophore synthesis in *Klebsiella pneumoniae*. *Genome Med.* 2018, 10, 77. [PubMed: 30371343]
- (318). Konopka K; Neilands JB Effect of serum albumin on siderophore-mediated utilization of transferrin iron. *Biochemistry* 1984, 23, 2122–7. [PubMed: 6234017]
- (319). Fischbach MA; Lin H; Zhou L; Yu Y; Abergel RJ; Liu DR; Raymond KN; Wanner BL; Strong RK; Walsh CT; Aderem A; Smith KD The pathogen-associated *iroA* gene cluster mediates bacterial evasion of lipocalin 2. *Proc. Natl. Acad. Sci. U. S. A* 2006, 103, 16502–7. [PubMed: 17060628]
- (320). Searle LJ; Meric G; Porcelli I; Sheppard SK; Lucchini S Variation in siderophore biosynthetic gene distribution and production across environmental and faecal populations of *Escherichia coli*. *PLoS One* 2015, 10, No. e0117906. [PubMed: 25756870]
- (321). Der Vartanian M Differences in excretion and efficiency of the aerobactin and enterochelin siderophores in a bovine pathogenic strain of *Escherichia coli*. *Infect. Immun* 1988, 56, 413–8. [PubMed: 2962945]
- (322). Valvano MA; Crosa JH Aerobactin iron transport genes commonly encoded by certain ColV plasmids occur in the chromosome of a human invasive strain of *Escherichia coli* K1. *Infect. Immun* 1984, 46, 159–67. [PubMed: 6237061]
- (323). Russo TA; Marr CM Hypervirulent *Klebsiella pneumoniae*. *Clin. Microbiol. Rev* 2019, 32, e00001–19. [PubMed: 31092506]
- (324). Bailey DC; Alexander E; Rice MR; Drake EJ; Mydy LS; Aldrich CC; Gulick AM Structural and functional delineation of aerobactin biosynthesis in hypervirulent *Klebsiella pneumoniae*. *J. Biol. Chem* 2018, 293, 7841–7852. [PubMed: 29618511]
- (325). Russo TA; Olson R; Macdonald U; Metzger D; Maltese LM; Drake EJ; Gulick AM Aerobactin mediates virulence and accounts for increased siderophore production under iron-limiting conditions by hypervirulent (hypermucoviscous) *Klebsiella pneumoniae*. *Infect. Immun* 2014, 82, 2356–67. [PubMed: 24664504]
- (326). Bachman MA; Oyler JE; Burns SH; Caza M; Lepine F; Dozois CM; Weiser JN *Klebsiella pneumoniae* yersiniabactin promotes respiratory tract infection through evasion of lipocalin 2. *Infect. Immun* 2011, 79, 3309–16. [PubMed: 21576334]
- (327). Magistro G; Hoffmann C; Schubert S The salmochelin receptor IroN itself, but not salmochelin-mediated iron uptake promotes biofilm formation in extraintestinal pathogenic *Escherichia coli* (ExPEC). *Int. J. Med. Microbiol* 2015, 305, 435–445. [PubMed: 25921426]
- (328). Gehring AM; DeMoll E; Fetherston JD; Mori I; Mayhew GF; Blattner FR; Walsh CT; Perry RD Iron acquisition in plague: modular logic in enzymatic biogenesis of yersiniabactin by *Yersinia pestis*. *Chem. Biol* 1998, 5, 573–86. [PubMed: 9818149]
- (329). Haag H; Hantke K; Drechsel H; Stojiljkovic I; Jung G; Zahner H Purification of yersiniabactin: a siderophore and possible virulence factor of *Yersinia enterocolitica*. *J. Gen. Microbiol* 1993, 139, 2159–65. [PubMed: 8245841]
- (330). Forman S; Paulley JT; Fetherston JD; Cheng YQ; Perry RD *Yersinia* ironomics: comparison of iron transporters among *Yersinia pestis* biotypes and its nearest neighbor, *Yersinia pseudotuberculosis*. *BioMetals* 2010, 23, 275–94. [PubMed: 20049509]
- (331). O’Connor L; Fetherston JD; Perry RD The *feoABC* Locus of *Yersinia pestis* Likely Has Two Promoters Causing Unique Iron Regulation. *Front. Cell. Infect. Microbiol* 2017, 7, 331. [PubMed: 28785546]
- (332). Perry RD; Fetherston JD Yersiniabactin iron uptake: mechanisms and role in *Yersinia pestis* pathogenesis. *Microbes Infect.* 2011, 13, 808–17. [PubMed: 21609780]

- (333). Bobrov AG; Kirillina O; Fetherston JD; Miller MC; Burlison JA; Perry RD The Yersinia pestis siderophore, yersiniabactin, and the ZnuABC system both contribute to zinc acquisition and the development of lethal septicaemic plague in mice. *Mol. Microbiol* 2014, 93, 759–75. [PubMed: 24979062]
- (334). Fetherston JD; Kirillina O; Bobrov AG; Paulley JT; Perry RD The yersiniabactin transport system is critical for the pathogenesis of bubonic and pneumonic plague. *Infect. Immun* 2010, 78, 2045–52. [PubMed: 20160020]
- (335). Garcia EC; Brumbaugh AR; Mobley HL Redundancy and specificity of Escherichia coli iron acquisition systems during urinary tract infection. *Infect. Immun* 2011, 79, 1225–35. [PubMed: 21220482]
- (336). Brumbaugh AR; Smith SN; Mobley HL Immunization with the yersiniabactin receptor, FyuA, protects against pyelonephritis in a murine model of urinary tract infection. *Infect. Immun* 2013, 81, 3309–16. [PubMed: 23798537]
- (337). Vigil PD; Stapleton AE; Johnson JR; Hooton TM; Hodges AP; He Y; Mobley HL Presence of putative repeat-in-toxin gene *tosA* in Escherichia coli predicts successful colonization of the urinary tract. *mBio* 2011, 2, No. e00066–11. [PubMed: 21540363]
- (338). Chaturvedi KS; Hung CS; Giblin DE; Urushidani S; Austin AM; Dinauer MC; Henderson JP Cupric yersiniabactin is a virulence-associated superoxide dismutase mimic. *ACS Chem. Biol* 2014, 9, 551–61. [PubMed: 24283977]
- (339). Cornelis P; Dingemans J Pseudomonas aeruginosa adapts its iron uptake strategies in function of the type of infections. *Front. Cell. Infect. Microbiol* 2013, 3, 75. [PubMed: 24294593]
- (340). Fang Z; Sampson SL; Warren RM; Gey van Pittius NC; Newton-Foot M Iron acquisition strategies in mycobacteria. *Tuberculosis (Oxford, U. K.)* 2015, 95, 123–30.
- (341). Lemos ML; Osorio CR Heme, an iron supply for vibrios pathogenic for fish. *BioMetals* 2007, 20, 615–26. [PubMed: 17206385]
- (342). Lyles KV; Eichenbaum Z From Host Heme To Iron: The Expanding Spectrum of Heme Degrading Enzymes Used by Pathogenic Bacteria. *Front. Cell. Infect. Microbiol* 2018, 8, 198. [PubMed: 29971218]
- (343). Richard KL; Kelley BR; Johnson JG Heme Uptake and Utilization by Gram-Negative Bacterial Pathogens. *Front. Cell. Infect. Microbiol* 2019, 9, 81. [PubMed: 30984629]
- (344). Siudeja K; Olczak T [Mechanisms and regulation of iron and heme utilization in Gram-negative bacteria]. *Postepy Biochem.* 2005, 51, 198–208. [PubMed: 16209357]
- (345). Tong Y; Guo M Bacterial heme-transport proteins and their heme-coordination modes. *Arch. Biochem. Biophys* 2009, 481, 1–15. [PubMed: 18977196]
- (346). de Léséleuc L; Harris G; KuoLee R; Xu HH; Chen W Serum resistance, gallium nitrate tolerance and extrapulmonary dissemination are linked to heme consumption in a bacteremic strain of *Acinetobacter baumannii*. *Int. J. Med. Microbiol* 2014, 304, 360–9. [PubMed: 24440358]
- (347). Wilks A; Ikeda-Saito M Heme utilization by pathogenic bacteria: not all pathways lead to biliverdin. *Acc. Chem. Res* 2014, 47, 2291–8. [PubMed: 24873177]
- (348). Jin B; Newton SM; Shao Y; Jiang X; Charbit A; Klebba PE Iron acquisition systems for ferric hydroxamates, haemin and haemoglobin in *Listeria monocytogenes*. *Mol. Microbiol* 2006, 59, 1185–1198. [PubMed: 16430693]
- (349). Kokesová A; Frolová L; Kverka M; Sokol D; Rossmann P; Bártová J; Tlaskalová-Hogenová H Oral administration of probiotic bacteria (*E. coli* Nissle, *E. coli* O83, *Lactobacillus casei*) influences the severity of dextran sodium sulfate-induced colitis in BALB/c mice. *Folia Microbiol. (Dordrecht, Neth.)* 2006, 51, 478–84. [PubMed: 17176771]
- (350). Blattner FR; Plunkett G 3rd; Bloch CA; Perna NT; Burland V; Riley M; Collado-Vides J; Glasner JD; Rode CK; Mayhew GF; Gregor J; Davis NW; Kirkpatrick HA; Goeden MA; Rose DJ; Mau B; Shao Y The complete genome sequence of *Escherichia coli* K-12. *Science (Washington, DC, U. S.)* 1997, 277, 1453–62.
- (351). Nash JH; Villegas A; Kropinski AM; Aguilar-Valenzuela R; Konczyk P; Mascarenhas M; Ziebell K; Torres AG; Karmali MA; Coombes BK Genome sequence of adherent-invasive *Escherichia*



- coli and comparative genomic analysis with other *E. coli* pathotypes. *BMC Genomics* 2010, 11, 667. [PubMed: 21108814]
- (352). Chhibber S; Aggarwal S; Yadav V Contribution of capsular and lipopolysaccharide antigens to the pathogenesis of *Klebsiella pneumoniae* respiratory tract infection. *Folia Microbiol. (Dordrecht, Neth.)* 2003, 48, 699–702. [PubMed: 14976731]
- (353). Evrard B; Balestrino D; Dosgilbert A; Bouya-Gachancard JL; Charbonnel N; Forestier C; Tridon A Roles of capsule and lipopolysaccharide O antigen in interactions of human monocyte-derived dendritic cells and *Klebsiella pneumoniae*. *Infect. Immun* 2010, 78, 210–9. [PubMed: 19841082]
- (354). Fresno S; Jimenez N; Canals R; Merino S; Corsaro MM; Lanzetta R; Parrilli M; Pieretti G; Regue M; Tomas JM A second galacturonic acid transferase is required for core lipopolysaccharide biosynthesis and complete capsule association with the cell surface in *Klebsiella pneumoniae*. *J. Bacteriol* 2007, 189, 1128–37. [PubMed: 17142396]
- (355). Hetem DJ; Bootsma MCJ; Troelstra A; Bonten MJM Transmissibility of livestock-associated methicillin-resistant *Staphylococcus aureus*. *Emerging Infect. Dis* 2013, 19, 1797–1802.
- (356). Hsieh PF; Lin TL; Yang FL; Wu MC; Pan YJ; Wu SH; Wang JT Lipopolysaccharide O1 antigen contributes to the virulence in *Klebsiella pneumoniae* causing pyogenic liver abscess. *PLoS One* 2012, 7, No. e33155. [PubMed: 22427976]
- (357). Mehling JS; Lavender H; Clegg S A Dam methylation mutant of *Klebsiella pneumoniae* is partially attenuated. *FEMS Microbiol. Lett* 2007, 268, 187–93. [PubMed: 17328745]
- (358). Lawlor MS; O'Connor C; Miller VL Yersiniabactin is a virulence factor for *Klebsiella pneumoniae* during pulmonary infection. *Infect. Immun* 2007, 75, 1463–72. [PubMed: 17220312]
- (359). Munoz-Price LS; Poirel L; Bonomo RA; Schwaber MJ; Daikos GL; Cormican M; Cornaglia G; Garau J; Gniadkowski M; Hayden MK; Kumarasamy K; Livermore DM; Maya JJ; Nordmann P; Patel JB; Paterson DL; Pitout J; Villegas MV; Wang H; Woodford N; Quinn JP Clinical epidemiology of the global expansion of *Klebsiella pneumoniae* carbapenemases. *Lancet Infect. Dis* 2013, 13, 785–96. [PubMed: 23969216]
- (360). Tumbarello M; Viale P; Viscoli C; Trecarichi EM; Tumietto F; Marchese A; Spanu T; Ambretti S; Ginocchio F; Cristini F; Losito AR; Tedeschi S; Cauda R; Bassetti M Predictors of mortality in bloodstream infections caused by *Klebsiella pneumoniae* carbapenemase-producing *K. pneumoniae*: importance of combination therapy. *Clin. Infect. Dis* 2012, 55, 943–50. [PubMed: 22752516]
- (361). Iwasaki Y; Inokuchi R; Harada S; Aoki K; Ishii Y; Shinohara K Bacterial Meningitis Caused by Hypervirulent *Klebsiella pneumoniae* Capsular Genotype K54 with Development of Granuloma-like Nodal Enhancement in the Brain during the Subacute Phase. *Intern. Med* 2017, 56, 373–376. [PubMed: 28154286]
- (362). Kwon JM; Jung HL; Shim JW; Kim DS; Shim JY; Park MS *Klebsiella pneumoniae* liver abscess in an immunocompetent child. *Korean J. Pediatr* 2013, 56, 407–10. [PubMed: 24223603]
- (363). Ng D; Frazee B Necrotizing fasciitis caused by hypermucoviscous *Klebsiella pneumoniae* in a Filipino female in North America. *West J. Emerg Med* 2015, 16, 165–8. [PubMed: 25671032]
- (364). Prokesch BC; TeKippe M; Kim J; Raj P; TeKippe EM; Greenberg DE Primary osteomyelitis caused by hypervirulent *Klebsiella pneumoniae*. *Lancet Infect. Dis* 2016, 16, e190–e195. [PubMed: 27402393]
- (365). Takahashi K; Miura A; Yamaguchi T; Kanematsu M Novel cord-like structures on MRI in a case of hypervirulent *Klebsiella pneumoniae*. *Intern. Med* 2015, 54, 355–6. [PubMed: 25748749]
- (366). Vandeveld A; Stepanovic B On a Boat: A Case in Australia of Endophthalmitis and Pyogenic Liver, Prostatic, and Lung Abscesses in a Previously Well Patient due to *Klebsiella pneumoniae*. *Case Rep. Infect Dis* 2014, 2014, 137248. [PubMed: 25309763]
- (367). Paczosa MK; Mecsas J *Klebsiella pneumoniae*: Going on the Offense with a Strong Defense. *Microbiol. Mol. Biol. Rev* 2016, 80, 629–61. [PubMed: 27307579]
- (368). Miethke M; Marahiel MA Siderophore-based iron acquisition and pathogen control. *Microbiol. Mol. Biol. Rev* 2007, 71, 413–51. [PubMed: 17804665]

- (369). Brock JH; Williams PH; Licéaga J; Wooldridge KG Relative availability of transferrin-bound iron and cell-derived iron to aerobactin-producing and enterochelin-producing strains of *Escherichia coli* and to other microorganisms. *Infect. Immun* 1991, 59, 3185–90. [PubMed: 1831796]
- (370). Lai YC; Peng HL; Chang HY Identification of genes induced in vivo during *Klebsiella pneumoniae* CG43 infection. *Infect. Immun* 2001, 69, 7140–5. [PubMed: 11598090]
- (371). Lawlor MS; O'Connor C; Miller VL Yersiniabactin is a virulence factor for *Klebsiella pneumoniae* during pulmonary infection. *Infect. Immun* 2007, 75, 1463–72. [PubMed: 17220312]
- (372). Wasserman SI; Soter NA; Center DM; Austen KF Cold urticaria. Recognition and characterization of a neutrophil chemotactic factor which appears in serum during experimental cold challenge. *J. Clin. Invest* 1977, 60, 189–96. [PubMed: 874083]
- (373). Heesemann J; Hantke K; Vocke T; Saken E; Rakin A; Stojiljkovic I; Berner R Virulence of *Yersinia enterocolitica* is closely associated with siderophore production, expression of an iron-repressible outer membrane polypeptide of 65,000 Da and pesticin sensitivity. *Mol. Microbiol* 1993, 8, 397–408. [PubMed: 8316088]
- (374). Perry RD; Balbo PB; Jones HA; Fetherston JD; DeMoll E Yersiniabactin from *Yersinia pestis*: biochemical characterization of the siderophore and its role in iron transport and regulation. *Microbiology* 1999, 145, 1181–1190. [PubMed: 10376834]
- (375). Fetherston JD; Bertolino VJ; Perry RD YbtP and YbtQ: two ABC transporters required for iron uptake in *Yersinia pestis*. *Mol. Microbiol* 1999, 32, 289–99. [PubMed: 10231486]
- (376). Koh EI; Hung CS; Henderson JP The Yersiniabactin-Associated ATP Binding Cassette Proteins YbtP and YbtQ Enhance *Escherichia coli* Fitness during High-Titer Cystitis. *Infect. Immun* 2016, 84, 1312–1319. [PubMed: 26883590]
- (377). Gibson F; Magrath DI The isolation and characterization of a hydroxamic acid (aerobactin) formed by *Aerobacter aerogenes* 62-I. *Biochim. Biophys. Acta, Gen. Subj* 1969, 192, 175–84.
- (378). Vernet V; Philippon A; Madoulet C; Vistelle R; Jaussaud R; Chippaux C Virulence factors (aerobactin and mucoid phenotype) in *Klebsiella pneumoniae* and *Escherichia coli* blood culture isolates. *FEMS Microbiol. Lett* 1995, 130, 51–57. [PubMed: 7557296]
- (379). Koczura R; Kaznowski A Occurrence of the *Yersinia* high-pathogenicity island and iron uptake systems in clinical isolates of *Klebsiella pneumoniae*. *Microb. Pathog* 2003, 35, 197–202. [PubMed: 14521878]
- (380). Warner PJ; Williams PH; Bindereif A; Neilands JB ColV plasmid-specific aerobactin synthesis by invasive strains of *Escherichia coli*. *Infect. Immun* 1981, 33, 540–5. [PubMed: 6456229]
- (381). Russo TA; Gulick AM Aerobactin Synthesis Proteins as Antivirulence Targets in Hypervirulent *Klebsiella pneumoniae*. *ACS Infect. Dis* 2019, 5, 1052–1054. [PubMed: 31032610]
- (382). Oudega B; van der Molen J; de Graaf FK In vitro binding of cloacin DF13 to its purified outer membrane receptor protein and effect of peptidoglycan on bacteriocin-receptor interaction. *J. Bacteriol* 1979, 140, 964–70. [PubMed: 533771]
- (383). Russo TA; Olson R; Macdonald U; Metzger D; Maltese LM; Drake EJ; Gulick AM Aerobactin mediates virulence and accounts for increased siderophore production under iron-limiting conditions by hypervirulent (hypermucoviscous) *Klebsiella pneumoniae*. *Infect. Immun* 2014, 82, 2356–67. [PubMed: 24664504]
- (384). Ayobami O; Willrich N; Harder T; Okeke IN; Eckmanns T; Markwart R The incidence and prevalence of hospital-acquired (carbapenem-resistant) *Acinetobacter baumannii* in Europe, Eastern Mediterranean and Africa: a systematic review and meta-analysis. *Emerging Microbes Infect.* 2019, 8, 1747–1759.
- (385). Wong D; Nielsen TB; Bonomo RA; Pantapalangkoor P; Luna B; Spellberg B Clinical and Pathophysiological Overview of *Acinetobacter* Infections: a Century of Challenges. *Clin. Microbiol. Rev* 2017, 30, 409–447. [PubMed: 27974412]
- (386). Actis LA; Tolmasky ME; Crosa LM; Crosa JH Effect of iron-limiting conditions on growth of clinical isolates of *Acinetobacter baumannii*. *J. Clin. Microbiol* 1993, 31, 2812–5. [PubMed: 8253994]

- (387). Daniel C; Haentjens S; Bissinger MC; Courcol RJ Characterization of the *Acinetobacter baumannii* Fur regulator: cloning and sequencing of the fur homolog gene. *FEMS Microbiol. Lett* 1999, 170, 199–209. [PubMed: 9919669]
- (388). Dorsey CW; Beglin MS; Actis LA Detection and analysis of iron uptake components expressed by *Acinetobacter baumannii* clinical isolates. *Journal of clinical microbiology* 2003, 41, 4188–93. [PubMed: 12958246]
- (389). Goel VK; Kapil A; Das B; Rao DN Influence of iron on growth and extracellular products of *Acinetobacter baumannii*. *Jpn. J. Med. Sci. Biol* 1998, 51, 25–33. [PubMed: 10211429]
- (390). Yamamoto S; Okujo N; Sakakibara Y Isolation and structure elucidation of acinetobactin, a novel siderophore from *Acinetobacter baumannii*. *Arch. Microbiol* 1994, 162, 249–54. [PubMed: 7802543]
- (391). Eijkelkamp BA; Hassan KA; Paulsen IT; Brown MH Investigation of the human pathogen *Acinetobacter baumannii* under iron limiting conditions. *BMC Genomics* 2011, 12, 126. [PubMed: 21342532]
- (392). Nwugo CC; Gaddy JA; Zimble DL; Actis LA Deciphering the iron response in *Acinetobacter baumannii*: A proteomics approach. *J. Proteomics* 2011, 74, 44–58. [PubMed: 20692388]
- (393). Runci F; Gentile V; Frangipani E; Rampioni G; Leoni L; Lucidi M; Visaggio D; Harris G; Chen W; Stahl J; Averhoff B; Visca P Contribution of Active Iron Uptake to *Acinetobacter baumannii* Pathogenicity. *Infect. Immun* 2019, 87, e00755–18. [PubMed: 30718286]
- (394). Mihara K; Tanabe T; Yamakawa Y; Funahashi T; Nakao H; Narimatsu S; Yamamoto S Identification and transcriptional organization of a gene cluster involved in biosynthesis and transport of acinetobactin, a siderophore produced by *Acinetobacter baumannii* ATCC 19606T. *Microbiology* 2004, 150, 2587–97. [PubMed: 15289555]
- (395). De Silva PM; Chong P; Fernando DM; Westmacott G; Kumar A Effect of Incubation Temperature on Antibiotic Resistance and Virulence Factors of *Acinetobacter baumannii* ATCC 17978. *Antimicrob. Agents Chemother* 2018, 62, e01514–17. [PubMed: 29061747]
- (396). Jacobs AC; Sayood K; Olmsted SB; Blanchard CE; Hinrichs S; Russell D; Dunman PM Characterization of the *Acinetobacter baumannii* growth phase-dependent and serum responsive transcriptomes. *FEMS Immunol. Med. Microbiol* 2012, 64, 403–12. [PubMed: 22211672]
- (397). Tuttobene MR; Cribb P; Mussi MA *BlsA* integrates light and temperature signals into iron metabolism through *Fur* in the human pathogen *Acinetobacter baumannii*. *Sci. Rep* 2018, 8, 7728. [PubMed: 29769610]
- (398). Penwell WF; DeGrace N; Tentarelli S; Gauthier L; Gilbert CM; Arivett BA; Miller AA; Durand-Reville TF; Joubran C; Actis LA Discovery and Characterization of New Hydroxamate Siderophores, *Baumannoferrin A* and *B*, produced by *Acinetobacter baumannii*. *ChemBioChem* 2015, 16, 1896. [PubMed: 26235845]
- (399). Proschak A; Lubuta P; Grun P; Lohr F; Wilharm G; De Berardinis V; Bode HB Structure and biosynthesis of *fimsbactins A-F*, siderophores from *Acinetobacter baumannii* and *Acinetobacter baylyi*. *ChemBioChem* 2013, 14, 633–8. [PubMed: 23456955]
- (400). Antunes LC; Imperi F; Towner KJ; Visca P Genome-assisted identification of putative iron-utilization genes in *Acinetobacter baumannii* and their distribution among a genotypically diverse collection of clinical isolates. *Res. Microbiol* 2011, 162, 279–84. [PubMed: 21144895]
- (401). Dorsey CW; Tolmasky ME; Crosa JH; Actis LA Genetic organization of an *Acinetobacter baumannii* chromosomal region harbouring genes related to siderophore biosynthesis and transport. *Microbiology* 2003, 149, 1227–38. [PubMed: 12724384]
- (402). Echenique JR; Arienti H; Tolmasky ME; Read RR; Staneloni RJ; Crosa JH; Actis LA Characterization of a high-affinity iron transport system in *Acinetobacter baumannii*. *J. Bacteriol* 1992, 174, 7670–9. [PubMed: 1447137]
- (403). Yakkala H; Samantarrai D; Gribskov M; Siddavattam D Comparative genome analysis reveals niche-specific genome expansion in *Acinetobacter baumannii* strains. *PLoS One* 2019, 14, No. e0218204. [PubMed: 31194814]
- (404). Vallenet D; Nordmann P; Barbe V; Poirel L; Mangenot S; Bataille E; Dossat C; Gas S; Kreimeyer A; Lenoble P; Oztas S; Poulain J; Segurens B; Robert C; Abergel C; Claverie JM;

- Raoult D; Médigue C; Weissenbach J; Cruveiller S Comparative analysis of Acinetobacters: three genomes for three lifestyles. *PLoS One* 2008, 3, No. e1805. [PubMed: 18350144]
- (405). Dorsey CW; Tomaras AP; Connerly PL; Tolmasky ME; Crosa JH; Actis LA The siderophore-mediated iron acquisition systems of *Acinetobacter baumannii* ATCC 19606 and *Vibrio anguillarum* 775 are structurally and functionally related. *Microbiology* 2004, 150, 3657–67. [PubMed: 15528653]
- (406). Wuest WM; Sattely ES; Walsh CT Three siderophores from one bacterial enzymatic assembly line. *J. Am. Chem. Soc* 2009, 131, 5056–7. [PubMed: 19320483]
- (407). Penwell WF; Arivett BA; Actis LA The *Acinetobacter baumannii* entA gene located outside the acinetobactin cluster is critical for siderophore production, iron acquisition and virulence. *PLoS One* 2012, 7, No. e36493. [PubMed: 22570720]
- (408). Shapiro JA; Wencewicz TA Acinetobactin Isomerization Enables Adaptive Iron Acquisition in *Acinetobacter baumannii* through pH-Triggered Siderophore Swapping. *ACS Infect. Dis* 2016, 2, 157–68. [PubMed: 27624967]
- (409). Harding CM; Hennon SW; Feldman MF Uncovering the mechanisms of *Acinetobacter baumannii* virulence. *Nat. Rev. Microbiol* 2018, 16, 91–102. [PubMed: 29249812]
- (410). Bailey DC; Bohac TJ; Shapiro JA; Giblin DE; Wencewicz TA; Gulick AM Crystal Structure of the Siderophore Binding Protein BauB Bound to an Unusual 2:1 Complex Between Acinetobactin and Ferric Iron. *Biochemistry* 2018, 57, 6653–6661. [PubMed: 30406986]
- (411). Bohac TJ; Fang L; Giblin DE; Wencewicz TA Fimsbactin and Acinetobactin Compete for the Periplasmic Siderophore Binding Protein BauB in Pathogenic *Acinetobacter baumannii*. *ACS Chem. Biol* 2019, 14, 674–687. [PubMed: 30785725]
- (412). Shapiro JA; Wencewicz TA Structure-function studies of acinetobactin analogs. *Metallomics: integrated biometal science* 2017, 9, 463–470. [PubMed: 28440833]
- (413). Moynié L; Serra I; Scorciapino MA; Oueis E; Page MG; Ceccarelli M; Naismith JH Preacinetobactin not acinetobactin is essential for iron uptake by the BauA transporter of the pathogen *Acinetobacter baumannii*. *eLife* 2018, 7, e42270. [PubMed: 30558715]
- (414). Subashchandrabose S; Mobley HL Back to the metal age: battle for metals at the host-pathogen interface during urinary tract infection. *Metallomics: integrated biometal science* 2015, 7, 935–42. [PubMed: 25677827]
- (415). Gaddy JA; Arivett BA; McConnell MJ; Lopez-Rojas R; Pachon J; Actis LA Role of acinetobactin-mediated iron acquisition functions in the interaction of *Acinetobacter baumannii* strain ATCC 19606T with human lung epithelial cells, *Galleria mellonella* caterpillars, and mice. *Infect. Immun* 2012, 80, 1015–24. [PubMed: 22232188]
- (416). Russo TA; MacDonald U The *Galleria mellonella* Infection Model Does Not Accurately Differentiate between Hypervirulent and Classical *Klebsiella pneumoniae*. *mSphere* 2020, 5, e00850–19. [PubMed: 31915230]
- (417). Fleming ID; Krezalek MA; Belogortseva N; Zaborin A; Defazio J; Chandrasekar L; Actis LA; Zaborina O; Alverdy JC Modeling *Acinetobacter baumannii* wound infections: The critical role of iron. *J. Trauma Acute Care Surg* 2017, 82, 557–565. [PubMed: 28030490]
- (418). Wilson BR; Bogdan AR; Miyazawa M; Hashimoto K; Tsuji Y Siderophores in Iron Metabolism: From Mechanism to Therapy Potential. *Trends Mol. Med* 2016, 22, 1077–1090. [PubMed: 27825668]
- (419). de Léséleuc L; Harris G; KuoLee R; Chen W In vitro and in vivo biological activities of iron chelators and gallium nitrate against *Acinetobacter baumannii*. *Antimicrob. Agents Chemother* 2012, 56, 5397–400. [PubMed: 22825117]
- (420). Okujo N; Sakakibara Y; Yoshida T; Yamamoto S Structure of acinetoferrin, a new citrate-based dihydroxamate siderophore from *Acinetobacter haemolyticus*. *BioMetals* 1994, 7, 170–176. [PubMed: 8148619]
- (421). Rohrbach MR; Braun V; Koster W Ferrichrome transport in *Escherichia coli* K-12: altered substrate specificity of mutated periplasmic FhuD and interaction of FhuD with the integral membrane protein FhuB. *Journal of bacteriology* 1995, 177, 7186–93. [PubMed: 8522527]

- (422). Thulasiraman P; Newton SM; Xu J; Raymond KN; Mai C; Hall A; Montague MA; Klebba PE Selectivity of ferric enterobactin binding and cooperativity of transport in gram-negative bacteria. *J. Bacteriol* 1998, 180, 6689–96. [PubMed: 9852016]
- (423). Fiester SE; Arivett BA; Schmidt RE; Beckett AC; Ticak T; Carrier MV; Ghosh R; Ohneck EJ; Metz ML; Sellin Jeffries MK; Actis LA Iron-Regulated Phospholipase C Activity Contributes to the Cytolytic Activity and Virulence of *Acinetobacter baumannii*. *PLoS One* 2016, 11, No. e0167068. [PubMed: 27875572]
- (424). Camarena L; Bruno V; Euskirchen G; Poggio S; Snyder M Molecular mechanisms of ethanol-induced pathogenesis revealed by RNA-sequencing. *PLoS Pathog.* 2010, 6, No. e1000834. [PubMed: 20368969]
- (425). Jacobs AC; Hood I; Boyd KL; Olson PD; Morrison JM; Carson S; Sayood K; Iwen PC; Skaar EP; Dunman PM Inactivation of phospholipase D diminishes *Acinetobacter baumannii* pathogenesis. *Infect. Immun* 2010, 78, 1952–62. [PubMed: 20194595]
- (426). Stahl J; Bergmann H; Göttig S; Ebersberger I; Averhoff B *Acinetobacter baumannii* Virulence Is Mediated by the Concerted Action of Three Phospholipases D. *PLoS One* 2015, 10, No. e0138360. [PubMed: 26379240]
- (427). Choi SR; Britigan BE; Narayanasamy P Iron/Heme Metabolism-Targeted Gallium(III) Nanoparticles Are Active against Extracellular and Intracellular *Pseudomonas aeruginosa* and *Acinetobacter baumannii*. *Antimicrob. Agents Chemother.* 2019, 63, e02643–18. [PubMed: 30782994]
- (428). de Leseleuc L; Harris G; KuoLee R; Xu HH; Chen W Serum resistance, gallium nitrate tolerance and extrapulmonary dissemination are linked to heme consumption in a bacteremic strain of *Acinetobacter baumannii*. *Int. J. Med. Microbiol* 2014, 304, 360–9. [PubMed: 24440358]
- (429). Giardina BJ; Shahzad S; Huang W; Wilks A Heme uptake and utilization by hypervirulent *Acinetobacter baumannii* LAC-4 is dependent on a canonical heme oxygenase (abHemO). *Arch. Biochem. Biophys* 2019, 672, 108066. [PubMed: 31398314]
- (430). Zimpler DL; Penwell WF; Gaddy JA; Menke SM; Tomaras AP; Connerly PL; Actis LA Iron acquisition functions expressed by the human pathogen *Acinetobacter baumannii*. *BioMetals* 2009, 22, 23–32. [PubMed: 19130255]
- (431). Subashchandrabose S; Smith S; DeOrnellas V; Crepin S; Kole M; Zahdeh C; Mobley HL *Acinetobacter baumannii* Genes Required for Bacterial Survival during Bloodstream Infection. *mSphere* 2016, 1, e00013–15. [PubMed: 27303682]
- (432). Moynié L; Luscher A; Rolo D; Pletzer D; Tortajada A; Weingart H; Braun Y; Page MG; Naismith JH; Köhler T Structure and Function of the PiuA and PirA Siderophore-Drug Receptors from *Pseudomonas aeruginosa* and *Acinetobacter baumannii*. *Antimicrob. Agents Chemother* 2017, 61, e02531–16. [PubMed: 28137795]
- (433). Catel-Ferreira M; Marti S; Guillon L; Jara L; Coadou G; Molle V; Bouffartigues E; Bou G; Shalk I; Jouenne T; Vila-Farrés X; Dé E The outer membrane porin OmpW of *Acinetobacter baumannii* is involved in iron uptake and colistin binding. *FEBS Lett.* 2016, 590, 224–31. [PubMed: 26823169]
- (434). Zimpler DL; Arivett BA; Beckett AC; Menke SM; Actis LA Functional features of TonB energy transduction systems of *Acinetobacter baumannii*. *Infect. Immun* 2013, 81, 3382–94. [PubMed: 23817614]
- (435). Álvarez-Fraga L; Vázquez-Ucha JC; Martínez-Guitián M; Vallejo JA; Bou G; Beceiro A; Poza M Pneumonia infection in mice reveals the involvement of the *feoA* gene in the pathogenesis of *Acinetobacter baumannii*. *Virulence* 2018, 9, 496–509. [PubMed: 29334313]
- (436). Newton SM; Klebba PE; Raynaud C; Shao Y; Jiang X; Dubail I; Archer C; Frehel C; Charbit A The *svpA-srtB* locus of *Listeria monocytogenes*: Fur-mediated iron regulation and effect on virulence. *Mol. Microbiol* 2005, 55, 927–940. [PubMed: 15661014]
- (437). Lamont IL; Konings AF; Reid DW Iron acquisition by *Pseudomonas aeruginosa* in the lungs of patients with cystic fibrosis. *BioMetals* 2009, 22, 53–60. [PubMed: 19130260]

- (438). Peek ME; Bhatnagar A; McCarty NA; Zughaier SM Pyoverdine, the Major Siderophore in *Pseudomonas aeruginosa*, Evades NGAL Recognition. *Interdiscip. Perspect. Infect. Dis* 2012, 2012, 843509. [PubMed: 22973307]
- (439). Brandel J; Humbert N; Elhabiri M; Schalk IJ; Mislin GL; Albrecht-Gary AM Pyochelin, a siderophore of *Pseudomonas aeruginosa*: physicochemical characterization of the iron(III), copper(II) and zinc(II) complexes. *Dalton Trans* 2012, 41, 2820–34. [PubMed: 22261733]
- (440). Dumas Z; Ross-Gillespie A; Kummerli R Switching between apparently redundant iron-uptake mechanisms benefits bacteria in changeable environments. *Proc. R. Soc. London, Ser. B* 2013, 280, 20131055.
- (441). Albrecht-Gary AM; Blanc S; Rochel N; Ocaktan AZ; Abdallah MA Bacterial iron transport: coordination properties of pyoverdin PaA, a peptidic siderophore of *Pseudomonas aeruginosa*. *Inorg. Chem* 1994, 33, 6391–6402.
- (442). Cezard C; Farvacques N; Sonnet P Chemistry and biology of pyoverdines, *Pseudomonas* primary siderophores. *Curr. Med. Chem* 2014, 22, 165–86.
- (443). Meyer JM; Neely A; Stintzi A; Georges C; Holder IA Pyoverdin is essential for virulence of *Pseudomonas aeruginosa*. *Infection and immunity* 1996, 64, 518–23. [PubMed: 8550201]
- (444). Xiao R; Kisaalita WS Iron acquisition from transferrin and lactoferrin by *Pseudomonas aeruginosa* pyoverdin. *Microbiology* 1997, 143, 2509–15.
- (445). Teintze M; Hossain MB; Barnes CL; Leong J; van der Helm D Structure of ferric pseudobactin, a siderophore from a plant growth promoting *Pseudomonas*. *Biochemistry* 1981, 20, 6446–57. [PubMed: 7306518]
- (446). Teintze M; Leong J Structure of pseudobactin A, a second siderophore from plant growth promoting *Pseudomonas* B10. *Biochemistry* 1981, 20, 6457–62. [PubMed: 7306519]
- (447). Xiong YQ; Vasil ML; Johnson Z; Ochsner UA; Bayer AS The oxygen- and iron-dependent sigma factor *pvdS* of *Pseudomonas aeruginosa* is an important virulence factor in experimental infective endocarditis. *J. Infect. Dis* 2000, 181, 1020–6. [PubMed: 10720526]
- (448). Minandri F; Imperi F; Frangipani E; Bonchi C; Visaggio D; Facchini M; Pasquali P; Bragonzi A; Visca P Role of Iron Uptake Systems in *Pseudomonas aeruginosa* Virulence and Airway Infection. *Infect. Immun* 2016, 84, 2324–35. [PubMed: 27271740]
- (449). Lamont IL; Beare PA; Ochsner U; Vasil AI; Vasil ML Siderophore-mediated signaling regulates virulence factor production in *Pseudomonas aeruginosa*. *Proc. Natl. Acad. Sci. U. S. A* 2002, 99, 7072–7. [PubMed: 11997446]
- (450). Gi M; Lee KM; Kim SC; Yoon JH; Yoon SS; Choi JY A novel siderophore system is essential for the growth of *Pseudomonas aeruginosa* in airway mucus. *Sci. Rep* 2015, 5, 14644. [PubMed: 26446565]
- (451). Becker R; Grun M; Scholz G Nicotianamine and the distribution of iron into the apoplasm and symplasm of tomato (*Lycopersicon esculentum* Mill.): I. Determination of the apoplasmic and symplasmic iron pools in roots and leaves of the cultivar Bonner Beste and its nicotianamine-less mutant chloronerva. *Planta* 1992, 187, 48–52. [PubMed: 24177965]
- (452). Takahashi M; Terada Y; Nakai I; Nakanishi H; Yoshimura E; Mori S; Nishizawa NK Role of nicotianamine in the intracellular delivery of metals and plant reproductive development. *Plant Cell* 2003, 15, 1263–80. [PubMed: 12782722]
- (453). Dean CR; Poole K Expression of the ferric enterobactin receptor (PfeA) of *Pseudomonas aeruginosa*: involvement of a two-component regulatory system. *Mol. Microbiol* 1993, 8, 1095–103. [PubMed: 8361354]
- (454). Dean CR; Poole K Cloning and characterization of the ferric enterobactin receptor gene (*pfeA*) of *Pseudomonas aeruginosa*. *J. Bacteriol* 1993, 175, 317–24. [PubMed: 8419284]
- (455). Cornelis P; Bodilis J A survey of TonB-dependent receptors in fluorescent pseudomonads. *Environ. Microbiol. Rep* 2009, 1, 256–62. [PubMed: 23765855]
- (456). Llamas MA; Sparrius M; Kloet R; Jimenez CR; Vandenbroucke-Grauls C; Bitter W The heterologous siderophores ferrioxamine B and ferrichrome activate signaling pathways in *Pseudomonas aeruginosa*. *J. Bacteriol* 2006, 188, 1882–91. [PubMed: 16484199]
- (457). Ó Cuiv P; Keogh D; Clarke P; O'Connell M FoxB of *Pseudomonas aeruginosa* functions in the utilization of the xenosiderophores ferrichrome, ferrioxamine B, and schizokinen: evidence

- for transport redundancy at the inner membrane. *J. Bacteriol* 2007, 189, 284–287. [PubMed: 17056746]
- (458). Banin E; Lozinski A; Brady KM; Berenshtein E; Butterfield PW; Moshe M; Chevion M; Greenberg EP; Banin E The potential of desferrioxamine-gallium as an anti-*Pseudomonas* therapeutic agent. *Proc. Natl. Acad. Sci. U. S. A* 2008, 105, 16761–6. [PubMed: 18931304]
- (459). Llamas MA; Mooij MJ; Sparrius M; Vandenbroucke-Grauls CM; Ratledge C; Bitter W Characterization of five novel *Pseudomonas aeruginosa* cell-surface signalling systems. *Mol. Microbiol* 2008, 67, 458–72. [PubMed: 18086184]
- (460). Marshall B; Stintzi A; Gilmour C; Meyer JM; Poole K Citrate-mediated iron uptake in *Pseudomonas aeruginosa*: involvement of the citrate-inducible FecA receptor and the FeoB ferrous iron transporter. *Microbiology* 2009, 155, 305–315. [PubMed: 19118371]
- (461). Cuiv PO; Clarke P; O’Connell M Identification and characterization of an iron-regulated gene, *chtA*, required for the utilization of the xenosiderophores aerobactin, rhizobactin 1021 and schizokinen by *Pseudomonas aeruginosa*. *Microbiology* 2006, 152, 945–54. [PubMed: 16549659]
- (462). Elias S; Degtyar E; Banin E FvbA is required for vibriobactin utilization in *Pseudomonas aeruginosa*. *Microbiology* 2011, 157, 2172–2180. [PubMed: 21546589]
- (463). Galet J; Deveau A; Hotel L; Frey-Klett P; Leblond P; Aigle B *Pseudomonas fluorescens* pirates both ferrioxamine and ferricoelichelin siderophores from *Streptomyces ambofaciens*. *Appl. Environ. Microbiol* 2015, 81, 3132–41. [PubMed: 25724953]
- (464). Ochsner UA; Johnson Z; Vasil ML Genetics and regulation of two distinct haem-uptake systems, *phu* and *has*, in *Pseudomonas aeruginosa*. *Microbiology* 2000, 146, 185–198. [PubMed: 10658665]
- (465). Letoffe S; Redeker V; Wandersman C Isolation and characterization of an extracellular haem-binding protein from *Pseudomonas aeruginosa* that shares function and sequence similarities with the *Serratia marcescens* HasA haemophore. *Mol. Microbiol* 1998, 28, 1223–34. [PubMed: 9680211]
- (466). Wandersman C; Delepelaire P Bacterial iron sources: from siderophores to hemophores. *Annu. Rev. Microbiol* 2004, 58, 611–47. [PubMed: 15487950]
- (467). Wandersman C; Delepelaire P Haemophore functions revisited. *Mol. Microbiol* 2012, 85, 618–31. [PubMed: 22715905]
- (468). Smith AD; Modi AR; Sun S; Dawson JH; Wilks A Spectroscopic Determination of Distinct Heme Ligands in Outer- Membrane Receptors *PhuR* and *HasR* of *Pseudomonas aeruginosa*. *Biochemistry* 2015, 54, 2601–12. [PubMed: 25849630]
- (469). Smith AD; Wilks A Differential contributions of the outer membrane receptors *PhuR* and *HasR* to heme acquisition in *Pseudomonas aeruginosa*. *J. Biol. Chem* 2015, 290, 7756–66. [PubMed: 25616666]
- (470). Otero-Asman JR; Garcia-Garcia AI; Civantos C; Quesada JM; Llamas MA *Pseudomonas aeruginosa* possesses three distinct systems for sensing and using the host molecule haem. *Environ. Microbiol* 2019, 21, 4629–4647. [PubMed: 31390127]
- (471). Macedo MF; Cruz E; Lacerda R; Porto G; de Sousa M Low serum transferrin levels in HFE C282Y homozygous subjects are associated with low CD8(+) T lymphocyte numbers. *Blood Cells, Mol., Dis* 2005, 35, 319–25. [PubMed: 16140024]
- (472). Stites SW; Plautz MW; Bailey K; O’Brien-Ladner AR; Wesselius LJ Increased concentrations of iron and isoferritins in the lower respiratory tract of patients with stable cystic fibrosis. *Am. J. Respir. Crit. Care Med* 1999, 160, 796–801. [PubMed: 10471599]
- (473). Dehner C; Morales-Soto N; Behera RK; Shrout J; Theil EC; Maurice PA; Dubois JL Ferritin and ferrihydrite nanoparticles as iron sources for *Pseudomonas aeruginosa*. *JBIC, J. Biol. Inorg. Chem* 2013, 18, 371–81. [PubMed: 23417538]
- (474). Zimmermann L; Hantke K; Braun V Exogenous induction of the iron dicitrate transport system of *Escherichia coli* K-12. *J. Bacteriol* 1984, 159, 271–7. [PubMed: 6376472]
- (475). Harle C; Kim I; Angerer A; Braun V Signal transfer through three compartments: transcription initiation of the *Escherichia coli* ferric citrate transport system from the cell surface. *EMBO J.* 1995, 14, 1430–8. [PubMed: 7729419]

- (476). Brilllet K; Journet L; Celia H; Paulus L; Stahl A; Pattus F; Cobessi D A beta strand lock exchange for signal transduction in TonB-dependent transducers on the basis of a common structural motif. *Structure (Oxford, U. K.)* 2007, 15, 1383–91.
- (477). Wirth C; Meyer-Klaucke W; Pattus F; Cobessi D From the periplasmic signaling domain to the extracellular face of an outer membrane signal transducer of *Pseudomonas aeruginosa*: crystal structure of the ferric pyoverdine outer membrane receptor. *J. Mol. Biol* 2007, 368, 398–406. [PubMed: 17349657]
- (478). Cunliffe HE; Merriman TR; Lamont IL Cloning and characterization of pvdS, a gene required for pyoverdine synthesis in *Pseudomonas aeruginosa*: PvdS is probably an alternative sigma factor. *Journal of bacteriology* 1995, 177, 2744–50. [PubMed: 7751284]
- (479). Redly GA; Poole K Pyoverdine-mediated regulation of FpvA synthesis in *Pseudomonas aeruginosa*: involvement of a probable extracytoplasmic-function sigma factor, FpvI. *J. Bacteriol* 2003, 185, 1261–5. [PubMed: 12562796]
- (480). Beare PA; For RJ; Martin LW; Lamont IL Siderophore-mediated cell signalling in *Pseudomonas aeruginosa*: divergent pathways regulate virulence factor production and siderophore receptor synthesis. *Mol. Microbiol* 2003, 47, 195–207. [PubMed: 12492864]
- (481). Llamas MA; Imperi F; Visca P; Lamont IL Cell-surface signaling in *Pseudomonas*: stress responses, iron transport, and pathogenicity. *FEMS Microbiol Rev.* 2014, 38, 569–97. [PubMed: 24923658]
- (482). Flemming HC; Wingender J The biofilm matrix. *Nat. Rev. Microbiol* 2010, 8, 623–33. [PubMed: 20676145]
- (483). Kang D; Kirienko DR; Webster P; Fisher AL; Kirienko NV Pyoverdine, a siderophore from *Pseudomonas aeruginosa*, translocates into *C. elegans*, removes iron, and activates a distinct host response. *Virulence* 2018, 9, 804–817. [PubMed: 29532717]
- (484). Kang D; Kirienko NV High-Throughput Genetic Screen Reveals that Early Attachment and Biofilm Formation Are Necessary for Full Pyoverdine Production by *Pseudomonas aeruginosa*. *Front. Microbiol* 2017, 8, 1707. [PubMed: 28928729]
- (485). Alhede M; Bjarnsholt T; Givskov M; Alhede M *Pseudomonas aeruginosa* biofilms: mechanisms of immune evasion. *Adv. Appl. Microbiol* 2014, 86, 1–40. [PubMed: 24377853]
- (486). Banin E; Vasil ML; Greenberg EP Iron and *Pseudomonas aeruginosa* biofilm formation. *Proc. Natl. Acad. Sci. U. S. A* 2005, 102, 11076–81. [PubMed: 16043697]
- (487). Banin E; Brady KM; Greenberg EP Chelator-induced dispersal and killing of *Pseudomonas aeruginosa* cells in a biofilm. *Appl. Environ. Microbiol* 2006, 72, 2064–9. [PubMed: 16517655]
- (488). Andrews SC; Robinson AK; Rodriguez-Quinones F Bacterial iron homeostasis. *FEMS Microbiol Rev.* 2003, 27, 215–37. [PubMed: 12829269]
- (489). Hunter RC; Klepac-Ceraj V; Lorenzi MM; Grotzinger H; Martin TR; Newman DK Phenazine content in the cystic fibrosis respiratory tract negatively correlates with lung function and microbial complexity. *Am. J. Respir. Cell Mol. Biol* 2012, 47, 738–45. [PubMed: 22865623]
- (490). Hunter RC; Asfour F; Dingemans J; Osuna BL; Samad T; Malfroot A; Cornelis P; Newman DK Ferrous iron is a significant component of bioavailable iron in cystic fibrosis airways. *mBio* 2013, 4, e00557–13.
- (491). Cowan SW; Garavito RM; Jansonius JN; Jenkins JA; Karlsson R; Konig N; Pai EF; Pauptit RA; Rizkallah PJ; Rosenbusch JP; et al. The structure of OmpF porin in a tetragonal crystal form. *Structure (Oxford, U. K.)* 1995, 3, 1041–50.
- (492). Nakashige TG; Zhang B; Krebs C; Nolan EM Human calprotectin is an iron-sequestering host-defense protein. *Nat. Chem. Biol* 2015, 11, 765–71. [PubMed: 26302479]
- (493). Zygiel EM; Nelson CE; Brewer LK; Oglesby-Sherrouse AG; Nolan EM The human innate immune protein calprotectin induces iron starvation responses in *Pseudomonas aeruginosa*. *J. Biol. Chem* 2019, 294, 3549–3562. [PubMed: 30622135]
- (494). Zygiel EM; Nolan EM Exploring Iron Withholding by the Innate Immune Protein Human Calprotectin. *Acc. Chem. Res* 2019, 52, 2301–2308. [PubMed: 31381301]
- (495). Bonneau A; Roche B; Schalk IJ Iron acquisition in *Pseudomonas aeruginosa* by the siderophore pyoverdine: an intricate interacting network including periplasmic and membrane proteins. *Sci. Rep* 2020, 10, 120. [PubMed: 31924850]



- (496). Brillet K; Ruffenach F; Adams H; Journet L; Gasser V; Hoegy F; Guillon L; Hannauer M; Page A; Schalk IJ An ABC transporter with two periplasmic binding proteins involved in iron acquisition in *Pseudomonas aeruginosa*. *ACS Chem. Biol* 2012, 7, 2036–45. [PubMed: 23009327]
- (497). Vigouroux A; Aumont-Nicaise M; Boussac A; Marty L; Lo Bello L; Legrand P; Brillet K; Schalk IJ; Morera S A unique ferrous iron binding mode is associated with large conformational changes for the transport protein FpVC of *Pseudomonas aeruginosa*. *FEBS J.* 2020, 287, 295–309. [PubMed: 31318478]
- (498). Kirienko NV; Ausubel FM; Ruvkun G Mitophagy confers resistance to siderophore-mediated killing by *Pseudomonas aeruginosa*. *Proc. Natl. Acad. Sci. U. S. A* 2015, 112, 1821–6. [PubMed: 25624506]
- (499). Pollitzer R Plague; WHO, Geneva, 1954; pp 409–482.
- (500). Perry RD; Fetherston JD *Yersinia pestis*—etiologic agent of plague. *Clin. Microbiol. Rev* 1997, 10, 35–66. [PubMed: 8993858]
- (501). Hinnebusch B; Erickson D *Yersinia pestis* biofilm in the flea vector and its role in the transmission of plague. In *Bacterial Biofilms*; Springer, 2008; pp 229–248.
- (502). Fetherston JD; Kirillina O; Bobrov AG; Paulley JT; Perry RD The yersiniabactin transport system is critical for the pathogenesis of bubonic and pneumonic plague. *Infect. Immun* 2010, 78, 2045–2052. [PubMed: 20160020]
- (503). Guerinot ML Microbial iron transport. *Annu. Rev. Microbiol* 1994, 48, 743–772. [PubMed: 7826025]
- (504). Mietzner TA; Morse SA The role of iron-binding proteins in the survival of pathogenic bacteria. *Annu. Rev. Nutr* 1994, 14, 471–493. [PubMed: 7946530]
- (505). Crosa JH; Mey AR; Payne SM *Iron Transport in Bacteria*; ASM Press: Washington, DC, 2004; Vol. 410.
- (506). Payne SM; Mey AR *Pathogenic Escherichia coli, Shigella, and Salmonella. Iron transport in bacteria 2014*, 197–218.
- (507). Bearden SW; Fetherston JD; Perry RD Genetic organization of the yersiniabactin biosynthetic region and construction of avirulent mutants in *Yersinia pestis*. *Infection and immunity* 1997, 65, 1659–1668. [PubMed: 9125544]
- (508). Bearden SW; Staggs TM; Perry RD An ABC Transporter System of *Yersinia pestis* Allows Utilization of Chelated Iron by *Escherichia coli* SAB11. *J. Bacteriol* 1998, 180, 1135–1147. [PubMed: 9495751]
- (509). Bearden SW; Perry RD The Yfe system of *Yersinia pestis* transports iron and manganese and is required for full virulence of plague. *Mol. Microbiol* 1999, 32, 403–414. [PubMed: 10231495]
- (510). Gong S; Bearden SW; Geoffroy VA; Fetherston JD; Perry RD Characterization of the *Yersinia pestis* Yfu ABC Inorganic Iron Transport System. *Infect. Immun* 2001, 69, 2829–2837. [PubMed: 11292695]
- (511). Perry RD; Abney J; Mier I; Lee Y; Bearden SW; Fetherston JD Regulation of the *Yersinia pestis* Yfe and Ybt iron transport systems. In *The Genus Yersinia*; Springer, 2004; pp 275–283.
- (512). Kirillina O; Bobrov AG; Fetherston JD; Perry RD Hierarchy of iron uptake systems: Yfu and Yiu are functional in *Yersinia pestis*. *Infect. Immun* 2006, 74, 6171–6178. [PubMed: 16954402]
- (513). Perry RD; Mier I; Fetherston JD Roles of the Yfe and Feo transporters of *Yersinia pestis* in iron uptake and intracellular growth. *BioMetals* 2007, 20, 699. [PubMed: 17206386]
- (514). Forman S; Paulley JT; Fetherston JD; Cheng Y-Q; Perry RD *Yersinia ironomics: comparison of iron transporters among Yersiniapestis biotypes and its nearest neighbor, Yersinia pseudotuberculosis*. *BioMetals* 2010, 23, 275–294. [PubMed: 20049509]
- (515). Pieper R; Huang S-T; Parmar PP; Clark DJ; Alami H; Fleischmann RD; Perry RD; Peterson SN Proteomic analysis of iron acquisition, metabolic and regulatory responses of *Yersinia pestis* to iron starvation. *BMC Microbiol.* 2010, 10, 30. [PubMed: 20113483]
- (516). Perry R; Fetherston J Iron and heme uptake systems. In *Yersinia Molecular and Cellular Biology*; Horizon Bioscience: Norfolk, UK, 2004; pp 257–283
- (517). Iteman I; Guiyoule A; de Almeida A; Guilvout I; Baranton G; Carniel E Relationship between loss of pigmentation and deletion of the chromosomal iron-regulated *irp2* gene in *Yersinia*

- pestis: evidence for separate but related events. *Infect. Immun* 1993, 61, 2717–2722. [PubMed: 8500913]
- (518). Carniel E; Guilvout I; Prentice M Characterization of a large chromosomal” high-pathogenicity island” in biotype 1B *Yersinia enterocolitica*. *Journal of bacteriology* 1996, 178, 6743–6751. [PubMed: 8955291]
- (519). Rakin A; Noelting C; Schubert S; Heesemann J Common and specific characteristics of the high-pathogenicity island of *Yersinia enterocolitica*. *Infect. Immun* 1999, 67, 5265–5274. [PubMed: 10496905]
- (520). Lesic B; Carniel E The high pathogenicity island: a broad-host-range pathogenicity island. In *Yersinia Molecular and Cellular Biology*; Horizon Bioscience: Norfolk, UK, 2004; pp 285–306.
- (521). Perry RD; Balbo PB; Jones HA; Fetherston JD; DeMoll E *Yersiniabactin* from *Yersinia pestis*: biochemical characterization of the siderophore and its role in iron transport and regulation. *Microbiology* 1999, 145, 1181–1190. [PubMed: 10376834]
- (522). Rakin A; Saken E; Harmsen D; Heesemann J The pesticin receptor of *Yersinia enterocolitica*: a novel virulence factor with dual function. *Mol. Microbiol* 1994, 13, 253–263. [PubMed: 7984105]
- (523). Fetherston JD; Lillard J; Perry RD Analysis of the pesticin receptor from *Yersinia pestis*: role in iron-deficient growth and possible regulation by its siderophore. *J. Bacteriol* 1995, 177, 1824–1833. [PubMed: 7896707]
- (524). Fetherston JD; Bertolino VJ; Perry RD *YbtP* and *YbtQ*: two ABC transporters required for iron uptake in *Yersinia pestis*. *Mol. Microbiol* 1999, 32, 289–299. [PubMed: 10231486]
- (525). Sebbane F; Jarrett C; Gardner D; Long D; Hinnebusch BJ Role of the *Yersinia pestis* *yersiniabactin* iron acquisition system in the incidence of flea-borne plague. *PLoS One* 2010, 5, No. e14379. [PubMed: 21179420]
- (526). Tu J; Xue T; Qi K; Shao Y; Huang B; Wang X; Zhou X The *irp2* and *fyuA* genes in High Pathogenicity Islands are involved in the pathogenesis of infections caused by avian pathogenic *Escherichia coli* (APEC). *Pol. J. Vet. Sci* 2016, 19, 19–21.
- (527). Lukacik P; Barnard TJ; Keller PW; Chaturvedi KS; Seddiki N; Fairman JW; Noinaj N; Kirby TL; Henderson JP; Steven AC; Hinnebusch BJ; Buchanan SK Structural engineering of a phage lysin that targets gram-negative pathogens. *Proc. Natl. Acad. Sci. U. S. A* 2012, 109, 9857–62. [PubMed: 22679291]
- (528). Fetherston JD; Lillard JW Jr; Perry RD Analysis of the pesticin receptor from *Yersinia pestis*: role in iron-deficient growth and possible regulation by its siderophore. *Journal of bacteriology* 1995, 177, 1824–33. [PubMed: 7896707]
- (529). Xu H; Tie K; Zhang Y; Feng X; Cao Y; Han W Design, expression, and characterization of the hybrid antimicrobial peptide T-catesbeianin-1 based on *FyuA*. *J. Pept. Sci* 2018, 24, e3059.
- (530). Wang Z; Hu W; Zheng H Pathogenic siderophore ABC importer *YbtPQ* adopts a surprising fold of exporter. *Science advances* 2020, 6, No. eaay7997. [PubMed: 32076651]
- (531). Borths EL; Locher KP; Lee AT; Rees DC The structure of *Escherichia coli* *BtuF* and binding to its cognate ATP binding cassette transporter. *Proc. Natl. Acad. Sci. U. S. A* 2002, 99, 16642–7. [PubMed: 12475936]
- (532). Pinkett HW; Lee AT; Lum P; Locher KP; Rees DC An inward-facing conformation of a putative metal-chelate-type ABC transporter. *Science (Washington, DC, U. S.)* 2007, 315, 373–7.
- (533). Fetherston JD; Mier I; Truszczynska H; Perry RD The *Yfe* and *Feo* transporters are involved in microaerobic growth and virulence of *Yersinia pestis* in bubonic plague. *Infect. Immun* 2012, 80, 3880–3891. [PubMed: 22927049]
- (534). Une T; Brubaker RR In vivo comparison of avirulent *Vwa-* and *Pgm-* or *Pstr* phenotypes of *yersiniae*. *Infect. Immun* 1984, 43, 895–900. [PubMed: 6365786]
- (535). Skare JT; Ahmer B; Seachord CL; Darveau RP; Postle K Energy transduction between membranes. *TonB*, a cytoplasmic membrane protein, can be chemically cross-linked in vivo to the outer membrane receptor *FepA*. *J. Biol. Chem* 1993, 268, 16302–16308. [PubMed: 8344918]
- (536). Radka CD; DeLucas LJ; Wilson LS; Lawrenz MB; Perry RD; Aller SG Crystal structure of *Yersinia pestis* virulence factor *YfeA* reveals two polyspecific metal-binding sites. *Acta Crystallographica Section D: Structural Biology* 2017, 73, 557–572. [PubMed: 28695856]

- (537). Bezkorovainy A Antimicrobial properties of iron-binding proteins. *Advances in experimental medicine and biology* 1981, 135, 139–54. [PubMed: 6452038]
- (538). Crichton RR; Charlotiaux-Wauters M Iron transport and storage. *Eur. J. Biochem* 1987, 164, 485–506. [PubMed: 3032619]
- (539). Orsi N The antimicrobial activity of lactoferrin: current status and perspectives. *BioMetals* 2004, 17, 189–96. [PubMed: 15222464]
- (540). Otto BR; Verweij-Van Vught AM; MacLaren DM Transferrins and heme-compounds as iron sources for pathogenic bacteria. *Crit. Rev. Microbiol* 1992, 18, 217–33. [PubMed: 1532495]
- (541). Triebel S; Bläser J; Reinke H; Tschesche HA 25 kDa alpha 2-microglobulin-related protein is a component of the 125 kDa form of human gelatinase. *FEBS Lett.* 1992, 314, 386–8. [PubMed: 1281792]
- (542). Hraba-Renevey S; Türler H; Kress M; Salomon C; Weil R SV40-induced expression of mouse gene 24p3 involves a post-transcriptional mechanism. *Oncogene* 1989, 4, 601–608. [PubMed: 2542864]
- (543). Xiao X; Yeoh BS; Vijay-Kumar M Lipocalin 2: An Emerging Player in Iron Homeostasis and Inflammation. *Annu. Rev. Nutr* 2017, 37, 103–130. [PubMed: 28628361]
- (544). Yang J; Goetz D; Li JY; Wang W; Mori K; Setlik D; Du T; Erdjument-Bromage H; Tempst P; Strong R; Barasch J An iron delivery pathway mediated by a lipocalin. *Mol. Cell* 2002, 10, 1045–56. [PubMed: 12453413]
- (545). Devireddy LR; Hart DO; Goetz DH; Green MR A mammalian siderophore synthesized by an enzyme with a bacterial homolog involved in enterobactin production. *Cell* 2010, 141, 1006–17. [PubMed: 20550936]
- (546). Liu Z; Reba S; Chen WD; Porwal SK; Boom WH; Petersen RB; Rojas R; Viswanathan R; Devireddy L Regulation of mammalian siderophore 2,5-DHBA in the innate immune response to infection. *J. Exp. Med* 2014, 211, 1197–213. [PubMed: 24863067]
- (547). Fluckinger M; Haas H; Merschak P; Glasgow BJ; Redl B Human tear lipocalin exhibits antimicrobial activity by scavenging microbial siderophores. *Antimicrob. Agents Chemother* 2004, 48, 3367–72. [PubMed: 15328098]
- (548). Doneanu CE; Strong RK; Howald WN Characterization of a noncovalent lipocalin complex by liquid chromatography/electrospray ionization mass spectrometry. *J. Biomol. Tech* 2004, 15, 208–212. [PubMed: 15331587]
- (549). Holmes MA; Paulsene W; Jide X; Ratledge C; Strong RK Siderocalin (Lcn 2) also binds carboxymycobactins, potentially defending against mycobacterial infections through iron sequestration. *Structure (Oxford, U. K.)* 2005, 13, 29–41.
- (550). Lassagne H; Gachon AMF; Nakashima Y; Yanagita T; Ozawa M; Muramatsu T Cloning of a human lacrimal lipocalin secreted in tears. *Exp. Eye Res* 1993, 56, 605–609. [PubMed: 8500570]
- (551). Nelson AL; Barasch JM; Bunte RM; Weiser JN Bacterial colonization of nasal mucosa induces expression of siderocalin, an iron-sequestering component of innate immunity. *Cell. Microbiol* 2005, 7, 1404–17. [PubMed: 16153241]
- (552). Borregaard N; Cowland JB Neutrophil gelatinase-associated lipocalin, a siderophore-binding eukaryotic protein. *BioMetals* 2006, 19, 211–5. [PubMed: 16718606]
- (553). Wu H; Santoni-Rugiu E; Ralfkiaer E; Porse BT; Moser C; Hoiby N; Borregaard N; Cowland JB Lipocalin 2 is protective against *E. coli* pneumonia. *Respir. Res* 2010, 11, 96. [PubMed: 20633248]
- (554). Goetz DH; Holmes MA; Borregaard N; Bluhm ME; Raymond KN; Strong RK The neutrophil lipocalin NGAL is a bacteriostatic agent that interferes with siderophore-mediated iron acquisition. *Mol. Cell* 2002, 10, 1033–1043. [PubMed: 12453412]
- (555). Flo TH; Smith KD; Sato S; Rodriguez DJ; Holmes MA; Strong RK; Akira S; Aderem A Lipocalin 2 mediates an innate immune response to bacterial infection by sequestering iron. *Nature* 2004, 432, 917–921. [PubMed: 15531878]
- (556). Fischbach MA; Lin H; Zhou L; Yu Y; Abergel RJ; Liu DR; Raymond KN; Wanner BL; Strong RK; Walsh CT; et al. The pathogen-associated *iroA* gene cluster mediates bacterial evasion of lipocalin 2. *Proc. Natl. Acad. Sci. U. S. A* 2006, 103, 16502–16507. [PubMed: 17060628]

- (557). Dauner M; Eichinger A; Lücking G; Scherer S; Skerra A Reprogramming Human Siderocalin To Neutralize Petrobactin, the Essential Iron Scavenger of Anthrax Bacillus. *Angew. Chem., Int. Ed* 2018, 57, 14619–14623.
- (558). Dauner M; Skerra A Scavenging Bacterial Siderophores with Engineered Lipocalin Proteins as an Alternative Antimicrobial Strategy. *ChemBioChem* 2020, 21, 601–606. [PubMed: 31613035]
- (559). Heilmeyer L; Woehler F [Modern problems of hemochromatosis with special reference to desferrioxamine treatment]. *Dtsch. Med. Wochenschr* 1962, 87, 2661–7. [PubMed: 13953391]
- (560). Risell E; Schnack H [Experiences with a new iron compound, desferrioxamine]. *Wien Klin Wochenschr* 1962, 74, 577–580. [PubMed: 14492439]
- (561). Tripod J; Keberle H [Biological assay with desferrioxamine]. *Helv. Physiol. Pharmacol. Acta* 1962, 20, 291–293. [PubMed: 13994192]
- (562). Coulton JW; Naegeli HU; Braun V Iron supply of *Escherichia coli* with polymer-bound ferricrocin. *Eur. J. Biochem* 1979, 99, 39–47. [PubMed: 385320]
- (563). Plaha DS; Rogers HJ; Williams GW Studies of the antibacterial effect of the scandium complex of enterochelin. *J. Antibiot* 1984, 37, 588–95.
- (564). Rogers HJ; Synge C; Woods VE Antibacterial effect of scandium and indium complexes of enterochelin on *Klebsiella pneumoniae*. *Antimicrob. Agents Chemother* 1980, 18, 63–8. [PubMed: 6448022]
- (565). Ohi N; Aoki B; Shinozaki T; Moro K; Noto T; Nehashi T; Okazaki H; Matsunaga I Semisynthetic beta-lactam antibiotics. I. Synthesis and antibacterial activity of new ureidopenicillin derivatives having catechol moieties. *J. Antibiot* 1986, 39, 230–41.
- (566). Basker MJ; Branch CL; Finch SC; Guest AW; Milner PH; Pearson MJ; Ponsford RJ; Smale TC Studies on semi-synthetic 7 alpha-formamidocephalosporins. I. Structure-activity relationships in some semi-synthetic 7 alpha-formamidocephalosporins. *J. Antibiot* 1986, 39, 1788–91.
- (567). Burton G; Best DJ; Dixon RA; Kenyon RF; Lashford AG Studies on 6 alpha-substituted penicillins. II. Synthesis and structure-activity relationships of 6 beta-(2-aryl-2-sulfoacetamido)-6 alpha-methoxy penicillanic acids. *J. Antibiot* 1986, 39, 1419–29.
- (568). Mochida K; Ono Y; Yamasaki M; Shiraki C; Hirata T; Sato K; Okachi R Aminothiazolylglycyl derivatives of carbacephem antibiotics. II. Synthesis and antibacterial activity of novel aminothiazolyl cephem compounds with hydroxypyridone moiety. *J. Antibiot* 1987, 40, 182–9.
- (569). Nakagawa S; Sanada M; Matsuda K; Hazumi N; Tanaka N Biological activity of BO-1236, a new antipseudomonal cephalosporin. *Antimicrob. Agents Chemother* 1987, 31, 1100–5. [PubMed: 3116919]
- (570). Labott SM; Martin RB The stress-moderating effects of weeping and humor. *J. Human Stress* 1987, 13, 159–64.
- (571). Watanabe NA; Nagasu T; Katsu K; Kitoh K E-0702, a new cephalosporin, is incorporated into *Escherichia coli* cells via the tonB-dependent iron transport system. *Antimicrob. Agents Chemother* 1987, 31, 497–504. [PubMed: 3037997]
- (572). Carpenter C; Payne SM Regulation of iron transport systems in Enterobacteriaceae in response to oxygen and iron availability. *J. Inorg. Biochem* 2014, 133, 110–7. [PubMed: 24485010]
- (573). Miller MJ; McKee JA; Minnick AA; Dolence EK The design, synthesis and study of siderophore-antibiotic conjugates. Siderophore mediated drug transport. *Biol. Met* 1991, 4, 62–9. [PubMed: 1830210]
- (574). Curtis NA; Eisenstadt RL; East SJ; Cornford RJ; Walker LA; White AJ Iron-regulated outer membrane proteins of *Escherichia coli* K-12 and mechanism of action of catechol-substituted cephalosporins. *Antimicrob. Agents Chemother* 1988, 32, 1879–86. [PubMed: 3072926]
- (575). Dichtl S; Demetz E; Haschka D; Tymoszuk P; Petzer V; Nairz M; Seifert M; Hoffmann A; Brigo N; Wurzner R; Theurl I; Karlinsey JE; Fang FC; Weiss G Dopamine Is a Siderophore-Like Iron Chelator That Promotes *Salmonella enterica* Serovar Typhimurium Virulence in Mice. *mBio* 2019, 10, e02624–18. [PubMed: 30723125]
- (576). Armstrong SK; Brickman TJ; Suhadolc RJ Involvement of multiple distinct Bordetella receptor proteins in the utilization of iron liberated from transferrin by host catecholamine stress hormones. *Mol. Microbiol* 2012, 84, 446–62. [PubMed: 22458330]

- (577). Sandrini SM; Shergill R; Woodward J; Muralikuttan R; Haigh RD; Lyte M; Freestone PP Elucidation of the mechanism by which catecholamine stress hormones liberate iron from the innate immune defense proteins transferrin and lactoferrin. *J. Bacteriol* 2010, 192, 587–94. [PubMed: 19820086]
- (578). Hantke K Dihydroxybenzoylserine—a siderophore for *E. coli*. *FEMS Microbiol. Lett* 1990, 67, 5–8.
- (579). Lopez-Goni I; Moriyon I; Neilands JB Identification of 2,3-dihydroxybenzoic acid as a *Brucella abortus* siderophore. *Infect. Immun* 1992, 60, 4496–503. [PubMed: 1398964]
- (580). Young IG; Cox GB; Gibson F 2,3-Dihydroxybenzoate as a bacterial growth factor and its route of biosynthesis. *Biochim. Biophys. Acta, Gen. Subj* 1967, 141, 319–31.
- (581). Ito A; Nishikawa T; Matsumoto S; Yoshizawa H; Sato T; Nakamura R; Tsuji M; Yamano Y Siderophore Cephalosporin Cefiderocol Utilizes Ferric Iron Transporter Systems for Antibacterial Activity against *Pseudomonas aeruginosa*. *Antimicrob. Agents Chemother* 2016, 60, 7396–7401. [PubMed: 27736756]
- (582). Cody YS; Gross DC Characterization of Pyoverdin(pss), the Fluorescent Siderophore Produced by *Pseudomonas syringae* pv. *syringae*. *Appl. Environ. Microbiol* 1987, 53, 928–34. [PubMed: 16347352]
- (583). Huband MD; Ito A; Tsuji M; Sader HS; Fedler KA; Flamm RK Cefiderocol MIC quality control ranges in iron-depleted cation-adjusted Mueller-Hinton broth using a CLSI M23-A4 multi-laboratory study design. *Diagn. Microbiol. Infect. Dis* 2017, 88, 198–200. [PubMed: 28410852]
- (584). Schalk IJ; Yue WW; Buchanan SK Recognition of iron-free siderophores by TonB-dependent iron transporters. *Mol. Microbiol* 2004, 54, 14–22. [PubMed: 15458401]
- (585). Brilllet K; Reimmann C; Mislin GL; Noël S; Rognan D; Schalk IJ; Cobessi D Pyochelin enantiomers and their outer-membrane siderophore transporters in fluorescent pseudomonads: structural bases for unique enantiospecific recognition. *J. Am. Chem. Soc* 2011, 133, 16503–9. [PubMed: 21902256]
- (586). Hoegy F; Lee X; Noel S; Rognan D; Mislin GL; Reimmann C; Schalk IJ Stereospecificity of the siderophore pyochelin outer membrane transporters in fluorescent pseudomonads. *J. Biol. Chem* 2009, 284, 14949–57. [PubMed: 19297329]
- (587). Matzanke BF; Muller GI; Raymond KN Hydroxamate siderophore mediated iron uptake in *E. coli*: stereospecific recognition of ferric rhodotorulic acid. *Biochem. Biophys. Res. Commun* 1984, 121, 922–30. [PubMed: 6234892]
- (588). Neilands JB; Erickson TJ; Rastetter WH Stereospecificity of the ferric enterobactin receptor of *Escherichia coli* K-12. *J. Biol. Chem* 1981, 256, 3831–2. [PubMed: 6452456]
- (589). Youard ZA; Reimmann C Stereospecific recognition of pyochelin and enantio-pyochelin by the PchR proteins in fluorescent pseudomonads. *Microbiology* 2010, 156, 1772–1782. [PubMed: 20203054]
- (590). Ito AIN; Ishii R; Tsuji M; Maki H; Sato T; Yamano Y Changes of Responsible Iron-Transporters for the Activity of Cefiderocol against *Pseudomonas aeruginosa* Depending on the Culture Conditions. In *ASM Microbe*; ASM: San Francisco, CA, 2019.
- (591). Ito A; Nishikawa T; Ota M; Ito-Horiyama T; Ishibashi N; Sato T; Tsuji M; Yamano Y Stability and low induction propensity of cefiderocol against chromosomal AmpC  $\beta$ -lactamases of *Pseudomonas aeruginosa* and *Enterobacter cloacae*. *J. Antimicrob. Chemother* 2018, 73, 3049–3052. [PubMed: 30188999]
- (592). Ito A; Sato T; Ota M; Takemura M; Nishikawa T; Toba S; Kohira N; Miyagawa S; Ishibashi N; Matsumoto S; Nakamura R; Tsuji M; Yamano Y In Vitro Antibacterial Properties of Cefiderocol, a Novel Siderophore Cephalosporin, against Gram-Negative Bacteria. *Antimicrob. Agents Chemother* 2018, 62, e01454–17.
- (593). Moynie L; Milenkovic S; Mislin GLA; Gasser V; Mallocci G; Baco E; McCaughan RP; Page MGP; Schalk IJ; Ceccarelli M; Naismith JH The complex of ferric-enterobactin with its transporter from *Pseudomonas aeruginosa* suggests a two-site model. *Nat. Commun* 2019, 10, 3673. [PubMed: 31413254]

- (594). Luscher A; Moynie L; Auguste PS; Bumann D; Mazza L; Pletzer D; Naismith JH; Kohler T TonB-Dependent Receptor Repertoire of *Pseudomonas aeruginosa* for Uptake of Siderophore-Drug Conjugates. *Antimicrob. Agents Chemother* 2018, 62, e00097–18. [PubMed: 29555629]
- (595). van Delden C; Page MG; Kohler T Involvement of Fe uptake systems and AmpC beta-lactamase in susceptibility to the siderophore monosulfactam BAL30072 in *Pseudomonas aeruginosa*. *Antimicrob. Agents Chemother* 2013, 57, 2095–102. [PubMed: 23422914]
- (596). Kim A; Kutschke A; Ehmann DE; Patey SA; Crandon JL; Gorseth E; Miller AA; McLaughlin RE; Blinn CM; Chen A; Nayar AS; Dangel B; Tsai AS; Rooney MT; Murphy-Benenato KE; Eakin AE; Nicolau DP Pharmacodynamic Profiling of a Siderophore-Conjugated Monocarbam in *Pseudomonas aeruginosa*: Assessing the Risk for Resistance and Attenuated Efficacy. *Antimicrob. Agents Chemother* 2015, 59, 7743–52. [PubMed: 26438502]
- (597). McPherson CJ; Aschenbrenner LM; Lacey BM; Fahnoe KC; Lemmon MM; Finegan SM; Tadakamalla B; O'Donnell JP; Mueller JP; Tomaras AP Clinically relevant Gram-negative resistance mechanisms have no effect on the efficacy of MC-1, a novel siderophore-conjugated monocarbam. *Antimicrob. Agents Chemother* 2012, 56, 6334–42. [PubMed: 23027195]
- (598). de Lorenzo V; Giovannini F; Herrero M; Neilands JB Metal ion regulation of gene expression. Fur repressor-operator interaction at the promoter region of the aerobactin system of pColV-K30. *J. Mol. Biol* 1988, 203, 875–884. [PubMed: 3062182]
- (599). Escolar L; Perez-Martin J; de Lorenzo V Opening the iron box: transcriptional metalloregulation by the Fur protein. *J. Bacteriol* 1999, 181, 6223–9. [PubMed: 10515908]
- (600). Shields RK Case Commentary: the Need for Cefiderocol Is Clear, but Are the Supporting Clinical Data? *Antimicrob. Agents Chemother* 2020, 64, e00059–20. [PubMed: 32015037]
- (601). Wu JY; Srinivas P; Pogue JM Cefiderocol: A Novel Agent for the Management of Multidrug-Resistant Gram-Negative Organisms. *Infect Dis Ther* 2020, 9, 17–40. [PubMed: 32072491]
- (602). Yamano Y In Vitro Activity of Cefiderocol Against a Broad Range of Clinically Important Gram-negative Bacteria. *Clin. Infect. Dis* 2019, 69, S544–S551. [PubMed: 31724049]
- (603). Tomaras AP; Crandon JL; McPherson CJ; Banevicius MA; Finegan SM; Irvine RL; Brown MF; O'Donnell JP; Nicolau DP Adaptation-based resistance to siderophore-conjugated antibacterial agents by *Pseudomonas aeruginosa*. *Antimicrob. Agents Chemother* 2013, 57, 4197–207. [PubMed: 23774440]
- (604). Ghazi IM; Monogue ML; Tsuji M; Nicolau DP Humanized Exposures of Cefiderocol, a Siderophore Cephalosporin, Display Sustained in vivo Activity against Siderophore-Resistant *Pseudomonas aeruginosa*. *Pharmacology* 2018, 101, 278–284. [PubMed: 29471305]
- (605). Monogue ML; Tsuji M; Yamano Y; Echols R; Nicolau DP Efficacy of Humanized Exposures of Cefiderocol (S-649266) against a Diverse Population of Gram-Negative Bacteria in a Murine Thigh Infection Model. *Antimicrob. Agents Chemother* 2017, 61, e01022–17. [PubMed: 28848004]
- (606). Tomaras AP; Crandon JL; McPherson CJ; Nicolau DP Potentiation of antibacterial activity of the MB-1 siderophore-monobactam conjugate using an efflux pump inhibitor. *Antimicrob. Agents Chemother* 2015, 59, 2439–42. [PubMed: 25605364]
- (607). Vázquez-Ucha JC; Martínez-Gutián M; Maneiro M; Conde-Pérez K; Álvarez-Fraga L; Torrens G; Oliver A; Buynak JD; Bonomo RA; Bou G; González-Bello C; Poza M; Beceiro A Therapeutic Efficacy of LN-1–255 in Combination with Imipenem in Severe Infection Caused by Carbapenem-Resistant *Acinetobacter baumannii*. *Antimicrob. Agents Chemother* 2019, 63, e01092–19. [PubMed: 31383666]
- (608). Page MGP The Role of Iron and Siderophores in Infection, and the Development of Siderophore Antibiotics. *Clin. Infect. Dis* 2019, 69, S529–S537. [PubMed: 31724044]
- (609). Albomycin and grisein. *Br. Med. J* 1958, 1, 391.
- (610). Gamburg RL [Use of albomycin in pneumónia in children]. *Pediatrics* 1951, 5, 37–44. [PubMed: 14899972]
- (611). Luckey M; Pollack JR; Wayne R; Ames BN; Neilands JB Iron uptake in *Salmonella typhimurium*: utilization of exogenous siderochromes as iron carriers. *J. Bacteriol* 1972, 111, 731–8. [PubMed: 4559824]

- (612). Rafalowicz A [New antibiotic albomycin]. *Pol Tyg Lek (Wars)* 1953, 8, 957–958. [PubMed: 13088489]
- (613). Shorin VA; Luo S [Effect of aerobic and anaerobic conditions of growth of bacteria on antibacterial action of albomycin and of other antibiotics]. *Dokl. Akad. Nauk SSSR* 1954, 96, 645–647. [PubMed: 13173377]
- (614). Roosenberg JM 2nd; Miller MJ Total synthesis of the siderophore danoxamine. *J. Org. Chem* 2000, 65, 4833–8. [PubMed: 10956460]
- (615). Braun V; Pramanik A; Gwinner T; Köberle M; Bohn E Sideromycins: tools and antibiotics. *BioMetals* 2009, 22, 3–13. [PubMed: 19130258]
- (616). Liu R; Miller PA; Vakulenko SB; Stewart NK; Boggess WC; Miller MJ A Synthetic Dual Drug Sideromycin Induces Gram-Negative Bacteria To Commit Suicide with a Gram-Positive Antibiotic. *J. Med. Chem* 2018, 61, 3845–3854. [PubMed: 29554424]
- (617). Neumann W; Nolan EM Evaluation of a reducible disulfide linker for siderophore-mediated delivery of antibiotics. *JBIC, J. Biol. Inorg. Chem* 2018, 23, 1025–1036. [PubMed: 29968176]
- (618). Zheng T; Nolan EM Enterobactin-Mediated Delivery of beta-Lactam Antibiotics Enhances Antibacterial Activity against Pathogenic *Escherichia coli*. *J. Am. Chem. Soc* 2014, 136, 9677. [PubMed: 24927110]
- (619). Ji C; Miller MJ Chemical syntheses and in vitro antibacterial activity of two desferrioxamine B-ciprofloxacin conjugates with potential esterase and phosphatase triggered drug release linkers. *Bioorg. Med. Chem* 2012, 20, 3828–36. [PubMed: 22608921]
- (620). Silver LL A Gestalt approach to Gram-negative entry. *Bioorg. Med. Chem* 2016, 24, 6379–6389. [PubMed: 27381365]
- (621). Chen J; Yang J; Ren P; Zhou J Prokaryotic expression and function analysis of Lateolabrax japonica hepcidin. *Shuisheng Shengwu Xuebao* 2012, 34, 554–561.
- (622). Liu M; Tanaka WN; Zhu H; Xie G; Dooley DM; Lei B Direct hemin transfer from IsdA to IsdC in the iron-regulated surface determinant (Isd) heme acquisition system of *Staphylococcus aureus*. *J. Biol. Chem* 2008, 283, 6668–76. [PubMed: 18184657]
- (623). Ghosh M; Miller PA; Miller MJ Antibiotic repurposing: bis-catechol- and mixed ligand (bis-catechol-mono-hydroxamate)-teicoplanin conjugates are active against multidrug resistant *Acinetobacter baumannii*. *J. Antibiot* 2020, 73, 152–157.
- (624). Dahmen S; Mansour W; Charfi K; Boujaafar N; Arlet G; Bouallegue O Imipenem resistance in *Klebsiella pneumoniae* is associated to the combination of plasmid-mediated CMY-4 AmpC beta-lactamase and loss of an outer membrane protein. *Microb. Drug Resist* 2012, 18, 479–83. [PubMed: 22690752]
- (625). Martinez-Martinez L Extended-spectrum beta-lactamases and the permeability barrier. *Clin. Microbiol. Infect* 2008, 14, 82–9.
- (626). Nguyen Van JC; Gutmann L [Resistance to antibiotics caused by decrease of the permeability in gram-negative bacteria]. *Presse Med.* 1994, 23 (522), 527–531.
- (627). Nordmann P [Gram-negative bacteriae with resistance to carbapenems]. *Med. Sci. (Paris)* 2010, 26, 950–9. [PubMed: 21106177]
- (628). Broberg CA; Palacios M; Miller VL *Klebsiella*: a long way to go towards understanding this enigmatic jet-setter. *F1000Prime Rep.* 2014, 6, 64. [PubMed: 25165563]
- (629). Hsieh PF; Liu JY; Pan YJ; Wu MC; Lin TL; Huang YT; Wang JT *Klebsiella pneumoniae* peptidoglycan-associated lipoprotein and murein lipoprotein contribute to serum resistance, antiphagocytosis, and proinflammatory cytokine stimulation. *J. Infect. Dis* 2013, 208, 1580–9. [PubMed: 23911714]
- (630). Shon AS; Bajwa RP; Russo TA Hypervirulent (hypermucoviscous) *Klebsiella pneumoniae*: a new and dangerous breed. *Virulence.* 2013, 4, 107–18. [PubMed: 23302790]
- (631). Shon AS; Russo TA Hypervirulent *Klebsiella pneumoniae*: the next superbug? *Future Microbiol.* 2012, 7, 669–71. [PubMed: 22702521]
- (632). Hancock RE; Speert DP Antibiotic resistance in *Pseudomonas aeruginosa*: mechanisms and impact on treatment. *Drug Resist. Updates* 2000, 3, 247–255.
- (633). Nakae T Role of membrane permeability in determining antibiotic resistance in *Pseudomonas aeruginosa*. *Microbiol. Immunol* 1995, 39, 221–9. [PubMed: 7544425]

- (634). Poole K Aminoglycoside resistance in *Pseudomonas aeruginosa*. *Antimicrob. Agents Chemother* 2005, 49, 479–87. [PubMed: 15673721]
- (635). Sugawara E; Nagano K; Nikaido H Alternative folding pathways of the major porin OprF of *Pseudomonas aeruginosa*. *FEBS J.* 2012, 279, 910–8. [PubMed: 22240095]
- (636). Dong R; Guan C; Hu D; Xin TT; Qu Y The correlation study on antimicrobial resistance and biofilm related genes in clinical isolates of *Acinetobacter baumannii*. *Zhonghua Wei Zhong Bing Ji Jiu Yi Xue.* 2013, 25, 493–494. [PubMed: 24021047]
- (637). Smani Y; Pachon J Loss of the OprD homologue protein in *Acinetobacter baumannii*: impact on carbapenem susceptibility. *Antimicrob. Agents Chemother* 2013, 57, 677. [PubMed: 23275492]
- (638). Sugawara E; Nikaido H OprA is the principal nonspecific slow porin of *Acinetobacter baumannii*. *J. Bacteriol* 2012, 194, 4089–96. [PubMed: 22636785]
- (639). Oglesby-Sherrouse AG; Djapgne L; Nguyen AT; Vasil AI; Vasil ML The complex interplay of iron, biofilm formation, and mucoidy affecting antimicrobial resistance of *Pseudomonas aeruginosa*. *Pathog. Dis* 2014, 70, 307–20. [PubMed: 24436170]
- (640). Smith DJ; Lamont IL; Anderson GJ; Reid DW Targeting iron uptake to control *Pseudomonas aeruginosa* infections in cystic fibrosis. *Eur. Respir. J* 2013, 42, 1723–36. [PubMed: 23143541]
- (641). Wiens JR; Vasil AI; Schurr MJ; Vasil ML Iron-regulated expression of alginate production, mucoid phenotype, and biofilm formation by *Pseudomonas aeruginosa*. *mBio* 2014, 5, No. e01010–13. [PubMed: 24496793]
- (642). Chu BC; Peacock RS; Vogel HJ Bioinformatic analysis of the TonB protein family. *Biometals* 2007, 16, 467–483.
- (643). Hannavy K; Barr GC; Dorman CJ; Adamson J; Mazengera LR; Gallagher MP; Evans JS; Levine BA; Trayer IP; Higgins CF TonB protein of *Salmonella typhimurium*. A model for signal transduction between membranes. *J. Mol. Biol* 1990, 216, 897–910. [PubMed: 2266561]
- (644). Hannavy K; Higgins CF TonB; a model for signal transduction between membranes. *Biochem. Soc. Trans* 1991, 19, 530–2. [PubMed: 1889677]
- (645). Kodding J; Killig F; Polzer P; Howard SP; Diederichs K; Welte W Crystal structure of a 92-residue C-terminal fragment of TonB from *Escherichia coli* reveals significant conformational changes compared to structures of smaller TonB fragments. *J. Biol. Chem* 2005, 280, 3022–8. [PubMed: 15522863]
- (646). Peacock RS; Andrushchenko VV; Demcoe AR; Gehmlich M; Lu LS; Herrero AG; Vogel HJ Characterization of TonB interactions with the FepA cork domain and FecA N-terminal signaling domain. *BioMetals* 2006, 19, 127–42. [PubMed: 16718599]
- (647). Peacock RS; Weljie AM; Peter Howard S; Price FD; Vogel HJ The solution structure of the C-terminal domain of TonB and interaction studies with TonB box peptides. *J. Mol. Biol* 2005, 345, 1185–1197. [PubMed: 15644214]
- (648). Ginalski K Comparative modeling for protein structure prediction. *Curr. Opin. Struct. Biol* 2006, 16, 172–7. [PubMed: 16510277]
- (649). Kryshchovych A; Venclovas C; Fidelis K; Moult J Progress over the first decade of CASP experiments. *Proteins: Struct., Funct., Genet* 2005, 61 (7), 225–36. [PubMed: 16187365]
- (650). Neidhardt FC; Bloch PL; Smith DF Culture medium for enterobacteria. *J. Bacteriol* 1974, 119, 736–47. [PubMed: 4604283]
- (651). Do J; Zafar H; Saier MH, Jr Comparative genomics of transport proteins in probiotic and pathogenic *Escherichia coli* and *Salmonella enterica* strains. *Microb. Pathog* 2017, 107, 106–115. [PubMed: 28344124]
- (652). Bassford PJ, Jr; Kadner, R. J. Genetic analysis of components involved in vitamin B12 uptake in *Escherichia coli*. *J. Bacteriol* 1977, 132, 796–805. [PubMed: 336607]
- (653). Hantke K Dihydroxybenzoylserine—a siderophore for *E. coli*. *FEMS Microbiol. Lett* 1990, 67, 5–8.
- (654). Nikaido H; Rosenberg EY Cir and Fiu proteins in the outer membrane of *Escherichia coli* catalyze transport of monomeric catechols: study with beta-lactam antibiotics containing catechol and analogous groups. *J. Bacteriol* 1990, 172, 1361–1367. [PubMed: 2407721]

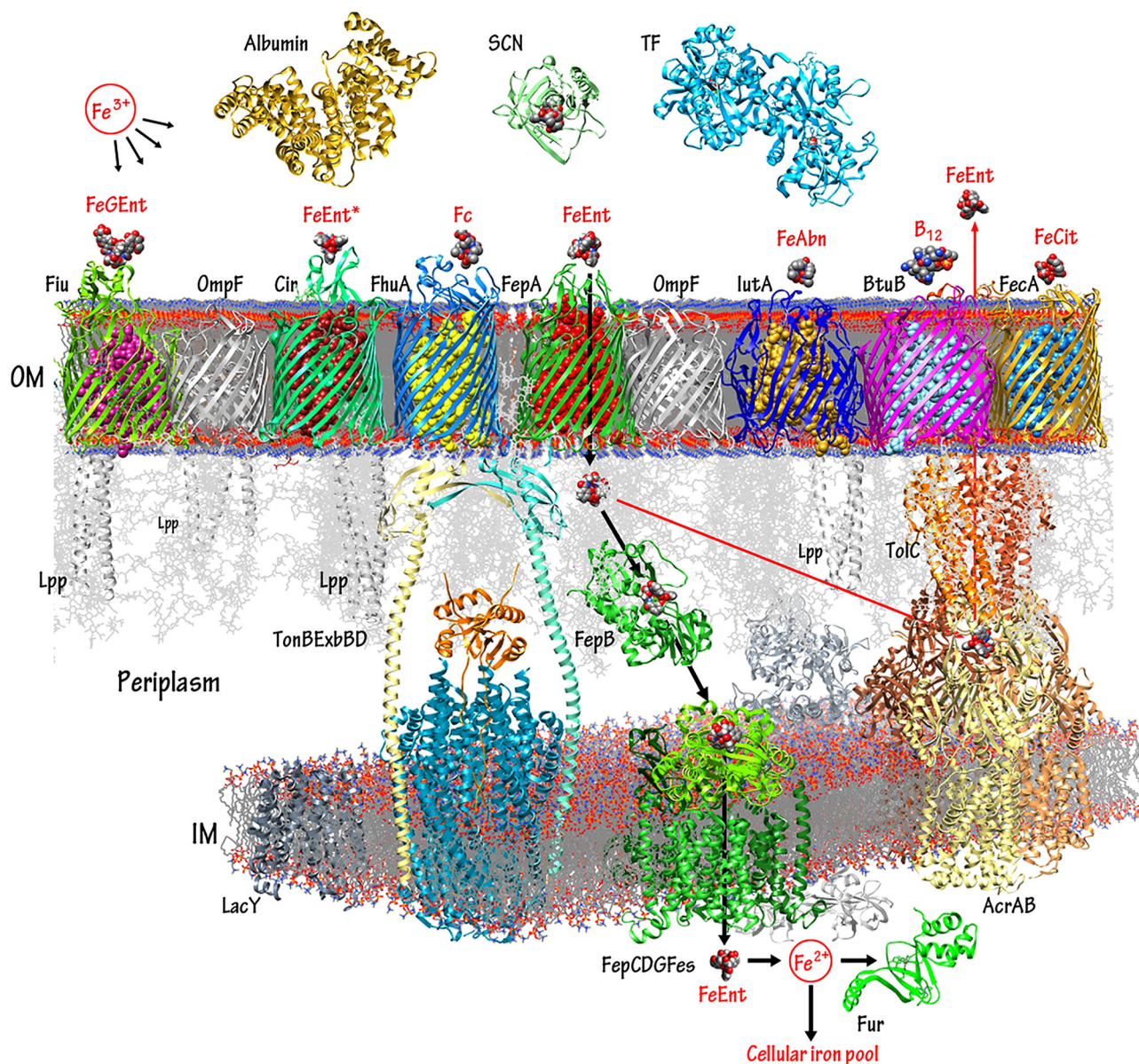


- (655). Bluhm ME; Hay BP; Kim SS; Dertz EA; Raymond KN Corynebactin and a serine trilactone based analogue: chirality and molecular modeling of ferric complexes. *Inorg. Chem* 2002, 41, 5475–8. [PubMed: 12377042]
- (656). Bluhm ME; Kim SS; Dertz EA; Raymond KN Corynebactin and enterobactin: related siderophores of opposite chirality. *J. Am. Chem. Soc* 2002, 124, 2436–7. [PubMed: 11890782]
- (657). May JJ; Wendrich TM; Marahiel MA The *dhb* operon of *Bacillus subtilis* encodes the biosynthetic template for the catecholic siderophore 2,3-dihydroxybenzoate-glycine-threonine trimeric ester bacillibactin. *J. Biol. Chem* 2001, 276, 7209–17. [PubMed: 11112781]
- (658). Lohmiller S; Hantke K; Patzer SI; Braun V TonB-dependent maltose transport by *Caulobacter crescentus*. *Microbiology* 2008, 154, 1748–54. [PubMed: 18524929]
- (659). Neugebauer H; Herrmann C; Kammer W; Schwarz G; Nordheim A; Braun V ExbBD-dependent transport of maltodextrins through the novel MalA protein across the outer membrane of *Caulobacter crescentus*. *J. Bacteriol* 2005, 187, 8300–11. [PubMed: 16321934]
- (660). Chairatana P; Zheng T; Nolan EM Targeting virulence: salmochelin modification tunes the antibacterial activity spectrum of  $\beta$ -lactams for pathogen-selective killing of *Escherichia coli*. *Chemical science* 2015, 6, 4458–4471. [PubMed: 28717471]
- (661). Payne MA; Igo JD; Cao Z; Foster SB; Newton SM; Klebba PE Biphasic binding kinetics between FepA and its ligands. *J. Biol. Chem* 1997, 272, 21950–5. [PubMed: 9268330]
- (662). Moynié L; Milenkovic S; Mislin GL; Gasser V; Mallocci G; Baco E; McCaughan RP; Page MG; Schalk IJ; Ceccarelli M The complex of ferric-enterobactin with its transporter from *Pseudomonas aeruginosa* suggests a two-site model. *Nat. Commun* 2019, 10, 3673. [PubMed: 31413254]
- (663). Grinter R; Lithgow T The structure of the bacterial iron-catecholate transporter Fiu suggests that it imports substrates via a two-step mechanism. *J. Biol. Chem* 2019, 294, 19523–19534. [PubMed: 31712312]
- (664). Larkin MA; Blackshields G; Brown NP; Chenna R; McGettigan PA; McWilliam H; Valentin F; Wallace IM; Wilm A; Lopez R; Thompson JD; Gibson TJ; Higgins DG Clustal W and Clustal X version 2.0. *Bioinformatics* 2007, 23, 2947–8. [PubMed: 17846036]
- (665). Dib L; Carbone A Protein fragments: functional and structural roles of their coevolution networks. *PLoS One* 2012, 7, No. e48124. [PubMed: 23139761]
- (666). Grytsyk N; Sugihara J; Kaback HR; Hellwig P pK(a) of Glu325 in LacY. *Proc. Natl. Acad. Sci. U. S. A* 2017, 114, 1530–1535. [PubMed: 28154138]
- (667). Kaback HR; Guan L It takes two to tango: The dance of the permease. *J. Gen. Physiol* 2019, 151, 878–886. [PubMed: 31147449]
- (668). Bradbeer C The proton motive force drives the outer membrane transport of cobalamin in *Escherichia coli*. *J. Bacteriol* 1993, 175, 3146–50. [PubMed: 8387997]
- (669). Majumdar A; Trinh V; Moore KJ; Smallwood CR; Kumar A; Yang T; Scott DC; Long NJ; Newton SM; Klebba PE Conformational rearrangements in the N-domain of *Escherichia coli* FepA during ferric enterobactin transport. *J. Biol. Chem* 2020, 295, 4974–4984. [PubMed: 32098871]
- (670). Esmailkhani H; Rasooli I; Hashemi M; Nazarian S; Sefid F Immunogenicity of Cork and Loop Domains of Recombinant *Baumannii acinetobactin Utilization Protein* in Murine Model. *Avicenna J. Med. Biotechnol* 2019, 11, 180–186. [PubMed: 31057721]
- (671). Lin J; Hogan JS; Smith KL Inhibition of in vitro growth of coliform bacteria by a monoclonal antibody directed against ferric enterobactin receptor FepA. *J. Dairy Sci* 1998, 81, 1267–74. [PubMed: 9621228]
- (672). Lin J; Hogan JS; Smith KL Growth responses of coliform bacteria to purified immunoglobulin G from cows immunized with ferric enterobactin receptor FepA. *J. Dairy Sci* 1999, 82, 86–92. [PubMed: 10022010]
- (673). Murphy CK; Kalve VI; Klebba PE Surface topology of the *Escherichia coli* K-12 ferric enterobactin receptor. *J. Bacteriol* 1990, 172, 2736–46. [PubMed: 2139651]
- (674). Wolf SL; Hogan JS; Smith KL Iron uptake by *Escherichia coli* cultured with antibodies from cows immunized with high-affinity ferric receptors. *J. Dairy Sci* 2004, 87, 2103–7. [PubMed: 15328222]

- (675). Kurupati P; Teh BK; Kumarasinghe G; Poh CL Identification of vaccine candidate antigens of an ESBL producing *Klebsiella pneumoniae* clinical strain by immunoproteome analysis. *Proteomics* 2006, 6, 836–44. [PubMed: 16372264]
- (676). Larrie-Bagha SM; Rasooli I; Mousavi-Gargari SL; Rasooli Z; Nazarian S Passive immunization by recombinant ferric enterobactin protein (FepA) from *Escherichia coli* O157. *Iran J. Microbiol* 2013, 5, 113–119. [PubMed: 23825727]
- (677). Lin J; Hogan JS; Aslam M; Smith KL Immunization of cows with ferric enterobactin receptor from coliform bacteria. *J. Dairy Sci* 1998, 81, 2151–8. [PubMed: 9749380]
- (678). Bentley AT; Klebba PE Effect of lipopolysaccharide structure on reactivity of antioporin monoclonal antibodies with the bacterial cell surface. *J. Bacteriol* 1988, 170, 1063–8. [PubMed: 2830227]
- (679). Klebba PE; Benson SA; Bala S; Abdullah T; Reid J; Singh SP; Nikaido H Determinants of OmpF porin antigenicity and structure. *J. Biol. Chem* 1990, 265, 6800–10. [PubMed: 1691177]
- (680). Tuntufye HN; Ons E; Pham AD; Luyten T; Van Gerven N; Bleyen N; Goddeeris BM *Escherichia coli* ghosts or live *E. coli* expressing the ferri-siderophore receptors FepA, FhuE, IroN and IutA do not protect broiler chickens against avian pathogenic *E. coli* (APEC). *Vet. Microbiol* 2012, 159, 470–478. [PubMed: 22633153]
- (681). Josts I; Veith K; Tidow H Ternary structure of the outer membrane transporter FoxA with resolved signalling domain provides insights into TonB-mediated siderophore uptake. *eLife* 2019, 8, e48528. [PubMed: 31385808]
- (682). Frillingos S; Ujwal ML; Sun J; Kaback HR The role of helix VIII in the lactose permease of *Escherichia coli*: I. Cys-scanning mutagenesis. *Protein Sci.* 1997, 6, 431–7. [PubMed: 9041646]
- (683). Frillingos S; Sahin-Toth M; Wu J; Kaback HR Cys-scanning mutagenesis: a novel approach to structure function relationships in polytopic membrane proteins. *FASEB J.* 1998, 12, 1281–99. [PubMed: 9761772]
- (684). Frillingos S; Gonzalez A; Kaback HR Cysteine-scanning mutagenesis of helix IV and the adjoining loops in the lactose permease of *Escherichia coli*: Glu126 and Arg144 are essential. *off. Biochemistry* 1997, 36, 14284–90. [PubMed: 9400367]
- (685). Nie Y; Ermolova N; Kaback HR Site-directed alkylation of LacY: effect of the proton electrochemical gradient. *J. Mol. Biol* 2007, 374, 356–64. [PubMed: 17920075]
- (686). Jiang X; Nie Y; Kaback HR Site-directed alkylation studies with LacY provide evidence for the alternating access model of transport. *Biochemistry* 2011, 50, 1634–40. [PubMed: 21254783]
- (687). Frillingos S; Kaback HR Probing the conformation of the lactose permease of *Escherichia coli* by in situ site-directed sulfhydryl modification. *Biochemistry* 1996, 35, 3950–6. [PubMed: 8672426]
- (688). Ermolova N; Madhvani RV; Kaback HR Site-directed alkylation of cysteine replacements in the lactose permease of *Escherichia coli*: helices I, III, VI, and XI. *Biochemistry* 2006, 45, 4182–9. [PubMed: 16566592]
- (689). Smirnova IN; Kasho VN; Kaback HR Direct sugar binding to LacY measured by resonance energy transfer. *Biochemistry* 2006, 45, 15279–87. [PubMed: 17176050]
- (690). Smirnova I; Kasho V; Sugihara J; Kaback HR Probing of the rates of alternating access in LacY with Trp fluorescence. *Proc. Natl. Acad. Sci. U. S. A* 2009, 106, 21561–6. [PubMed: 19959662]
- (691). Majumdar DS; Smirnova I; Kasho V; Nir E; Kong X; Weiss S; Kaback HR Single-molecule FRET reveals sugar-induced conformational dynamics in LacY. *Proc. Natl. Acad. Sci. U. S. A* 2007, 104, 12640–5. [PubMed: 17502603]
- (692). Jung K; Jung H; Kaback HR Dynamics of lactose permease of *Escherichia coli* determined by site-directed fluorescence labeling. *Biochemistry* 1994, 33, 3980–5. [PubMed: 8142402]
- (693). Voss J; Hubbell WL; Kaback HR Distance determination in proteins using designed metal ion binding sites and site-directed spin labeling: application to the lactose permease of *Escherichia coli*. *Proc. Natl. Acad. Sci. U. S. A* 1995, 92, 12300–3. [PubMed: 8618889]
- (694). Voss J; He MM; Hubbell WL; Kaback HR Site-directed spin labeling demonstrates that transmembrane domain XII in the lactose permease of *Escherichia coli* is an alpha-helix. *Biochemistry* 1996, 35, 12915–8. [PubMed: 8841136]

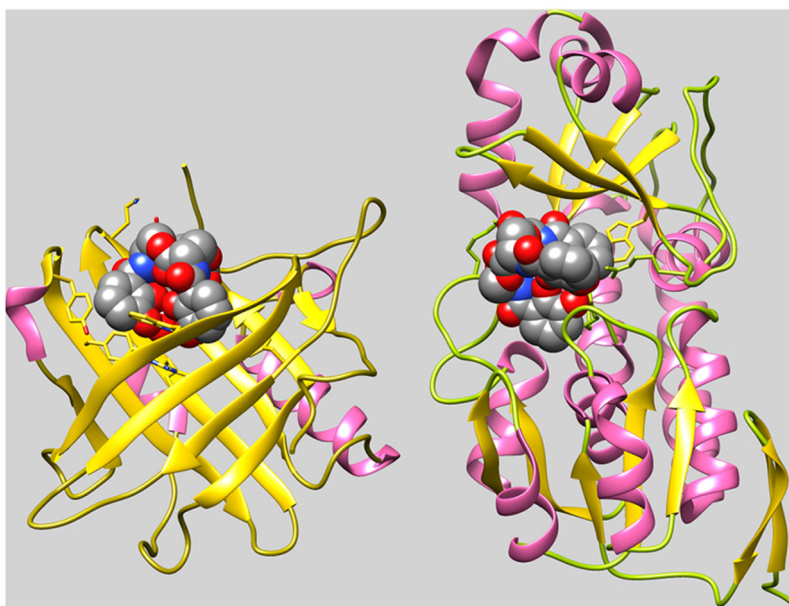
- (695). Wu J; Voss J; Hubbell WL; Kaback HR Site-directed spin labeling and chemical crosslinking demonstrate that helix V is close to helices VII and VIII in the lactose permease of *Escherichia coli*. *Proc. Natl. Acad. Sci. U. S. A* 1996, 93, 10123–7. [PubMed: 8816762]
- (696). Smirnova I; Kasho V; Choe JY; Altenbach C; Hubbell WL; Kaback HR Sugar binding induces an outward facing conformation of LacY. *Proc. Natl. Acad. Sci. U. S. A* 2007, 104, 16504–9. [PubMed: 17925435]
- (697). Liu J; Rutz JM; Klebba PE; Feix JB A site-directed spin-labeling study of ligand-induced conformational change in the ferric enterobactin receptor, FepA. *Biochemistry* 1994, 33, 13274–83. [PubMed: 7947735]
- (698). Cao Z; Warfel P; Newton SM; Klebba PE Spectroscopic observations of ferric enterobactin transport. *J. Biol. Chem* 2003, 278, 1022–8. [PubMed: 12409288]
- (699). Michelini E; Cevenini L; Mezzanotte L; Coppa A; Roda A Cell-based assays: fuelling drug discovery. *Anal. Bioanal. Chem* 2010, 398, 227–38. [PubMed: 20623273]
- (700). Cao Y; Bazemore-Walker CR Proteomic profiling of the surface-exposed cell envelope proteins of *Caulobacter crescentus*. *J. Proteomics* 2014, 97, 187–94. [PubMed: 23973469]
- (701). Nakae T; Nikaido H Multiple molecular forms of uridine diphosphate glucose pyrophosphorylase from *Salmonella typhimurium*. II. Genetic determination of multiple forms. *J. Biol. Chem* 1971, 246, 4397–403. [PubMed: 4937126]
- (702). Bailey DC; Buckley BP; Chernov MV; Gulick AM Development of a High-Throughput Biochemical Assay to Screen for Inhibitors of Aerobactin Synthetase IucA. *SLAS Discov* 2018, 23, 1070–1082. [PubMed: 29991301]
- (703). Hanson M; Jordan LD; Shipelskiy Y; Newton SM; Klebba PE High-Throughput Screening Assay for Inhibitors of TonB-Dependent Iron Transport. *J. Biomol. Screening* 2016, 21, 316–22.
- (704). Baell JB; Nissink JWM Seven Year Itch: Pan-Assay Interference Compounds (PAINS) in 2017-Utility and Limitations. *ACS Chem. Biol* 2018, 13, 36–44. [PubMed: 29202222]
- (705). Lagorce D; Oliveira N; Miteva MA; Villoutreix BO Pan-assay interference compounds (PAINS) that may not be too painful for chemical biology projects. *Drug Discovery Today* 2017, 22, 1131–1133. [PubMed: 28676405]
- (706). Pouliot M; Jeanmart S Pan Assay Interference Compounds (PAINS) and Other Promiscuous Compounds in Antifungal Research. *J. Med. Chem* 2016, 59, 497–503. [PubMed: 26313340]
- (707). Garcia-Herrero A; Peacock RS; Howard SP; Vogel HJ The solution structure of the periplasmic domain of the TonB system ExbD protein reveals an unexpected structural homology with siderophore-binding proteins. *Mol. Microbiol* 2007, 66, 872–89. [PubMed: 17927700]
- (708). Brewer S; Tolley M; Trayer IP; Barr GC; Dorman CJ; Hannavy K; Higgins CF; Evans JS; Levine BA; Wormald MR Structure and function of X-Pro dipeptide repeats in the TonB proteins of *Salmonella typhimurium* and *Escherichia coli*. *J. Mol. Biol* 1990, 216, 883–95. [PubMed: 2266560]
- (709). Brickman TJ; McIntosh MA Overexpression and purification of ferric enterobactin esterase from *Escherichia coli*. Demonstration of enzymatic hydrolysis of enterobactin and its iron complex. *J. Biol. Chem* 1992, 267, 12350–5. [PubMed: 1534808]
- (710). Escolar L; de Lorenzo V; Perez-Martin J Metalloregulation in vitro of the aerobactin promoter of *Escherichia coli* by the Fur (ferric uptake regulation) protein. *Mol. Microbiol* 1997, 26, 799–808. [PubMed: 9427409]
- (711). Escolar L; Perez-Martin J; de Lorenzo V Coordinated repression in vitro of the divergent fepA-fes promoters of *Escherichia coli* by the iron uptake regulation (Fur) protein. *J. Bacteriol* 1998, 180, 2579–82. [PubMed: 9573216]
- (712). Escolar L; Perez-Martin J; de Lorenzo V Binding of the fur (ferric uptake regulator) repressor of *Escherichia coli* to arrays of the GATAAT sequence. *J. Mol. Biol* 1998, 283, 537–47. [PubMed: 9784364]
- (713). Newton SM; Allen JS; Cao Z; Qi Z; Jiang X; Sprencel C; Igo JD; Foster SB; Payne MA; Klebba PE Double mutagenesis of a positive charge cluster in the ligand-binding site of the ferric enterobactin receptor, FepA. *Proc. Natl. Acad. Sci. U. S. A* 1997, 94, 4560–5. [PubMed: 9114029]

- (714). Annamalai R; Jin B; Cao Z; Newton SM; Klebba PE Recognition of ferric catecholates by FepA. *J. Bacteriol* 2004, 186, 3578–89. [PubMed: 15150246]
- (715). Cao Z; Qi Z; Sprencel C; Newton SM; Klebba PE Aromatic components of two ferric enterobactin binding sites in escherichia coli fepA. *Mol. Microbiol* 2000, 37, 1306–17. [PubMed: 10998164]
- (716). Pettersen EF; Goddard TD; Huang CC; Couch GS; Greenblatt DM; Meng EC; Ferrin TE UCSF Chimera—a visualization system for exploratory research and analysis. *J. Comput. Chem* 2004, 25, 1605–12. [PubMed: 15264254]

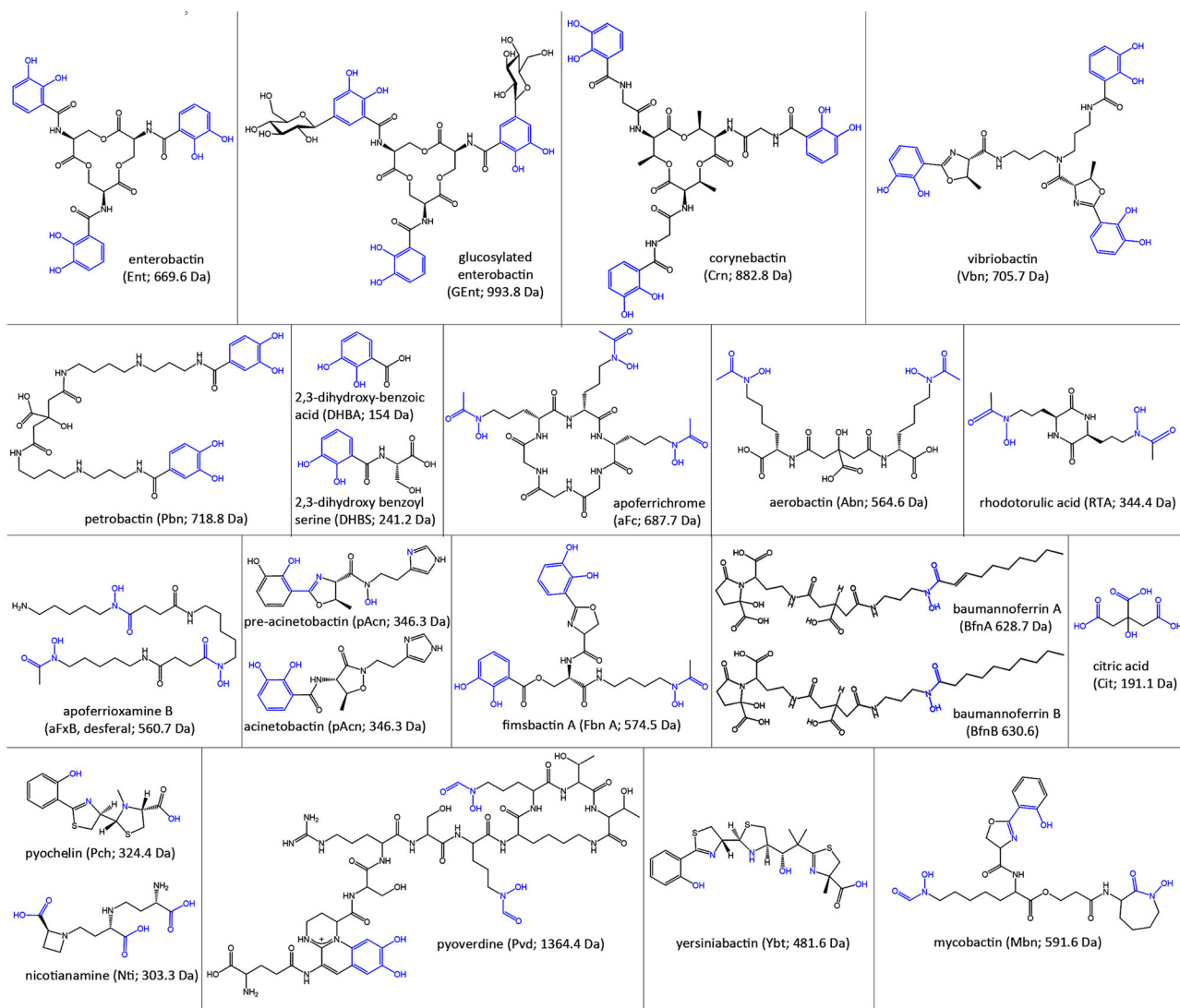


**Figure 1.** TonB-dependent iron and B<sub>12</sub> transport pathways in Gram (–) bacteria. The diagram displays selected components of the *E. coli* OM, periplasm, and IM, rendered by CHIMERA (UCSF) from their RCSB crystallographic coordinates. Proteins that participate in metal flux are portrayed in colors; other cell envelope components are shown in shades of gray. Bacteria and fungi secrete siderophores that chelate extracellular iron. In human and animal hosts, the innate immune system proteins albumin, SCN, and TF antagonize bacterial iron acquisition, by adsorbing siderophores, ferric siderophores, or free iron from blood, serum, lymph, and other fluids. Nevertheless, high affinity bacterial OM LGP bind specific ferric siderophores (or vitamin B<sub>12</sub>) and actively transport them into the periplasm. The bacterial TonB/ExbBD complex spans the cell envelope and utilizes IM PMF to energize the OM active transport reactions.<sup>91,237</sup> TonB/ExbBD is modeled from the

crystallographic coordinates of the TonB C-terminus,<sup>241</sup> the ExbBD proteins,<sup>232,233,707</sup> and other data;<sup>236,644,708</sup> the full complex was not yet structurally delineated. The import (black arrows) and export (red arrows) pathways of FeEnt typify those of other metal complexes: after binding and TonB-dependent internalization by FepA, FeEnt binds to the periplasmic protein FepB that delivers it to the IM ABC-transporter FepCDG, which hydrolyzes ATP as it transports the ferric siderophore to the cytoplasm. During or after the IM uptake process, Fes hydrolyzes the lactone backbone of FeEnt, which effectively releases Fe<sup>3+</sup> for reduction to Fe<sup>2+</sup>.<sup>709</sup> Ferrous iron enters cellular iron pools, and equilibrium with the global regulator, Fur.<sup>710-712</sup> Alternatively, if surplus FeEnt exists in the periplasm, then the AcrABTolC export complex expels the excess to the exterior.<sup>62</sup> The depiction of FepCDGFes was modeled from the crystal structure of BtuCD.

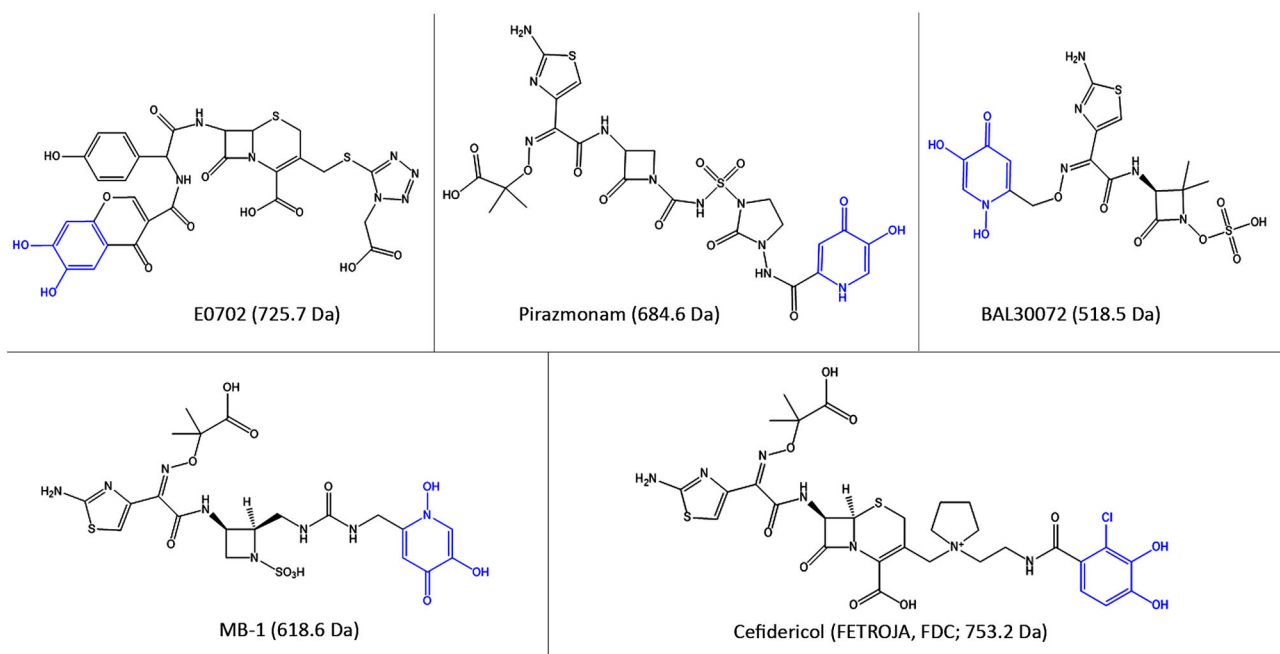


**Figure 2.** Binding of FeEnt by HsaSCN and EcoFepB. Comparison of the crystallographic structures of human SCN (3CMP) and *E. coli* FepB (3TLK), with bound FeEnt, shows two different structural folds for FeEnt binding. Both contain  $\alpha$ - (pink) and  $\beta$ - (gold) structures, but the former human serum protein binds FeEnt in the mouth of a seven-stranded  $\beta$ -barrel, whereas the latter periplasmic protein binds it in the central cleft of a bilobed globule. In both cases, however, affinity for the aromatic, triply negatively charged ferric siderophore derives from interactions with cationic (SCN: R81, R130, R134; FepB: R78, R242, R301) and aromatic (SCN: Y52, W79, Y100, Y106, F123, Y132; FepB: F300, W209) side chains in the binding protein. Adsorption of FeEnt to EcoFepA involves similar contributions of charge<sup>713</sup> and aromaticity<sup>714,715</sup> to the overall affinity.

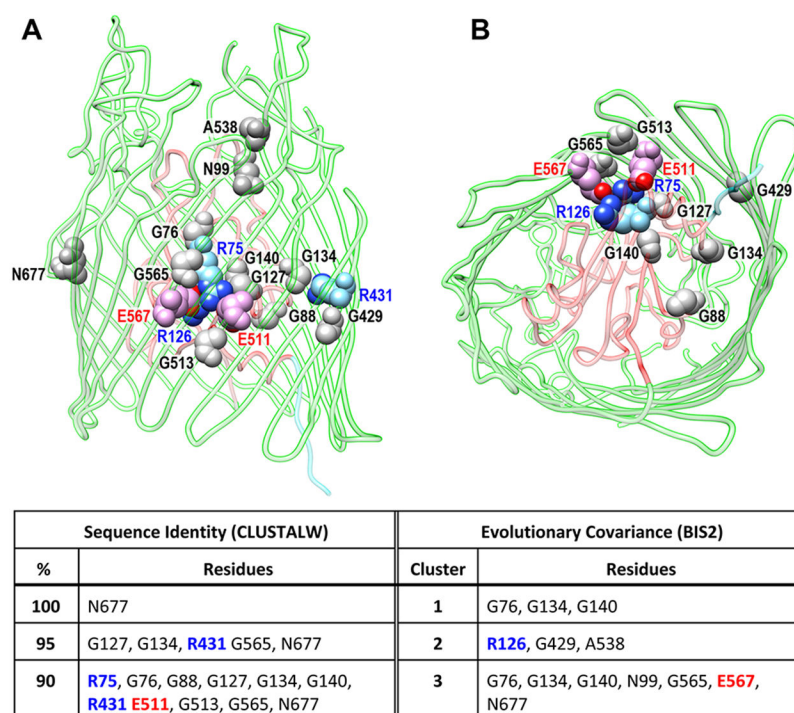


**Figure 3.** Siderophores. Pathogenic bacteria secrete and/or utilize a variety of catecholate, hydroxamate, and mixed chelation siderophores, usually less than 1000 Da in mass. The illustrations show the structures, abbreviations, and masses of the aposiderophores, with their iron chelation moieties colored blue.





**Figure 4.** Structures of siderophore- $\beta$ -lactam Trojan Horse antibiotics. These monocatecholate and hydroxypyridinone siderophore-antibiotic conjugates target ferric catecholate uptake pathways in Gram (–) cells. The iron chelation moieties are colored blue. Cefiderocol (FDC) contains a monocatecholate siderophore moiety and is the only FDA-approved siderophore-conjugated antibacterial drug.

**Figure 5.**

Conserved mechanistic charge cluster in the LGP interior. After aligning the primary structures of 79 LGP from commensal and pathogenic Gram (-) bacteria (Table 1) by CLUSTALW<sup>664</sup> and analyzing the aligned files for evolutionary covariance by BIS<sup>2,665</sup> we mapped 16 conserved (>90%) or coevolved amino acids to the tertiary structure of EcoFepA (PDB 1FEP) using CHIMERA (UCSF<sup>716</sup>). (A) Side view of EcoFepA: the N-domain (residues 1–150) is depicted in ribbon format and colored red; the C-domain  $\beta$ -barrel (residues 151–7240) is depicted in ribbon format and colored green. Among the 16 residues of interest (shown in space-filling format), one (N677, colored gray) was conserved in all the LGP. (B)  $-90^\circ$  X-axis rotation of the view in (A) creates a perspective inside the  $\beta$ -barrel, from the periplasm. Four polar charged side chains (R75, R126, E511, E567; colored sky blue and red, respectively; heteroatoms N and O colored blue and red, respectively) create an electrostatic lock that, in the absence of protonation, holds the N-domain to the  $\beta$ -barrel directly above the TonB-box region (in ribbon format, colored cyan). A group of eight glycines (colored gray), located in either the interior of the N-domain (G76, G88, G127, G134, G140) or in the strands of the  $\beta$ -barrel (G429, G513, G565), surround the charge cluster, potentially maximizing the flexibility of the protein structure in this region.

Table 1.

LGP of CRE/ESKAPE and Other Pathogens<sup>a</sup>

LGP <sup>b</sup>	strain <sup>c</sup>	metal complex <sup>d</sup>	protein ligands <sup>e</sup>	aa	mass <sup>f</sup>	pI <sup>g</sup>	<i>E. coli</i> K-12 orthologue <sup>h</sup>	NCBI ref <sup>i</sup>	PDB
Commensal <i>E. coli</i>									
FecA	MG1655	FeCit	ND	741	81 707	5.61	NSI	NP_418711.1	1PNZ
FepA	MG1655	FeEnt	colB, D; H8, mE495	724	79 771	5.4	53% Iron	NP_415116.1	1FEP
FhuA	MG1655	Fc	colM, T1, T5, $\phi$ 80	714	78 742	5.3	NSI	NP_414692.1	1BY5
Fiu	MG1655	FeDHBS	ND	727	78 432	5.75	NSI	NP_415326.1	6BPN
FhuE	MG1655	FeRta	ND	693	77 411	4.89	NSI	NP_415620.1	6E4V
Cir	MG1655	FeDHBS	colla, Ib,	638	71 149	5.2	35% FepA	NP_416660.1	2HDF
BtuB	MG1655	B12	ColE1, E3, BF23	594	66 325	5.35	NSI	NP_418401.1	INQE
Pathogenic <i>E. coli</i>									
YddB	UPEC 042	ND	ND	771	87 206	6.06	NSI	CBG34449.1	6OFR
TutA	083:HI <sup>j</sup>	FeAbn	cloacin DF13, colV	708	78 061	5.23	NSI	WP_000973516.1	ND
Iron	083:HI <sup>j</sup>	FeGEnt	ND	701	76 525	5.79	52% FepA	ADR29866.1	ND
YncD	UPEC C15	ND	ND	677	74 900	5.32	NSI	AKC11926.1	6V81
FyuA	0157:H7	FeYbt	pesticin	551	71 387	5.52	NSI	EFB2704300.1	ND
ChuA	0157:H7	Hn	ND	632	69 436	5.27	NSI	NP_312407.1	ND
LGP1	0157:H7	ND	ND	687	76 150	5.48	NSI	QGF16871.1	ND
LGP2	0157:H7	ND	ND	634	71 005	5.69	NSI	QGF15879.1	ND
<i>K. pneumoniae</i>									
FepA4	Kp52.145	FeEnt	ND	728	80 070	5.67	72% FepA	WP_004179434.1	ND
FepA1	Kp52.145	FeEnt	ND	717	79 665	5.41	81% FepA	CDO13414.1	ND
FhuA	Kp52.145	Fc	ND	715	79 054	5.34	89% FhuA	WP_048972727.1	ND
TutA	hvKPI	FeAbn	cloacin DF13	708	78 043	5.23	NSI	CDO11693.1	ND
Fiu	KP52.145	FeDHBS	ND	727	78 023	5.71	77% Fiu	WP_171841556.1	ND
FepA2	KP52.145	ND	ND	701	77 382	5.31	51% FepA	CDO16709.1	ND
FhuE	KP52.145	FeRTA <sup>k</sup>	ND	695	76 897	5.25	50% FhuE	AYK02175.1	ND
Iron	KP52.145 <sup>k</sup>	FeGEnt	ND	700	76 760	6.41	51% FepA	WP_042940746.1	ND
FcuA	KP52.145	ND	ND	703	76 166	5.57	NSI	EMB11413.1	ND

LGP <sup>b</sup>	strain <sup>c</sup>	metal complex <sup>d</sup>	protein ligands <sup>e</sup>	aa <sup>f</sup>	mass <sup>f</sup>	pI <sup>g</sup>	<i>E. coli</i> K-12 orthologue <sup>h</sup>	NCBI ref <sup>i</sup>	PDB
YncD	hvKP1	ND	ND	677	74 569	5.75	NSI	EMB10697.1	ND
FyuA	hvKP1	FeYbt	pesticin	652	71 400	5.52	NSI	CDO15344.1	ND
Cir	Kp52.145	FeDHBS		632	70 367	5.35	82% Cir	EMB11539.1	ND
ChuA	hvKP1	Hn	ND	613	67 571	5.27	100% ChuA	WP_001322816.1	ND
BtuB	KP52145	B12	ND	592	66 035	5.32	57% BtuB	CDO16333.1	ND
LGP1	KP52145	ND	ND	737	81 135	5.62	NSI	QDA45483.1	ND
LGP2	KP52145	ND	ND	680	74 658	5.64	33% FhuA	EMB11926.1	ND
<i>A. baumannii</i>									
Fiu	17978	FeDHBS	ND	771	84 285	6.89	34% Fiu	AZM59353.1	ND
BfnH	17978	FeBfn	ND	728	80 491	5.84	NSI	ABO12082.2	ND
FepA	17978	FeEnt	ND	730	80 248	5.67	45% FepA	WP_005135700.1	ND
PiuA	17978	FeDHBS	ND	736	80 054	6.23	31% Fiu	ABO10929.1	5FP1
PirA	17978	FeDHBS	ND	714	78 022	5.43	NSI	SCX98474.1	5FR8
BauA	17978	FeAcn	ND	712	77 497	7.6	NSI	ABO12804.2	ND
BauA	19606	FeAcn	ND	703	76 016	5.62	NSI	WP_001073039.1	6H7V
FhuA	19606	Fc	ND	679	75 739	5.59	25% FhuA	ABO12348.2	ND
FbsN	19606	FeFbn	ND	629	68 763	6.82	25% FhuA	ABO12983.2	ND
BtuB	19606	B12	ND	598	65 781	5.71	25% BtuB	ABO13283.2	ND
LGP1	19606	ND	ND	862	93 996	5.08	NSI	CAA0247590.1	ND
LGP2	19606	ND	ND	781	88 811	6.63	34% FecA	ABO13864.1	ND
LGP3	19606	ND	ND	697	78 847	5.8	NSI	ABO13728.2	ND
LGP4	19606	ND	ND	674	77 325	5.52	NSI	EEX02122.1	ND
LGP5	19606	ND	ND	681	75757	5.48	25% FhuA	ABO11495.2	ND
LGP6	19606	ND	ND	669	74 690	5.18	42% FepA	ABO13298.2	ND
<i>P. aeruginosa</i>									
HxuA	PAO1	Hn	ND	965	95 071	7.33	NSI	CRQ69633.1	ND
HasR	PAO1	Hn	ND	855	94 205	5.85	NSI	NP_252098.1	ND
FpvA	PAO1	FePvd	pyocins S2, S3, S4	772	86 469	5.27	NSI	NP_251088.1	2IAH
PupA	PAO1	FePeh	ND	777	86 005	5.28	NSI	AMU01031.1	ND
FoxA	PAO1	FxB	ND	773	85 273	5.05	32% FhuA	NP_251156.1	6196
ChuA	PAO1	Hn	ND	737	81 892	5.99	NSI	AAC13289.1	ND

LGP <sup>b</sup>	strain <sup>c</sup>	metal complex <sup>d</sup>	protein ligands <sup>e</sup>	aa	mass <sup>f</sup>	pI <sup>g</sup>	<i>E. coli</i> K-12 orthologue <sup>h</sup>	NCBI ref <sup>i</sup>	PDB
FepA1	PAOI	FeEnt?	ND	735	80 919	5.85	71% FepA	MXH37568.1	ND
PiuD	PAOI	FeDHBS	ND	731	80 149	5.68	NSI	WP_132667204.1	5NEC
FepA2	PAOI	FeEnt?	ND	717	79 687	5.19	81% FepA	MXH36562.1	5NEC
<i>P. aeruginosa</i>									
PfeA	PAOI	FeEnt	ND	721	78 503	5.8	60% Iron	NP_251378.1	6Q5E
PiuA	PAOI	ND	ND	729	78 313	5.7	77% Fiu	MXH35875.1	5FOK
CntA	PAOI	FeRTA <sup>j</sup>	ND	714	78 166	5.45	NSI	PTC33848.1	ND
IutA	PAOI	FeAbn	ND	708	78 161	4.96	72% IutA	MXH36073.1	ND
PirA	PAOI	FeDHBS	ND	714	77 992	5.43	56% FepA	AAG04320.1	5FP2
FhuA	PAOI	Fc	ND	702	77 881	5.37	61% FhuA	MXH37021.1	ND
Iron	PAOI	FeGEnt	ND	714	77 866	5.38	60% Iron	WP_058129121.1	ND
FptA	PAOI	FePch	pyocin E5	682	75 597	5.58	NSI	NP_252911.1	1XKW
FhuE	PAOI	FeRTA <sup>j</sup>	ND	689	75 467	5.14	46% FhuE	CRQ23141.1	ND
FvbA	PAOI	FeVbn	ND	665	73 731	5.46	NSI	WP_003093526.1	ND
Cir	PAOI	FeDHBS	ND	632	70 398	5.31	80% Cir	MXH34319.1	ND
BtuB	PAOI	B <sub>12</sub>	ND	598	66 521	5.38	57% BtuB	MXH38591.1	ND
LGP1	PAOI	ND	ND	821	92 251	6.39	NSI	BAQ41081.1	ND
<i>Y. pestis</i>									
HasR	KIM6+	Hn	ND	795	89 654	7.96	56% HasR	WP_002209485.1	ND
IutA	KIM6+	FeAbn	ND	745	82 439	5.36	67% IutA	WP_087813403.1	ND
FhuE	KIM6+	FeRTA <sup>j</sup>	ND	717	79 827	7.8	27% FhuE	WP_002211883.1	ND
FhuA	KIM6+	Fc	ND	716	78 382	5.99	26% FhuA	AAS63640.1	ND
huA	KIM6+	Hn	ND	690	75 802	5.24	68% ChuA	WP_002209062.1	ND
Cir	KIM6+	FeDHBS	ND	679	75 555	6.0	38% Cir	WP_071526008.1	ND
BtuB	KIM6+	B <sub>12</sub>	ND	672	72 172	5.45	65% BtuB	WP_058987704.1	ND
Psn	KIM6+	FeYbt	pesticin	651	71 442	5.62	NSI	AAC69592.1	4EPA
LGP1	KIM6+	Cu <sup>++</sup> ?	ND	698	76 423	8.82	28% BtuB	WP_002208882.1	ND
LGP2	KIM6+	Hn?	ND	667	76 274	5.34	45% YoeA	WP_002211632.1	ND
LGP3	KIM6+	FeDHBS	ND	678	74 129	6.2	31% Cir	AAM84435.1	ND

Other Gram (-) Pathogens

LGP <sup>b</sup>	strain <sup>c</sup>	metal complex <sup>d</sup>	protein ligands <sup>e</sup>	aa	mass <sup>f</sup>	pI <sup>g</sup>	<i>E. coli</i> K-12 orthologue <sup>h</sup>	NCBI ref <sup>i</sup>	PDB
HasR	<i>S. marcescens</i> <sup>m</sup>	Hn	ND	865	94 847	6.2	NSI	CAE46936.1	3CSN
FauA	<i>B. pertussis</i>	alcaligin	ND	699	77 593	6.75	NSI	WP_014905926.1	3EFM
FtpB	<i>N. meningitidis</i> <sup>n</sup>	FeEnt?	ND	692	76 823	9.42	NSI	AAF42315.1	4AIP

<sup>a</sup>We identified 79 LGP that participate in the uptake of ferric siderophores, heme or other metal complexes. This list, that is not fully comprehensive, illustrates the breadth of metal chelate recognition in Gram (-) bacterial pathogens. We used sequences of the mature proteins for analysis by CLUSTALΩ, the results of which appear in Figures S1 and 5.

<sup>b</sup>LGP reflect standard nomenclature; if function is unknown, the protein is enumerated: *e.g.*, EcoLGP1, EcoLGP2, *etc.*

<sup>c</sup>Bacterial strain from which the genomic information originated.

<sup>d</sup>Ferric siderophore or metal porphyrin; see text for abbreviations.

<sup>e</sup>Abbreviations: col, colicin; m, microcin.

<sup>f</sup>Mass (Da) of the mature protein.

<sup>g</sup>Isoelectric point of the mature protein.

<sup>h</sup>Extent of identity to the closest homologue in *E. coli* K-12 strain MG1655; NSI, NSI, no significant identity (*i.e.*, <25%).

<sup>i</sup>Entries originated from the NCBI PROTEIN database.

<sup>j</sup>Structural gene resides on pNRG857c in strain O83:H1.

<sup>k</sup>Structural gene resides on pLVPK in strain Kp52.145, also called pII.

<sup>l</sup>LGP that recognize RTA often also bind FxB or coprogen.

<sup>m</sup>*S. marcescens* strain SM365.

<sup>n</sup>*N. meningitidis* strain MC58.